NASA TECHNICAL MEMORANDUM

NASA TM X-3161

NASA TM X-3161

WIND-TUNNEL INVESTIGATION OF A SIMULATED GUNSHIP HELICOPTER ENGINE-EXHAUST—WINDSTREAM INTERACTION

by John C. Wilson and Raymond E. Mineck

Langley Directorate

U.S. Army Air Mobility R&D Laboratory

Hampton, Va. 23665

NATIONAL AERONAUTICS AND SPACE ADMINISTRATION • WASHINGTON, D. C. • DECEMBER 1974

1. Report No.	2. Government Accession No.	3. Recipient's Catalog No.
NASA TM X-3161		

4. Title and Subtitle	5. Report Date
WIND-TUNNEL INVESTIGATION OF A SIMULATED GUNSHIP HELICOPTER ENGINE-EXHAUST—WINDSTREAM INTERACTION	December 1974
	6. Performing Organization Code
7. Author(s) John C. Wilson and Raymond E. Mineck, Langley Directorate, U.S. Army Air Mobility R&D Laboratory	8. Performing Organization Report No. L-9923
	10. Work Unit No. 505-11-41-10
9. Performing Organization Name and Address NASA Langley Research Center Hampton, Va. 23665	11. Contract or Grant No.
	13. Type of Report and Period Covered Technical Memorandum
12. Sponsoring Agency Name and Address National Aeronautics and Space Administration Washington, D.C. 20546	14. Sponsoring Agency Code

15. Supplementary Notes

16. Abstract

A wind-tunnel investigation of the engine-exhaust—windstream flow interaction on a gunship helicopter model has been conducted in the Langley V/STOL tunnel. This program was sponsored jointly by the U.S. Army Aviation Systems Command and the National Aeronautics and Space Administration. The investigation utilized a flow-visualization technique employing neutrally buoyant helium-filled bubbles to determine the cause of exhaust-shield overheating during cruising flight and to evaluate means of eliminating the problem. The flow patterns were recorded with still cameras and on television magnetic tape. Exhaust-flow impingement on the exhaust shield during cruise was found to cause the problem. Several flow-altering devices were evaluated to find suitable ways to correct the problem. A flow deflector located on the model cowling upstream of the exhaust provides an effective solution.

17. Key Words (Suggested by Author(s))	18. Distribution Statement
Engine-exhaust—windstream interaction Helicopter exhaust Flow visualization Exhaust-flow impingement Flow deflector	Unclassified – Unlimited STAR Category 01

19. Security Classif. (of this report)	20. Security Classif. (of this page)	21. No. of Pages	22. Price*
Unclassified	Unclassified	69	$4.25

*For sale by the National Technical Information Service, Springfield, Virginia 22151

WIND-TUNNEL INVESTIGATION OF A SIMULATED GUNSHIP HELICOPTER ENGINE-EXHAUST—WINDSTREAM INTERACTION

By John C. Wilson and Raymond E. Mineck
Langley Directorate, U.S. Army Air Mobility R&D Laboratory

SUMMARY

A wind-tunnel investigation of the engine-exhaust—windstream flow interaction on a gunship helicopter model has been conducted in the Langley V/STOL tunnel. This program was sponsored jointly by the U.S. Army Aviation Systems Command and the National Aeronautics and Space Administration. The investigation utilized a flow-visualization technique employing neutrally buoyant helium-filled bubbles to determine the cause of exhaust-shield overheating during cruising flight and to evaluate means of eliminating the problem. The flow patterns were recorded with still cameras and on television magnetic tape. Exhaust-flow impingement on the exhaust shield during cruise was found to cause the problem. Several flow-altering devices were evaluated to find suitable ways to correct the problem. A flow deflector located on the model cowling upstream of the exhaust provides an effective solution.

INTRODUCTION

A problem encountered by a current gunship helicopter is that of engine-exhaust shield overheating during cruising flight. The problem area is shown in figure 1, and the helicopter under study is shown in figure 2. The problem is similar to one which was encountered by a light observation helicopter and which was investigated in wind-tunnel tests and flight tests. (See refs. 1 and 2.) The overheating was believed to be caused by the impingement of exhaust flow of the hot-exhaust gases on the external surfaces of the shield. The exhaust system of the gunship helicopter differs from that of the light observation helicopter in that it is a single moderately curved duct; whereas the exhaust system of the light observation helicopter had ducting with very complex curvature leading to two exhaust ducts.

The interaction of exhaust flow from curved ducting and free-stream flow is characterized by complex flow patterns originating within the duct (ref. 3) and becoming more complex upon egress from the duct (ref. 4). Within the duct, secondary flow patterns (swirl) originate because of viscous mixing, flow curvature, and engine swirl. Upon exiting, this swirl is accentuated. The result is that exhaust flow "quickly" mixes with

the windstream in the outboard regions of an exhaust jet. This mixing region impinges on the external surfaces of the exhaust shield. During tests in the Langley V/STOL tunnel (ref. 1), a flow deflector device was found to be an effective means of eliminating the exhaust impingement. The present investigation of the gunship helicopter exhaust system was intended to verify the effectiveness of a similar device and to evaluate the effectiveness of variations of this device for simulated flight conditions. A flow-visualization technique employing neutrally buoyant helium-filled soap bubbles was used to identify the exhaust flow path and its interaction with the free-stream flow. The development of the helium-bubble generator system which includes a unique set of equipment for bubble production, bubble illumination, and video recording is described in reference 5. The system includes a bubble generator, a set of lights, and a video recorder. The bubble generator produces helium-filled soap bubbles approximately 0.32 cm (0.125 in.) in diameter which are neutrally buoyant and follow the flow streamlines.

The primary simulation parameter, the ratio of effective windstream velocity to exhaust velocity, was varied from 0.6 to approximately 1.0. Previous research (ref. 6) has shown that when flow velocities and temperatures cannot be reproduced, realistic flow simulation is obtained by reproduction of the ratio of effective windstream velocity to exhaust velocity. Previous tests (refs. 1 and 2) for the OH-58A helicopter support this conclusion. The exhaust gas was simulated by compressed air at ambient temperatures.

SYMBOLS

The values used for physical quantities defined in this paper are given in both the U.S. Customary Units and International System of Units (SI). Factors relating these two systems of units are presented in reference 7.

$q_{exhaust}$ exhaust dynamic pressure, N/m^2 (lbf/ft^2)

q_∞ free-stream dynamic pressure, N/m^2 (lbf/ft^2)

V_{eff} ratio of effective windstream velocity to engine exhaust velocity, $\frac{V_\infty}{V_j} = \sqrt{\frac{q_\infty}{q_{exhaust}}}$

V_j jet-exhaust velocity, m/sec (ft/sec)

V_∞ free-stream velocity, m/sec (ft/sec)

α angle of attack (measured between free-stream velocity direction and the model baseline), deg

β angle of sideslip, deg

TESTS

Since the exhaust-heating problem was known to occur at cruise conditions for this helicopter configuration, tests were made for a range of V_{eff} from 0.6 to 1.0. Although tunnel dynamic pressure was as high as 2873 N/m^2 (60 lbf/ft^2), the best visualization of flow patterns was obtained at a dynamic pressure of 211 N/m^2 (4.4 lbf/ft^2). The angle-of-attack range was 0^o to -10^o and the model sideslip angle range was 10^o to -10^o.

Five flow deflector configurations were tested, as shown in figure 3. These configurations were (1) a flow deflector with the center cut out so that it would fit down over the entire cowling (fig. 3(a)); two modifications of this configuration are shown in figures 3(b) and 3(c); (2) a flow deflector with outboard sections canted downward (fig. 3(d)); and (3) a spoiler which is a standard installation (figs. 2 and 3(e)) on the gunship helicopter being investigated. The flow deflectors were mounted on two aluminum struts attached to the engine cowling.

APPARATUS

Model

The model was composed of the engine exhaust section attached to a wooden representation of a section of a helicopter pylon and fuselage structure. (See fig. 4.) A photograph of the helicopter exhaust system model installation in the V/STOL tunnel is shown in figure 5. Because the full-scale rotor diameter was greater than the tunnel width, the rotor was not installed. However, it was not considered necessary to have the effects of the rotor for the purposes of this investigation. An analysis of the rotor downwash utilizing the method of reference 8 indicates that at the cruise conditions, the tip vortex will pass high enough above the cowling to cause little influence upon the exhaust exit.

Flow-Visualization Equipment

The primary investigatory equipment was a helium-bubble generator system. This system is useful for airflow visualization when the flow temperature is less than 54^o C (130^o F) and flow velocity is less than 61 m/sec (200 ft/sec). Bubbles were released near the exhaust and inside the exhaust duct. These bubbles were illuminated by the

high-powered light source located downstream of the model. As the bubbles passed over the model, they were photographed from the left side (looking upstream) and top of the test section. Three still cameras were used to photograph the flow patterns. Two of the cameras (70 mm) were triggered together, one mounted above the model and the other mounted for a side view. The third camera was used to obtain supplementary side views of the flow patterns. The model was painted black to provide a nonreflecting background for enhanced photographic recording of the bubble streaks.

RESULTS AND DISCUSSION

The results of this investigation are shown in photographs utilizing the helium-bubble technique to show the flow patterns formed by the interaction of the free-stream flow and exhaust flow for the various flow deflector devices investigated. Some of the photographs in the figures are repetitive. They are presented to show patterns differing because of relocation of the bubble egress.

The identification of the problem (cause of the exhaust shield heating) is clearly shown in figure 6 for the gunship helicopter exhaust system without any of the deflector devices installed. The test condition shown is representative of cruising flight ($V_{eff} = 0.7$) for the helicopter under investigation. It can be seen that flow at the edge of the exhaust duct exit is drawn down and around the rear of the exhaust duct exit and impinges on the side of the system. This condition indicates that exhaust gas would follow the same path and that this condition becomes worse as the angle of attack increases negatively. Figure 7 shows directly that bubbles emanating from the interior of the system roll over the edge (as seen from the side and overhead) and down and around the back of the exhaust system.

When the flow swirler was installed in the exhaust duct, there was a moderate increase in the impingement spillover of the gas as shown in figures 8 and 9.

When the spoiler deflector device (shown in fig. 3(e)) was installed, it was found that at $V_{eff} = 0.7$, downward deflection of the flow patterns was diminished, but figure 10 still clearly shows substantial flow down and around the exhaust exit. Figure 11 shows an increased downward deflection at $V_{eff} = 0.9$ as well as the "stalled" or separated flow in the wake region aft of the spoiler. It can be said then that the spoiler reduced the flow impingement only moderately.

When flow deflector 1 (fig. 3(a)) was installed along with the swirler, the downward deflection of the flow pattern was effectively eliminated as shown in figure 12. Figure 12 shows a slight change of the exhaust pattern with an increase of V_{eff} from 0.7 to 1.0. Figures 13 and 14 show that bubbles emanating within the duct mix with a stalled flow region just rearward of the flow deflector center. As found in the tests of

references 1 and 2, the deflector causes the free-stream flow to be deflected upward in the region ahead of the exhaust, whereas vortices formed near the flow deflector tips provide additional upward deflection of the free-stream flow at the outboard regions of the exhaust exit.

Flow deflector 2 (fig. 3(b)) differs from flow deflector 1 in that it was moved back on the aluminum supports 2.54 cm (1.0 in.) to place the leading edge of the deflector tips at an angle of 0° with respect to the model reference axis. The swirler was installed in the exhaust duct for this installation Figures 15 and 16 indicate no significant change in the impingement when compared with deflector 1 (fig. 12), but they do indicate a larger stalled or separated flow in the wake region aft of the flow deflector such as that noted for the spoiler (fig. 11). Figures 17 to 26 present the results of a more detailed investigation of flow deflector 2 without the swirler installed in the exhaust duct. The ratio of effective windstream velocity to exhaust velocity, angle of attack, and sideslip angle were varied as well as the position of the exterior source of bubbles. Figure 17 indicates that as the angle of attack is increased negatively, the impingement increases. However, figures 18, 19, and 20 which present simultaneous side and top views show that the exhaust flow is dispersing laterally well clear of the external exhaust system. Varying V_{eff} (figs. 21, 22, and 23) causes slight change in the angle of the exhaust flow patterns and on the dispersion of the flow. Photographs of sideslip conditions are presented for sideslip angles of 5° and -5° at $V_{eff} = 0.7$ (figs. 24, 25, and 26). Although larger angles of 10° and -10° were tested, the photographs disclosed no greater effects than those shown for 5° and -5°. In summary, varying the ratio of effective windstream velocity to exhaust velocity, angle of attack, and sideslip angle did not diminish the effectiveness of the flow deflector.

Flow deflector 2 was modified by adding clay to the leading edge of the center section of the flow deflector and was designated flow deflector 3. (See fig. 3(c).) The purpose of this modification was to reduce stalled airflow just aft of the center section of the flow deflector. Figures 27 and 28 indicate that there were no significant reductions of the stalled or separated flow region aft of the flow deflector in the wake. However, figure 27(d) is of special interest in that it shows the tip vortex core generated by the flow deflector tip.

Flow deflector 4 (fig. 3(d)) had a constant chord of 25.4 cm (10 in.) and a span of 76.2 cm (30 in.) which was cut into three equal span sections. These sections were joined together so that the outboard sections canted downward 15° to cause the tip vortices shed from the tips of the flow deflector to flow past the exhaust system nearer the level of the exhaust exit. Figures 29 and 30 show no significant advantage of this configuration. In fact, figure 29(b) indicates that there is a slight impingement; this impingement indicates that the placement of the tip vortex might be too low. The stalled or separated flow in the wake region aft of the center section still exists as shown in figure 29(c).

SUMMARY OF RESULTS

A wind-tunnel investigation of the engine-exhaust—windstream flow interaction on a gunship helicopter model exhaust system gave the following results:

1. Exhaust flow impinges on the gunship helicopter exhaust system exterior without any of the deflector devices installed at cruising flight speeds (effective ratio of free-stream velocity to exit velocity from 0.7 to 1.0).

2. Exhaust-flow impingement on the exhaust shield can be eliminated by installing a flow deflector which causes the free-stream flow to be deflected upward in the region just upstream of the exhaust, whereas vortices formed near the tips of the flow deflector provide additional upward deflection of the free-stream flow at the outboard regions of the exhaust exit.

3. Variations of angle of attack and angle of sideslip do not diminish the effectiveness of the flow deflectors.

4. All configurations investigated, with the exception of the standard spoiler, reduced flow impingement to some degree; however, flow deflectors 1, 2, and 3 were better than flow deflector 4.

Langley Research Center,
National Aeronautics and Space Administration,
Hampton, Va., November 12, 1974.

REFERENCES

1. Shaw, Craig S.; and Wilson, John C.: Wind-Tunnel Investigation of Simulated Helicopter Engine Exhaust Interacting With Windstream. NASA TM X-3016, 1974.

2. Wilson, John C.: Flight Investigation of Temperature Reduction Modifications to the OH-58A Infrared Suppressor Exhaust Kits. NASA TM X-3081, 1974.

3. Schlichting, Hermann (J. Kestin, transl.): Boundary-Layer Theory. Sixth ed., McGraw-Hill Book Co., Inc., 1968.

4. Ramsey, J. W.; and Goldstein, R. J.: Interaction of a Heated Jet With a Deflecting Stream. Trans. ASME, Ser. C: J. Heat Transfer, vol. 93, no. 4, Nov. 1971, pp. 365-372.

5. Hale, R. W.; Tan, P.; Stowell, R. C.; and Ordway, D. E.: Development of Integrated System for Flow Visualization in Air Using Neutrally-Buoyant Bubbles. SAI-RR-7107 TR-2 (N00014-68-C-0434), Sage Action, Inc., Dec. 1971. (Available from DDC as AD 756 691.)

6. Williams, John; and Wood, Maurice N.: Aerodynamic Interference Effects With Jet-Lift V/STOL Aircraft Under Static and Forward-Speed Conditions. Tech. Rep. No. 66403, Brit. R.A.E., Dec. 1966.

7. Mechtly, E. A.: The International System of Units – Physical Constants and Conversion Factors (Second Revision). NASA SP-7012, 1973.

8. Clark, David R.; and Landgrebe, Anton J.: Wake and Boundary Layer Effects in Helicopter Rotor Aerodynamics. AIAA Paper No. 71-581, June 1971.

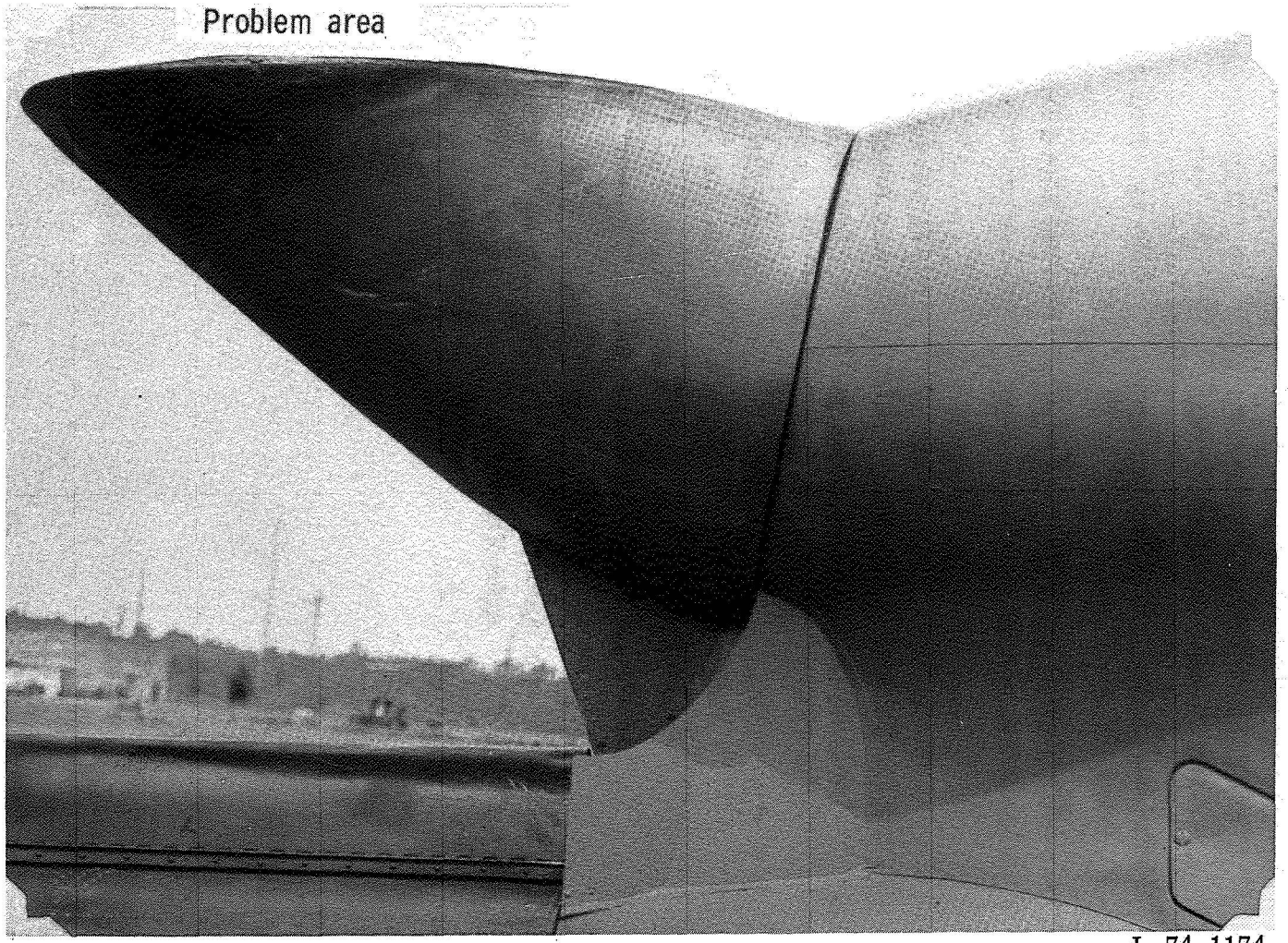

Figure 1.- Engine exhaust duct burned by exhaust gas.

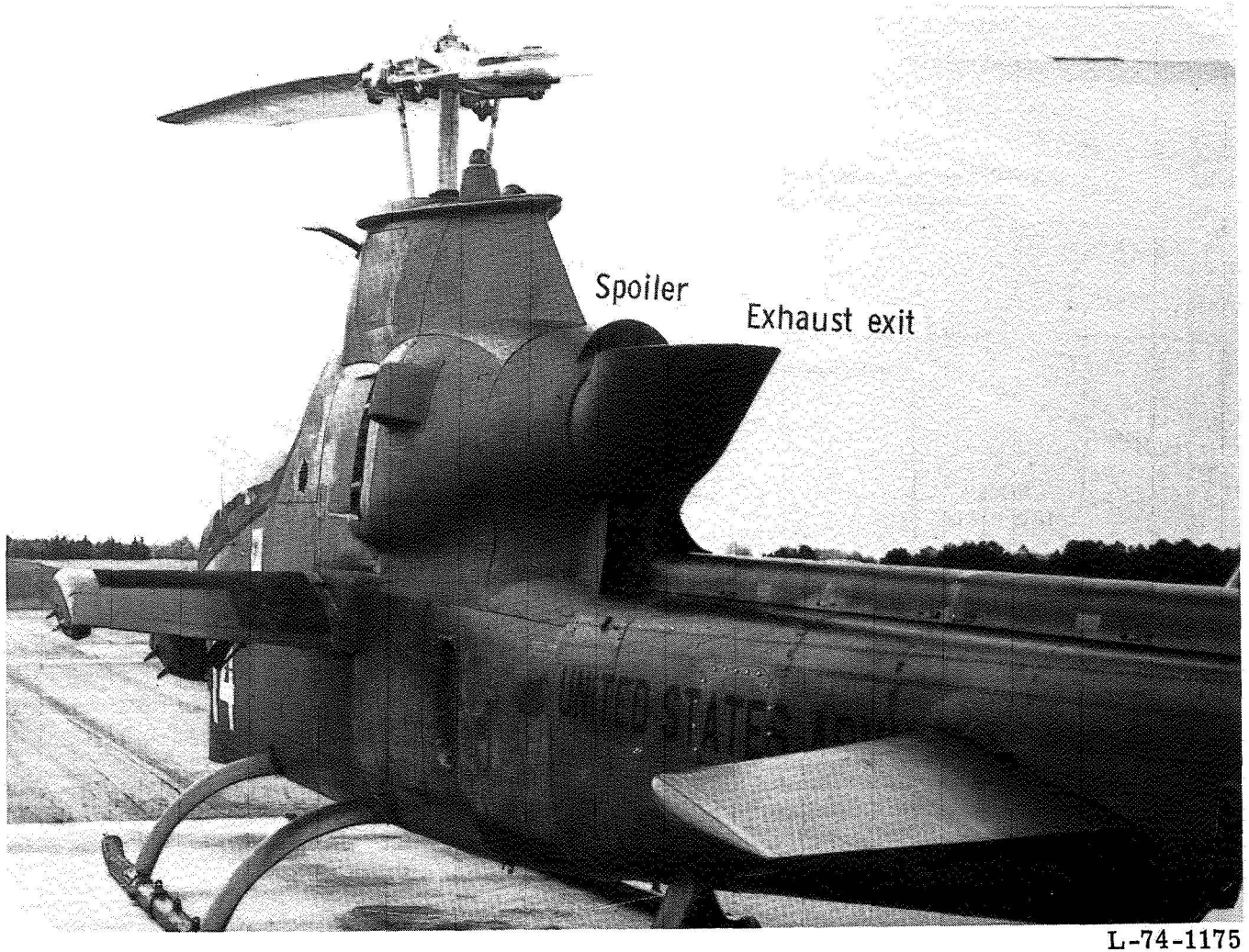

Figure 2.- Helicopter under study.

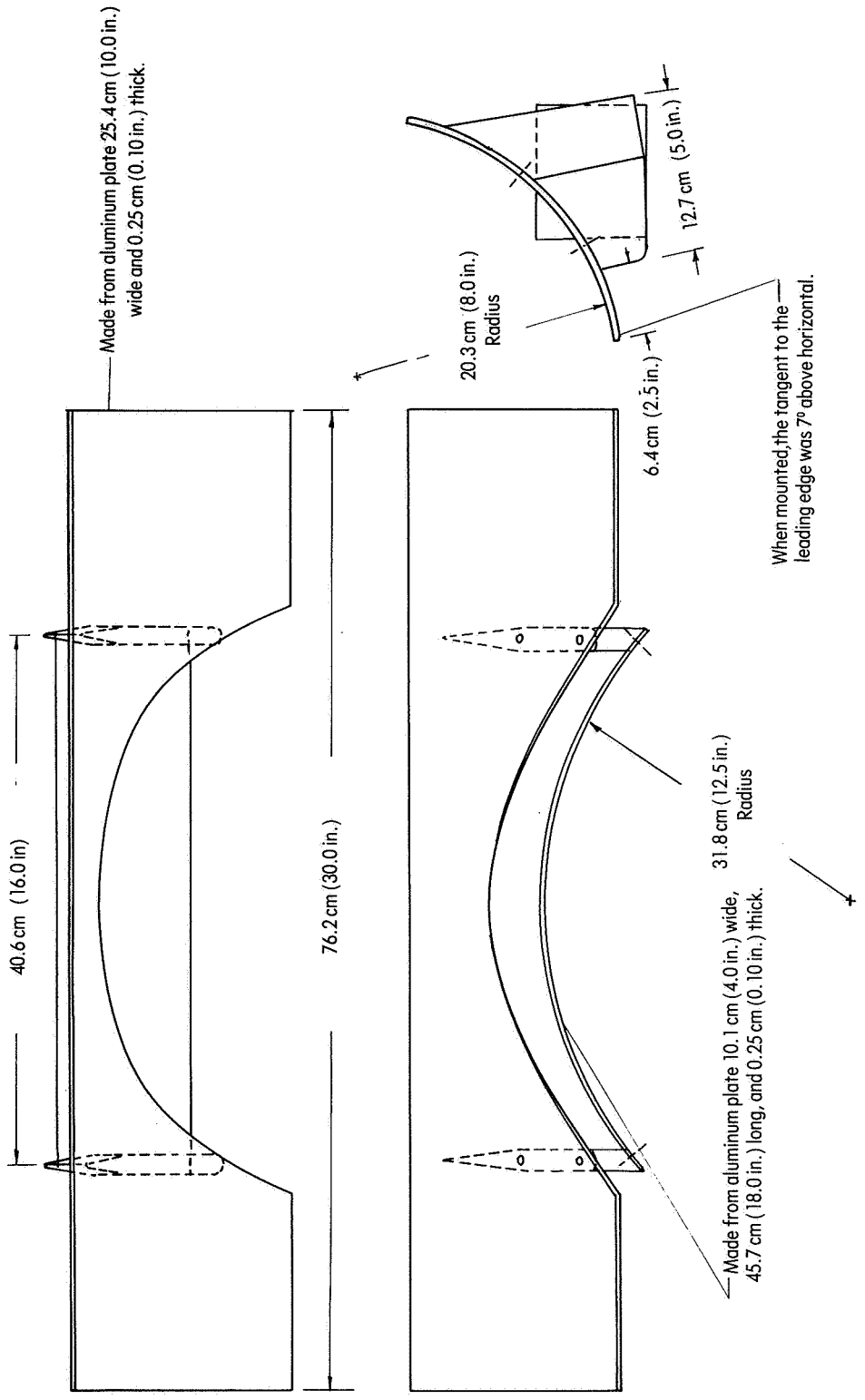

(a) Flow deflector 1.

Figure 3.- Modification components for the exhaust system under study.

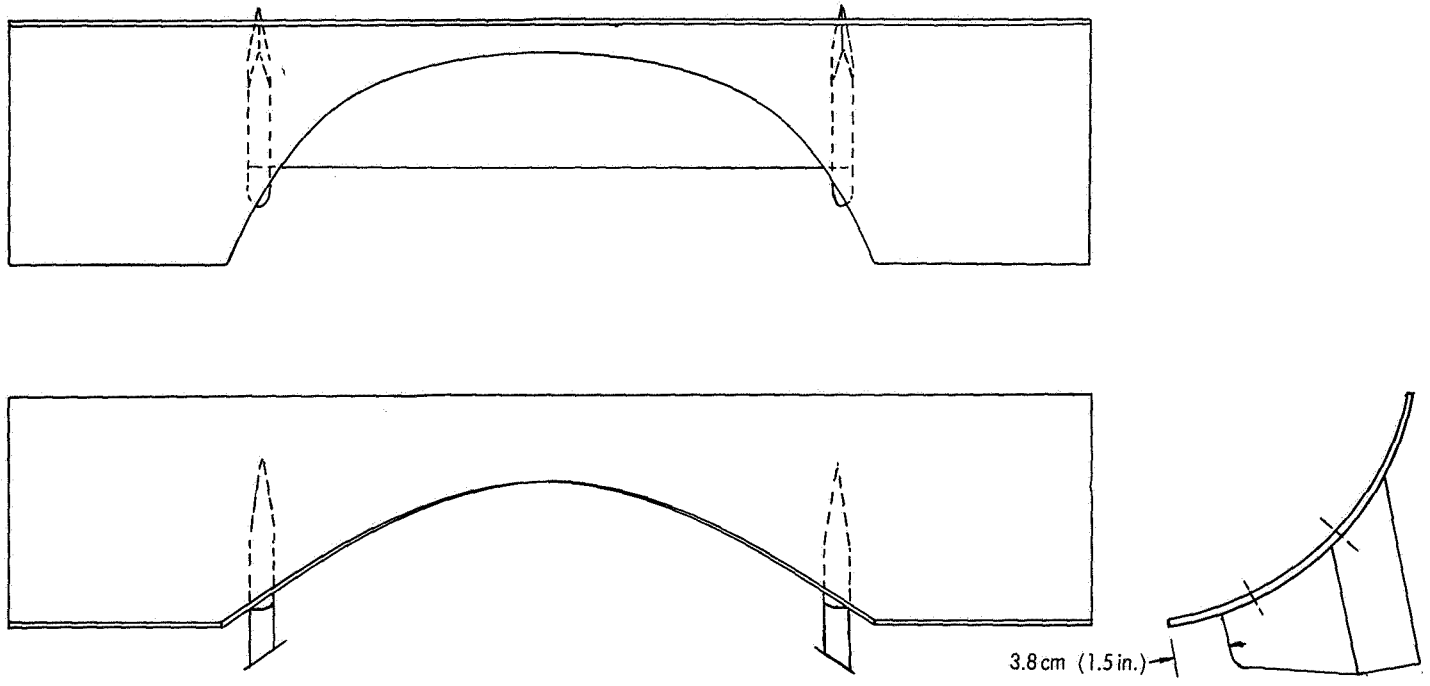

(b) Flow deflector 2.

Figure 3.- Continued.

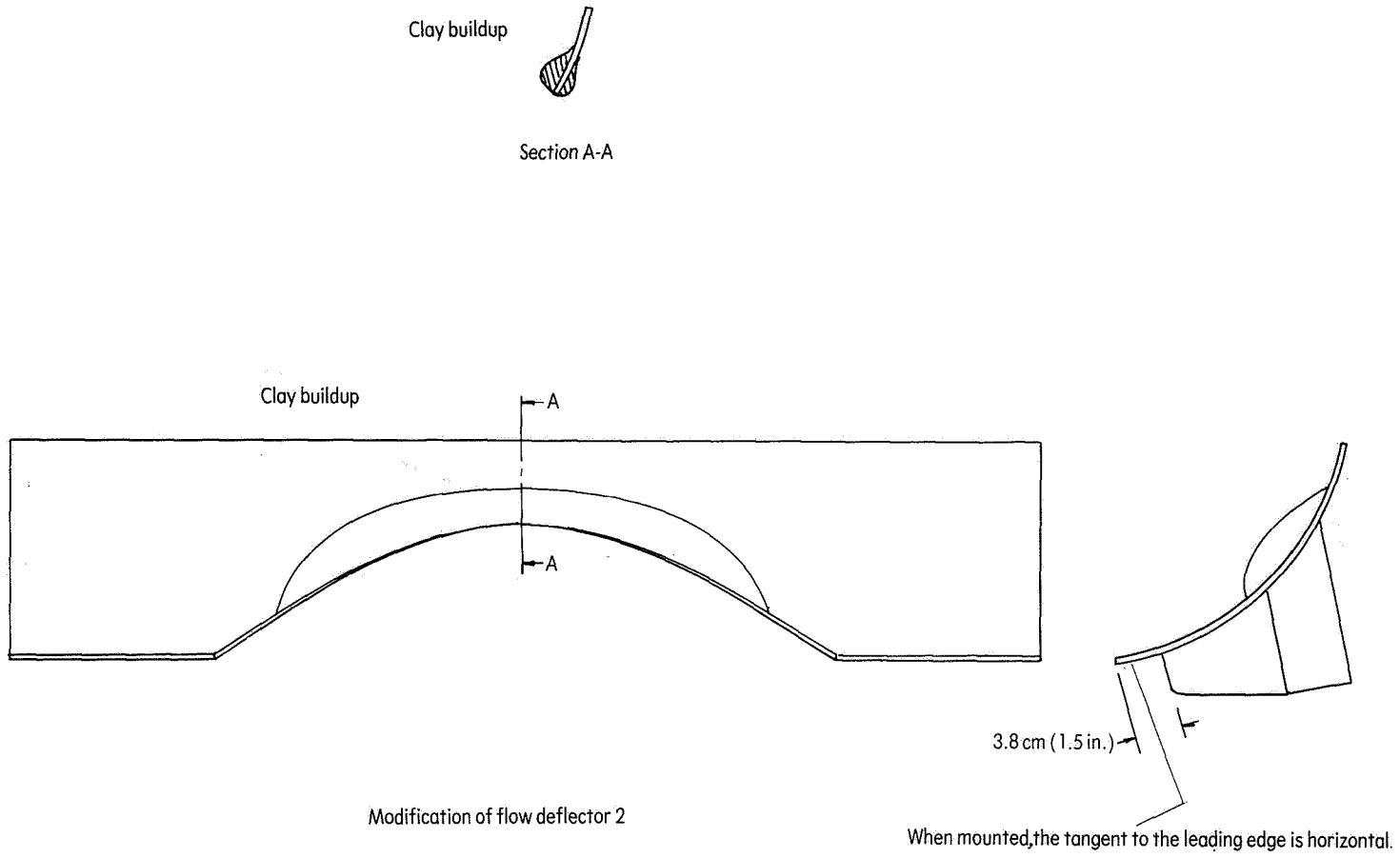

(c) Flow deflector 3.

Figure 3.- Continued.

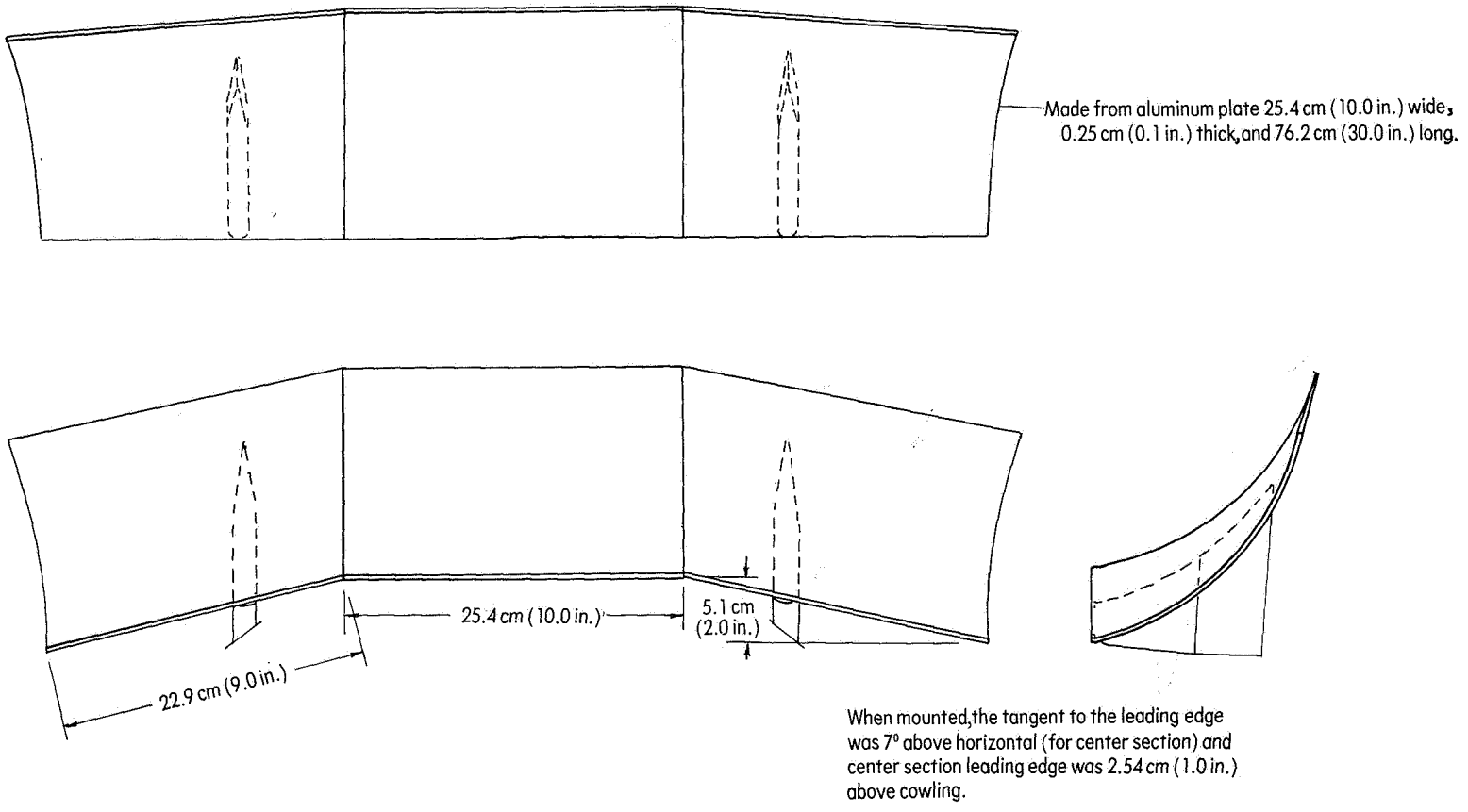

(d) Flow deflector 4.

Figure 3.- Continued.

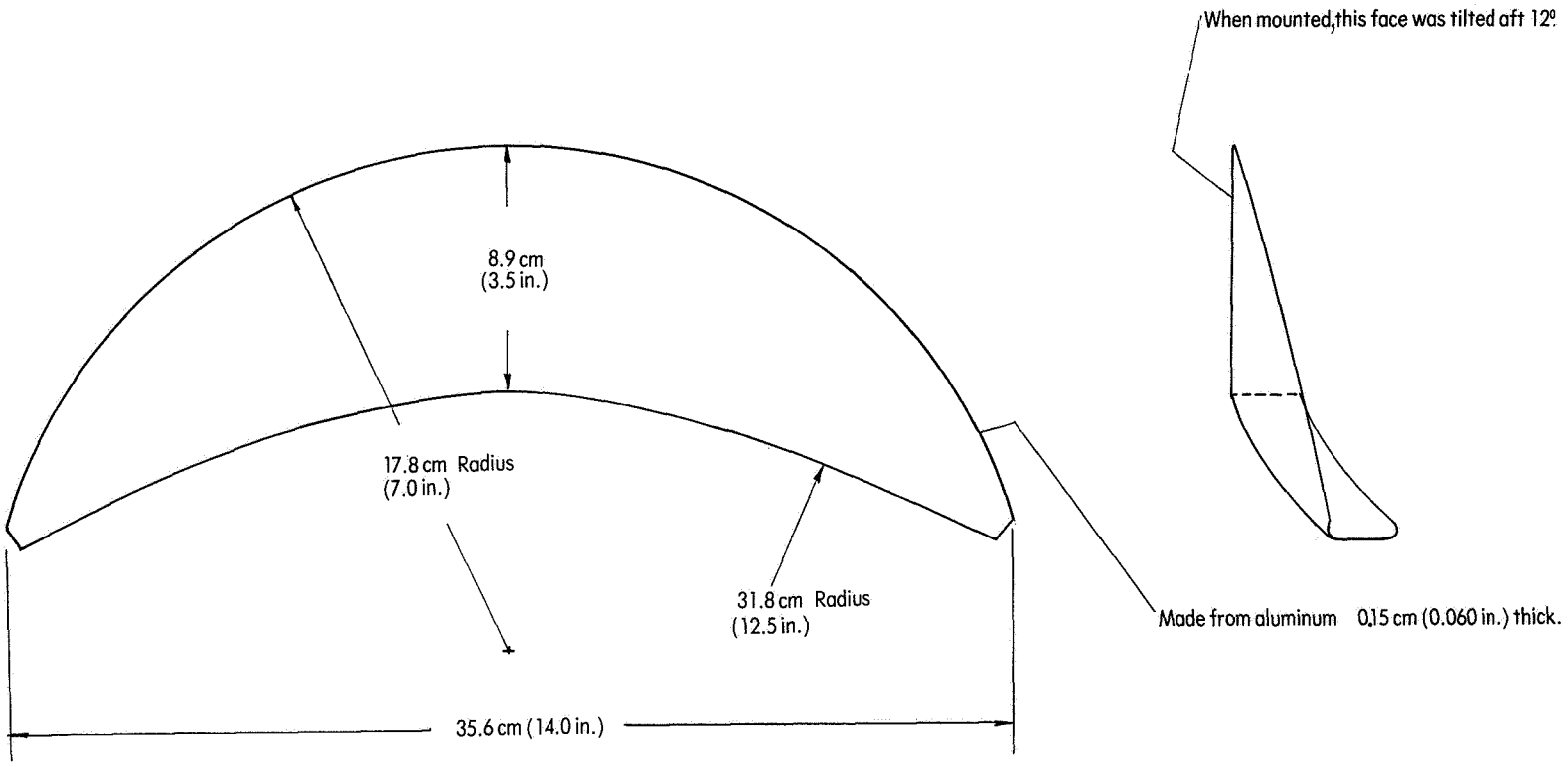

(e) Spoiler.

Figure 3.- Concluded.

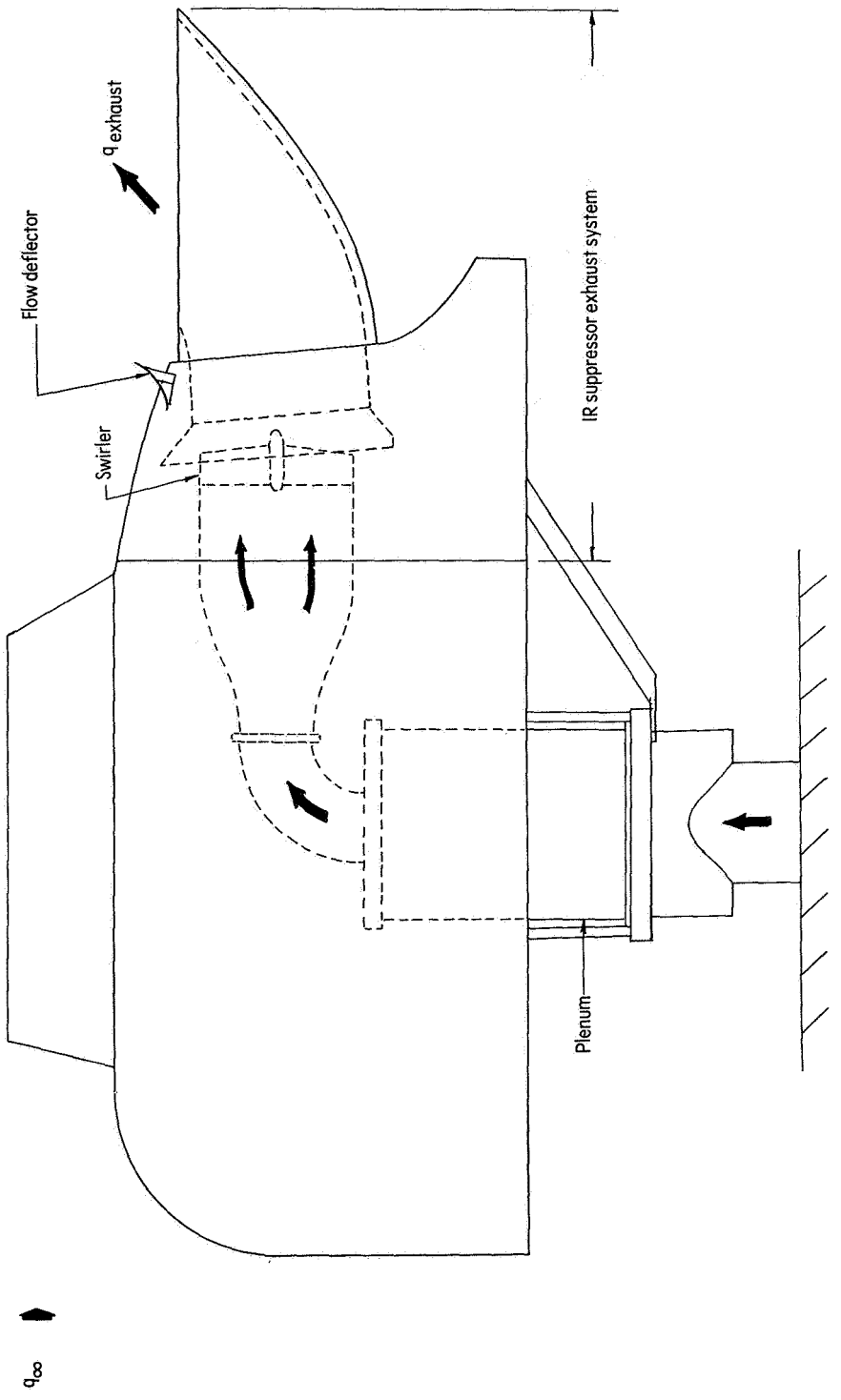

Figure 4.- Schematic of helicopter exhaust system tunnel installation.

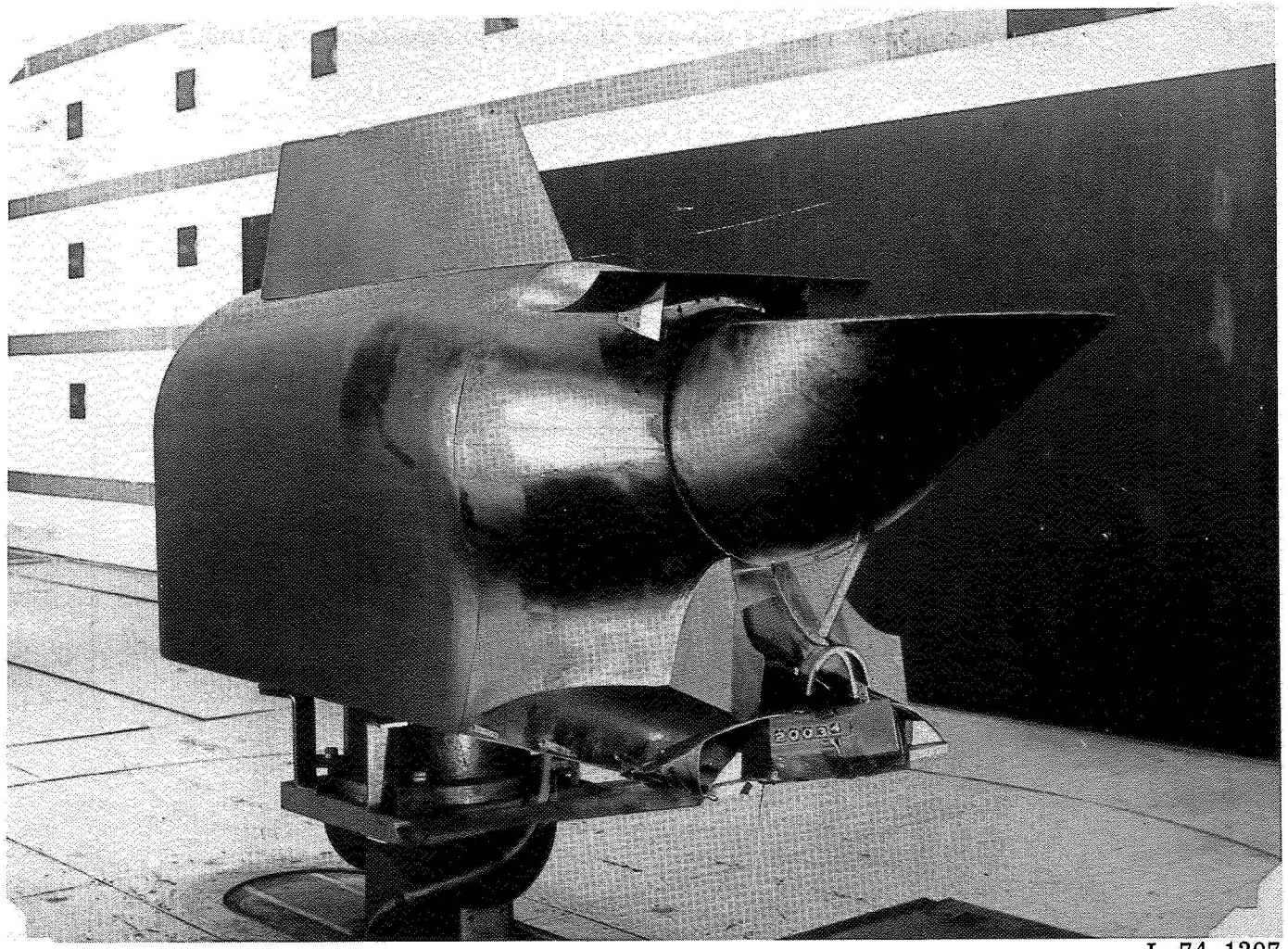

L-74-1297

Figure 5.- Installation of helicopter model exhaust system in the Langley V/STOL wind tunnel.

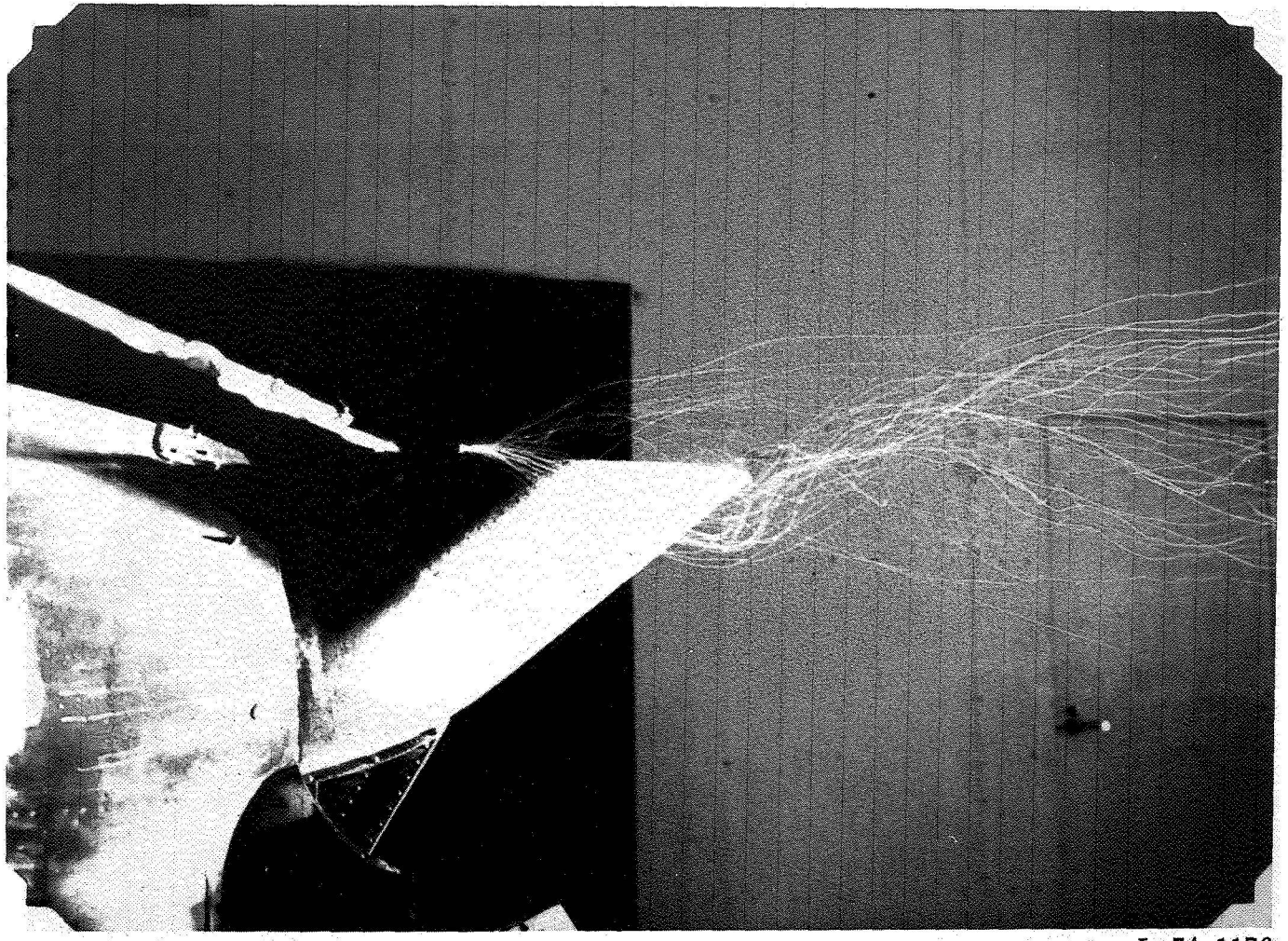

L-74-1176

(a) $\alpha = 0^{o}$; $V_{eff} = 0.7$.

Figure 6.- Identification of flow mechanism causing heating problem.

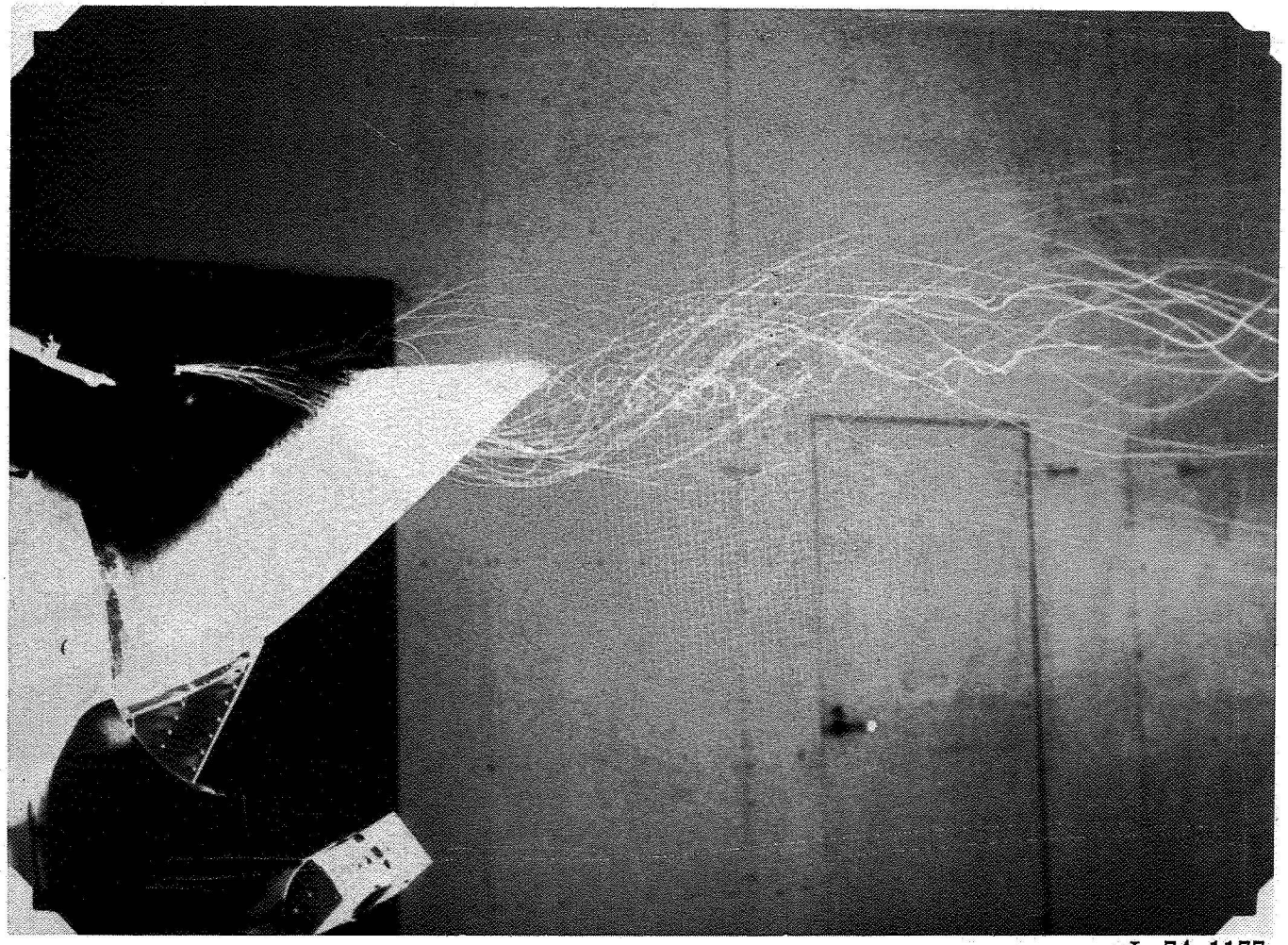

L-74-1177

(b) $\alpha = -5^{o}$; $V_{eff} = 0.7$.

Figure 6.- Continued.

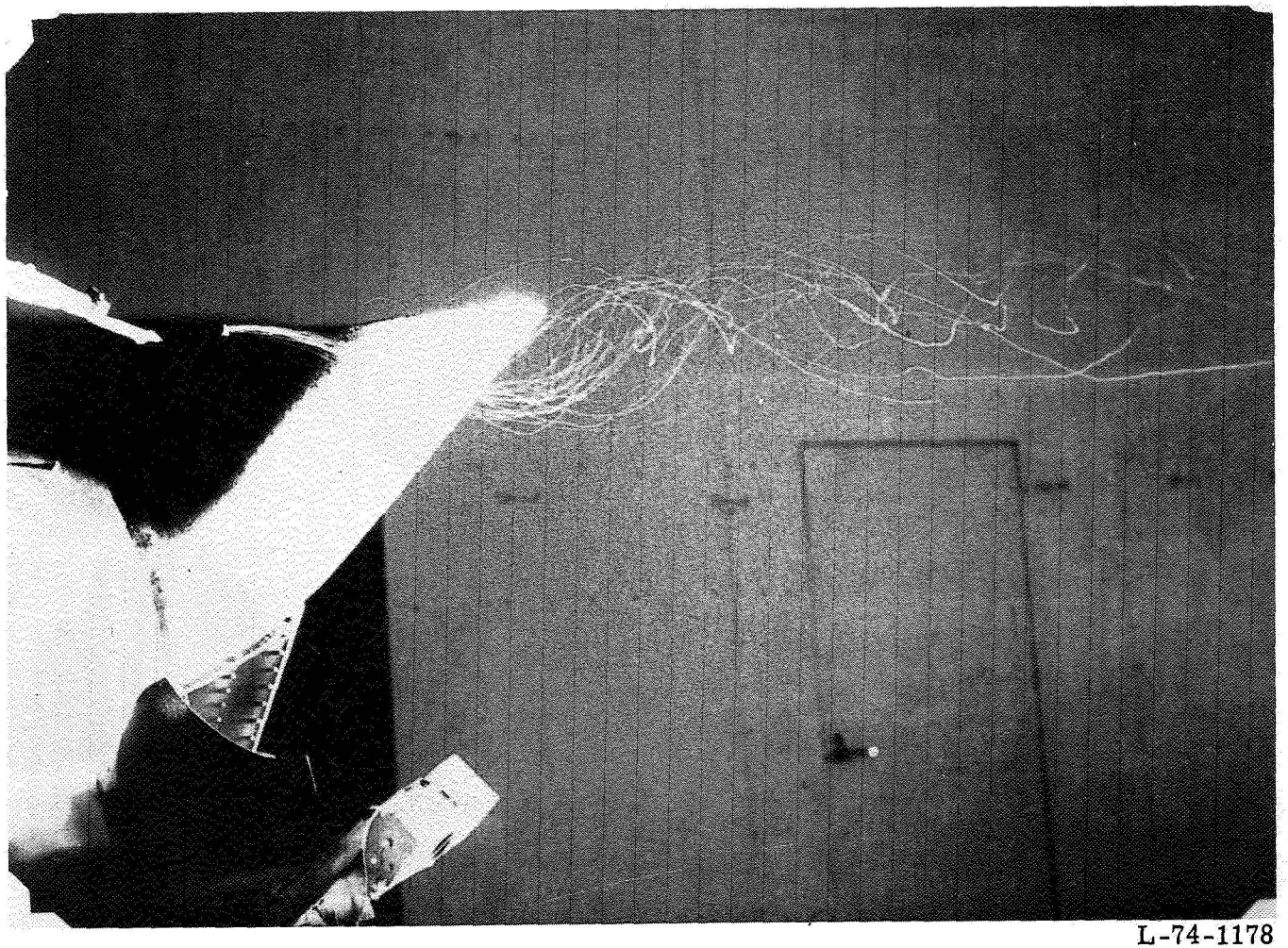

L-74-1178

(c) $\alpha = -10^{o}$; $V_{eff} = 0.7$.

Figure 6.- Concluded.

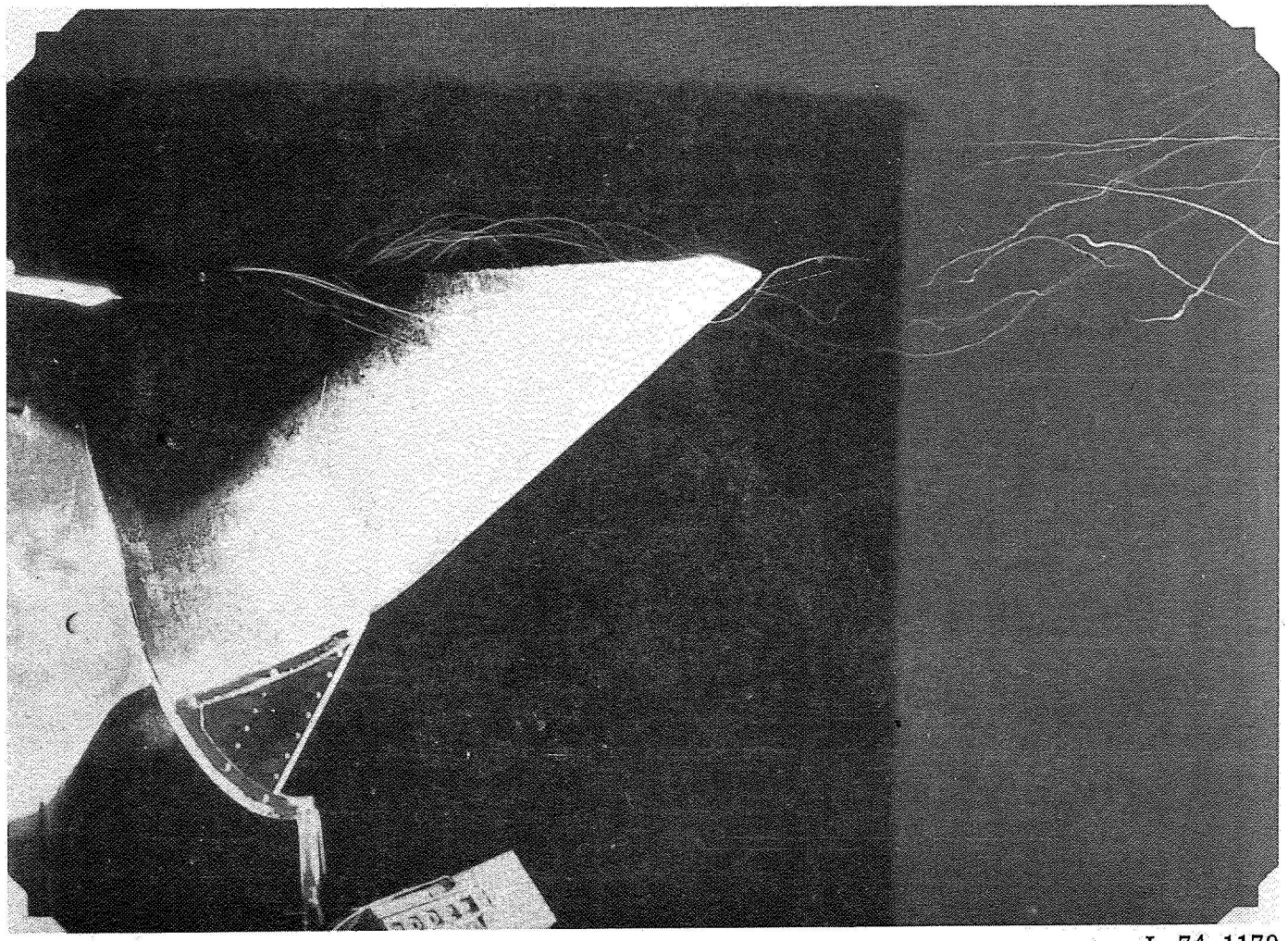

L-74-1179

(a) Side view.

Figure 7.- Side and top views, photographed simultaneously, of flow mechanism causing heating problem. $\alpha = 0^{o}$; $V_{eff} = 0.7$.

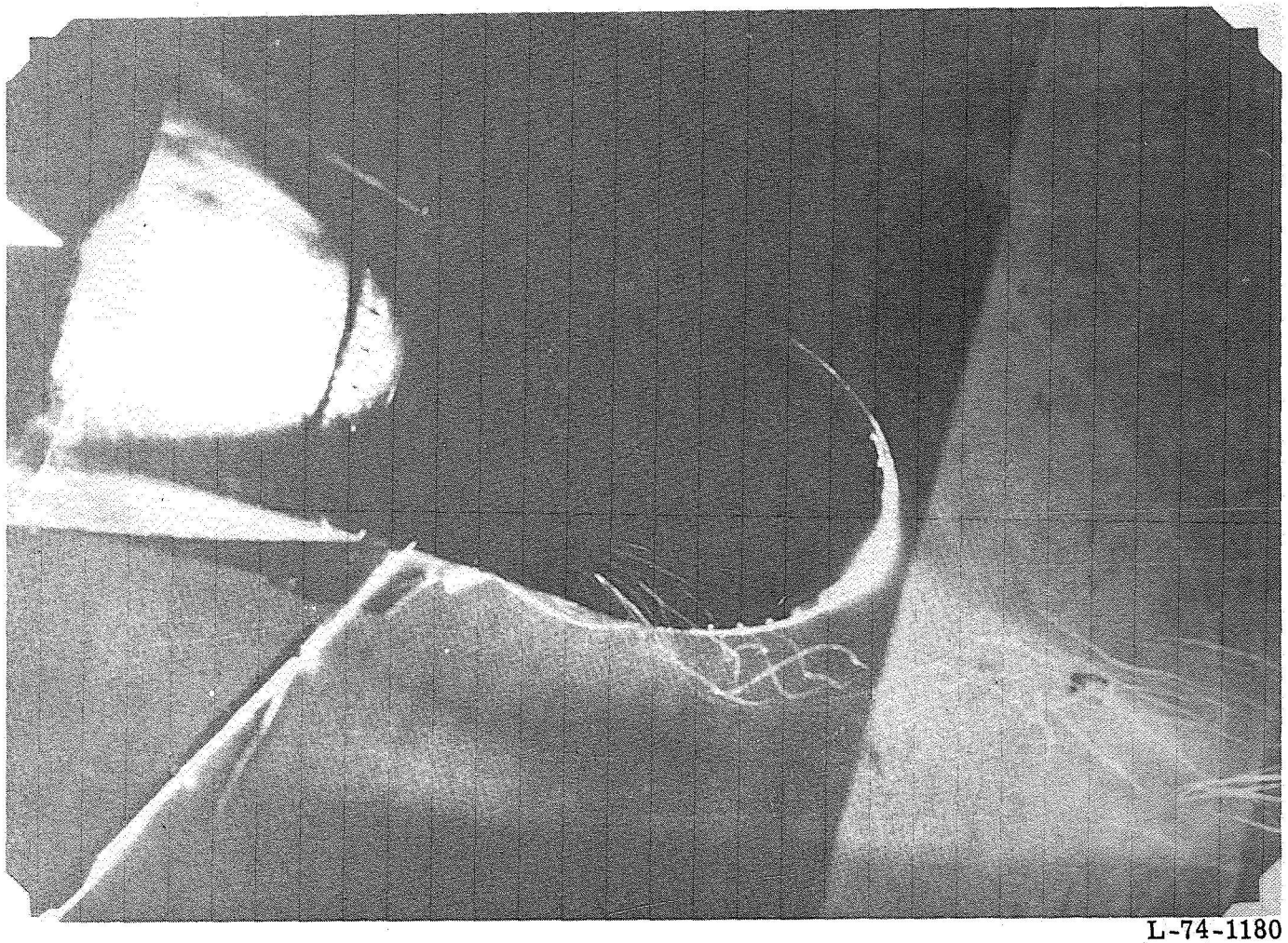

L-74-1180

(b) Top view.

Figure 7.- Concluded.

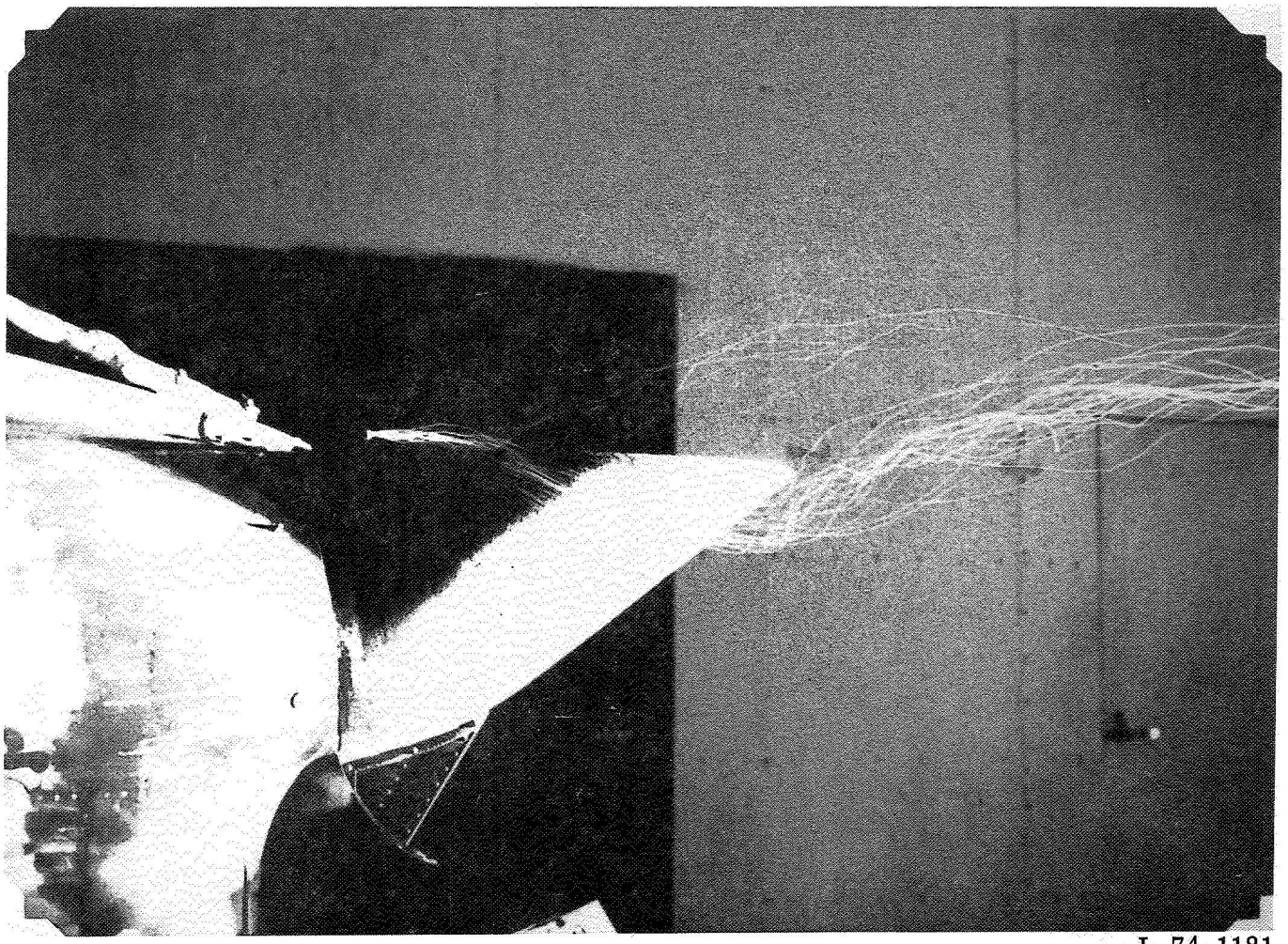

L-74-1181

Figure 8.- Effect of swirler on exhaust flow of exhaust system without modifications at $V_{eff} = 0.7$.

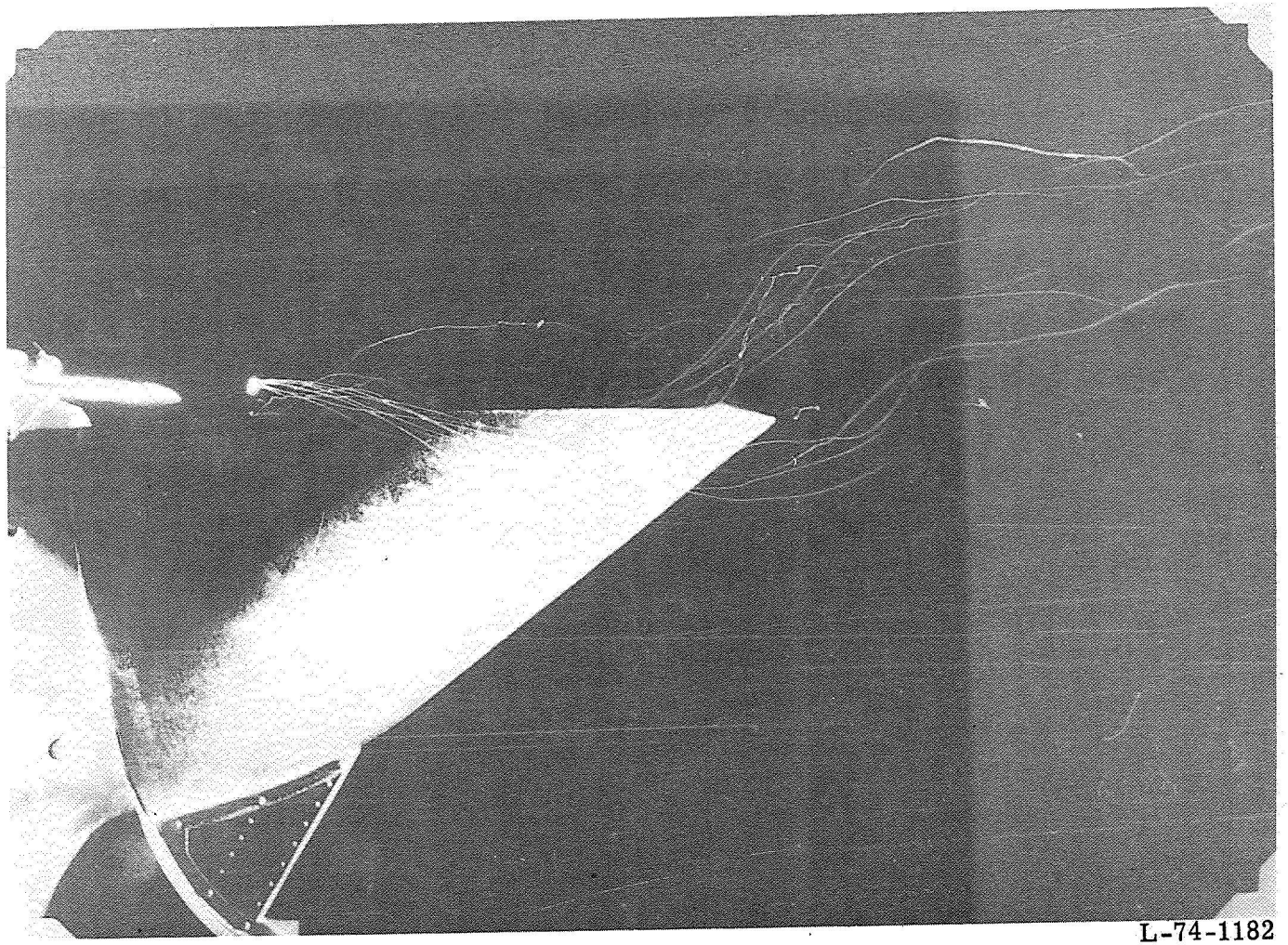

(a) Side view.

Figure 9.- Side and top views, photographed simultaneously, indicating the effect of the swirler on the flow of the exhaust system without flow deflector devices at $V_{eff} = 0.7$.

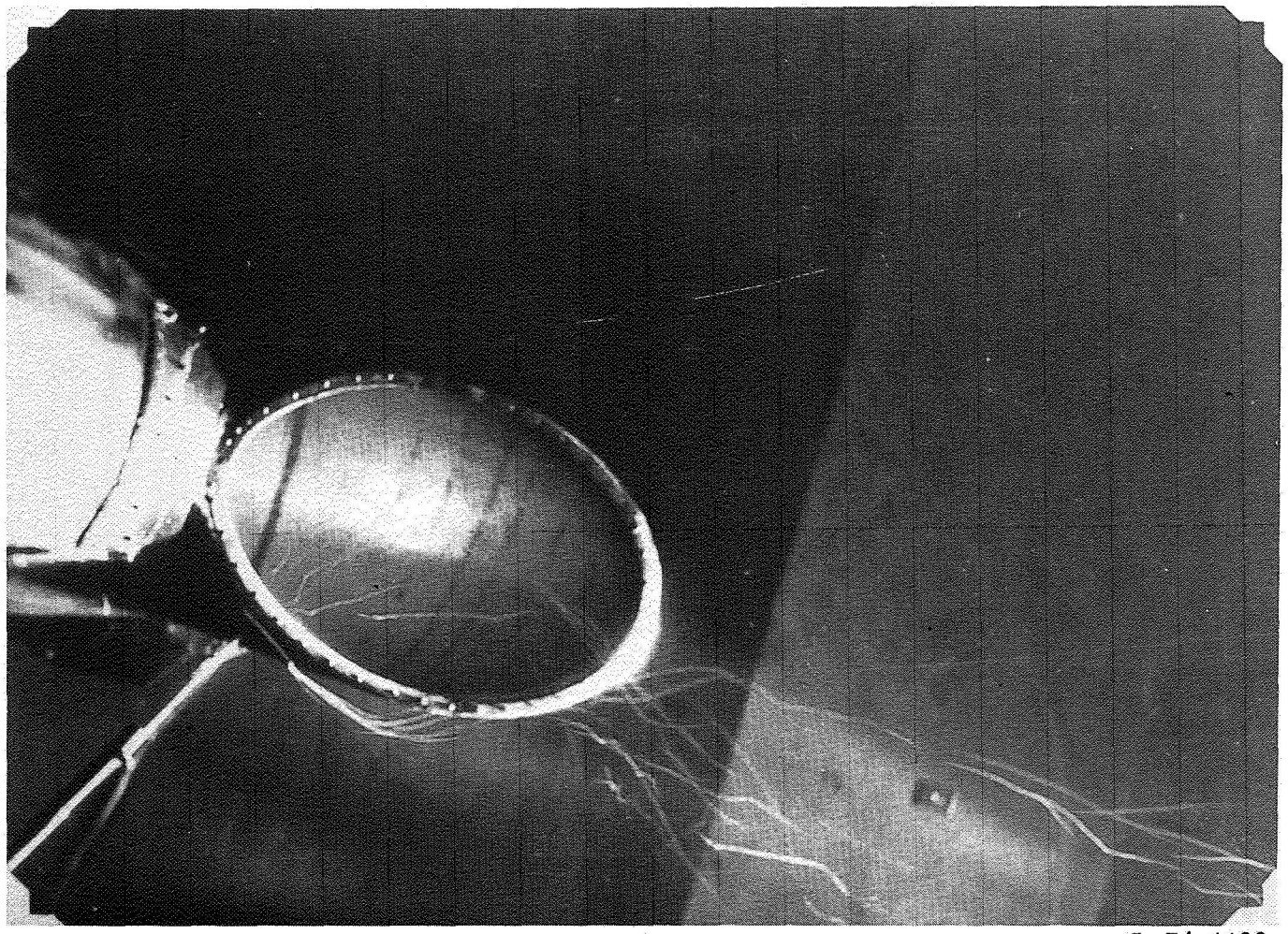

L-74-1183

(b) Top view.

Figure 9.- Concluded.

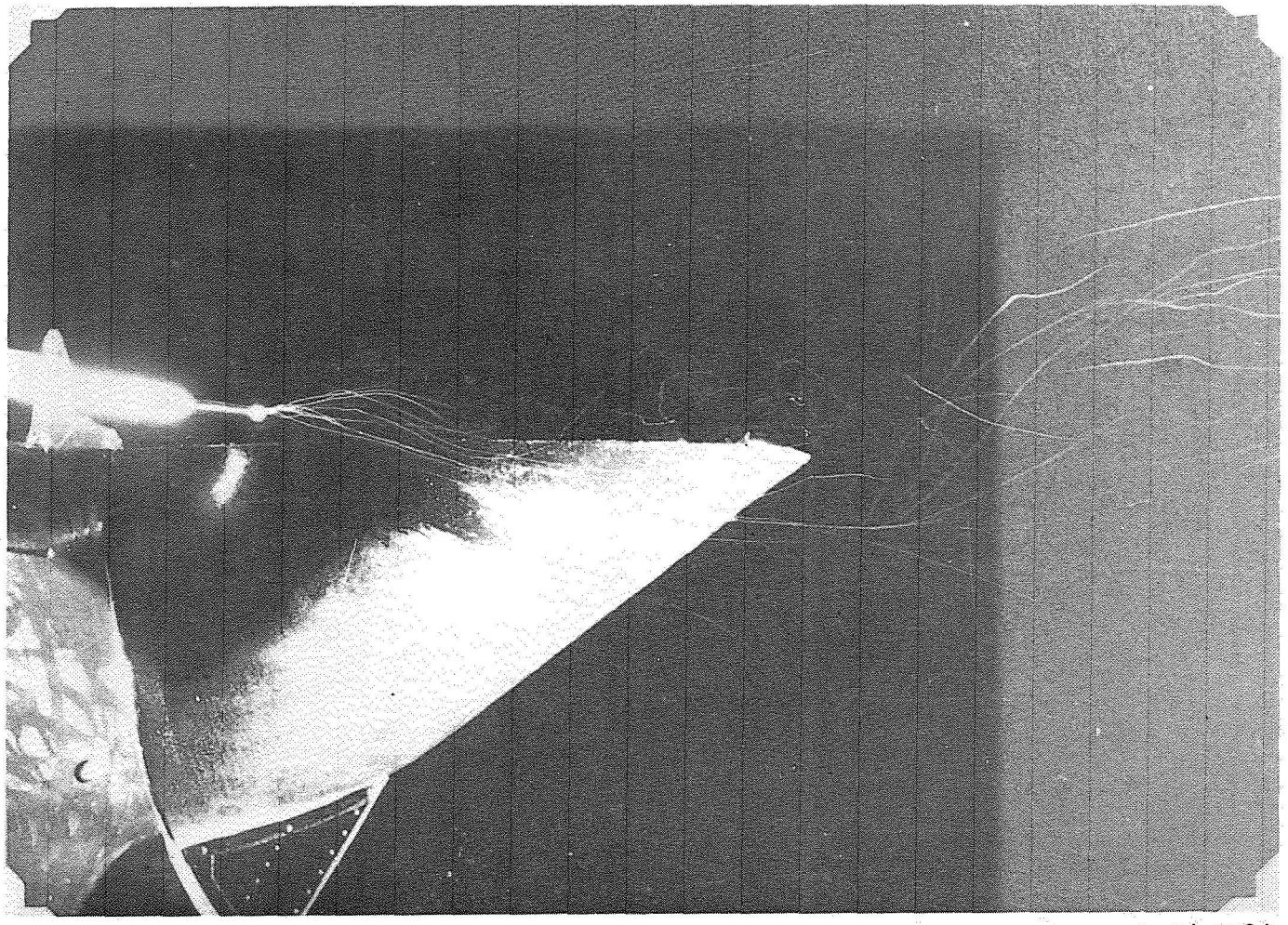

L-74-1184

(a) Side view.

Figure 10.- Effects of spoiler and swirler on exhaust flow at $V_{eff} = 0.7$.

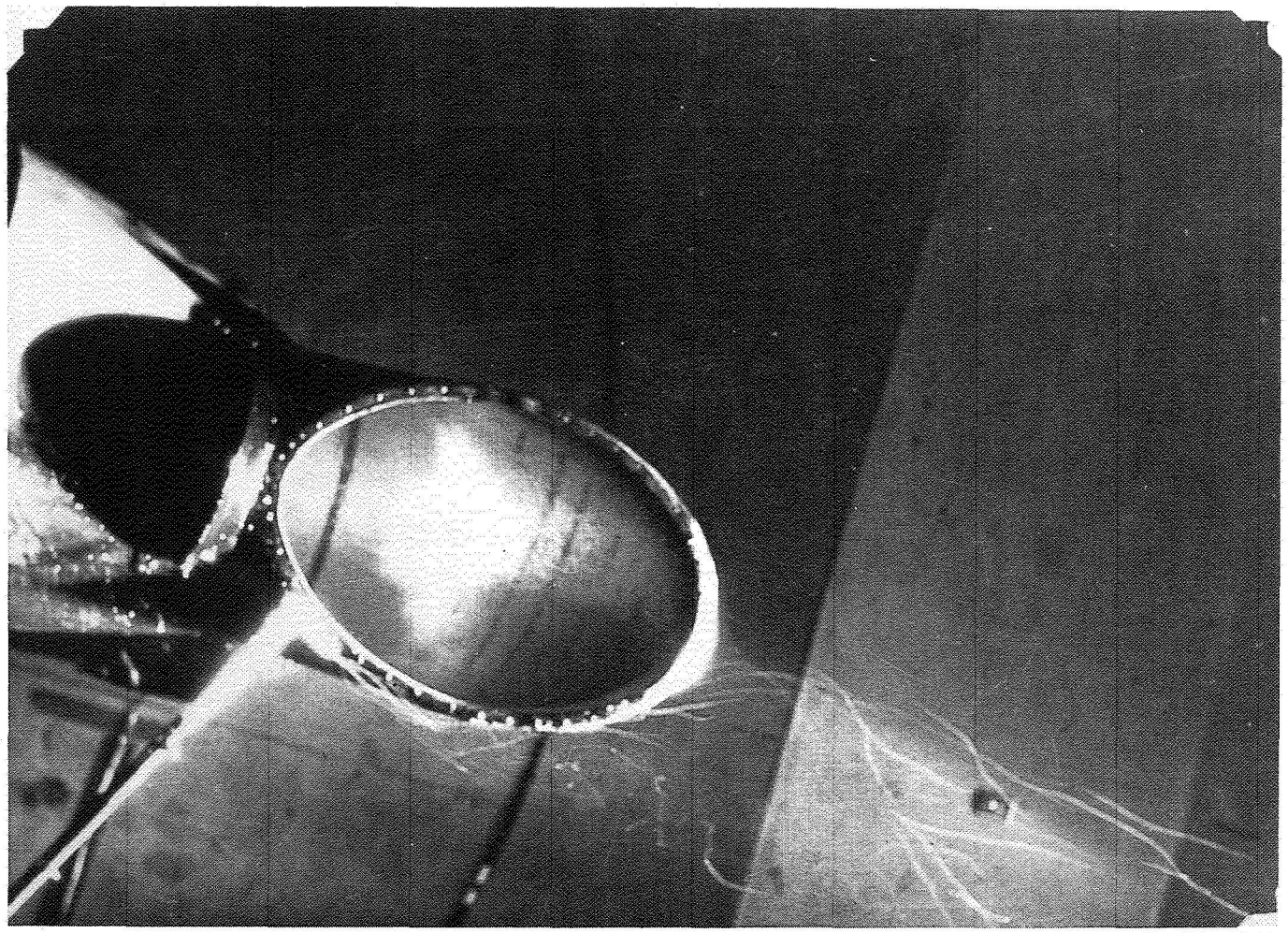

L-74-1185

(b) Top view.

Figure 10.- Concluded.

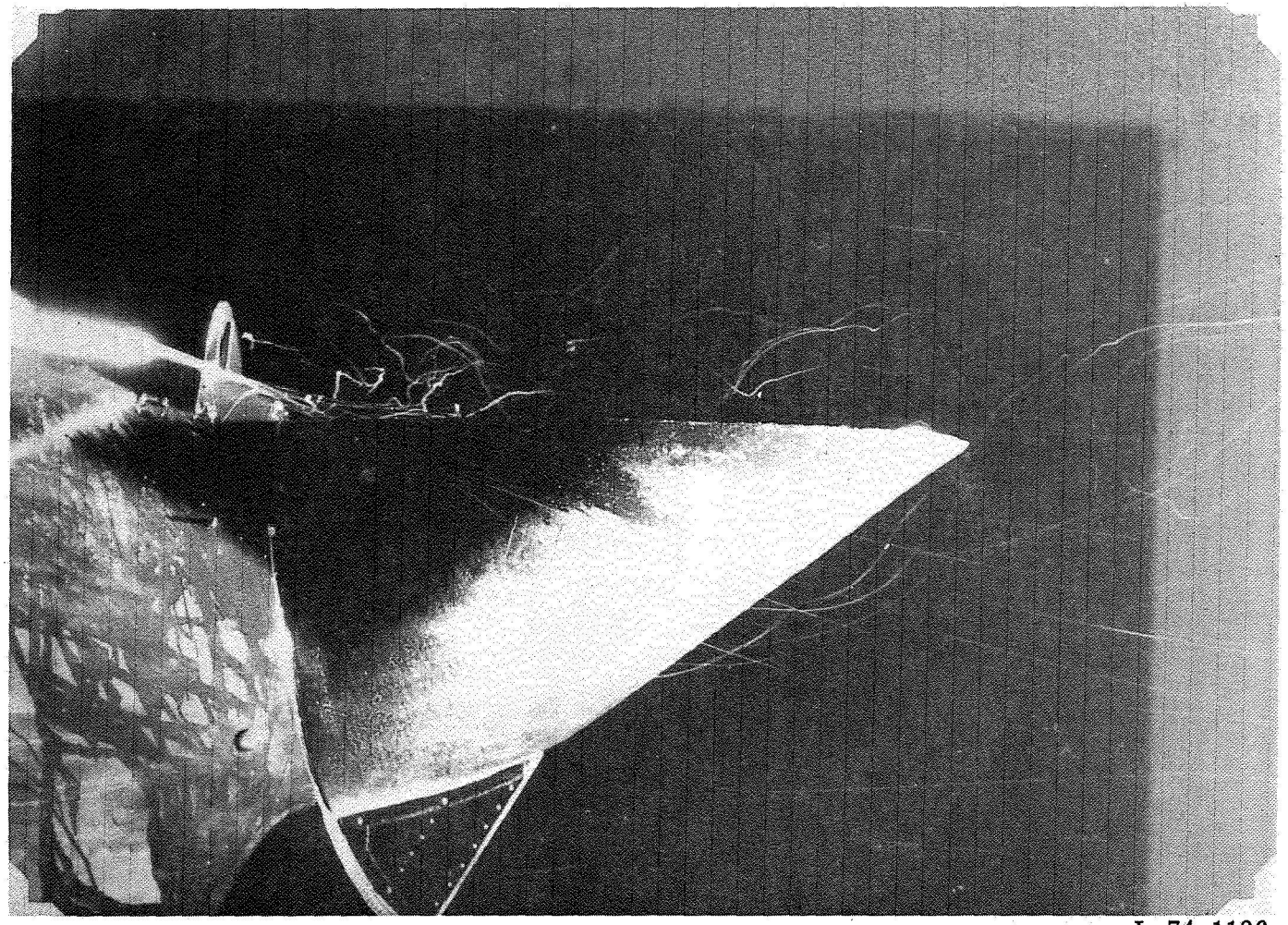

L-74-1186

(a) Side view.

Figure 11.- Effects of spoiler and swirler on exhaust flow at $V_{eff} = 0.9$.

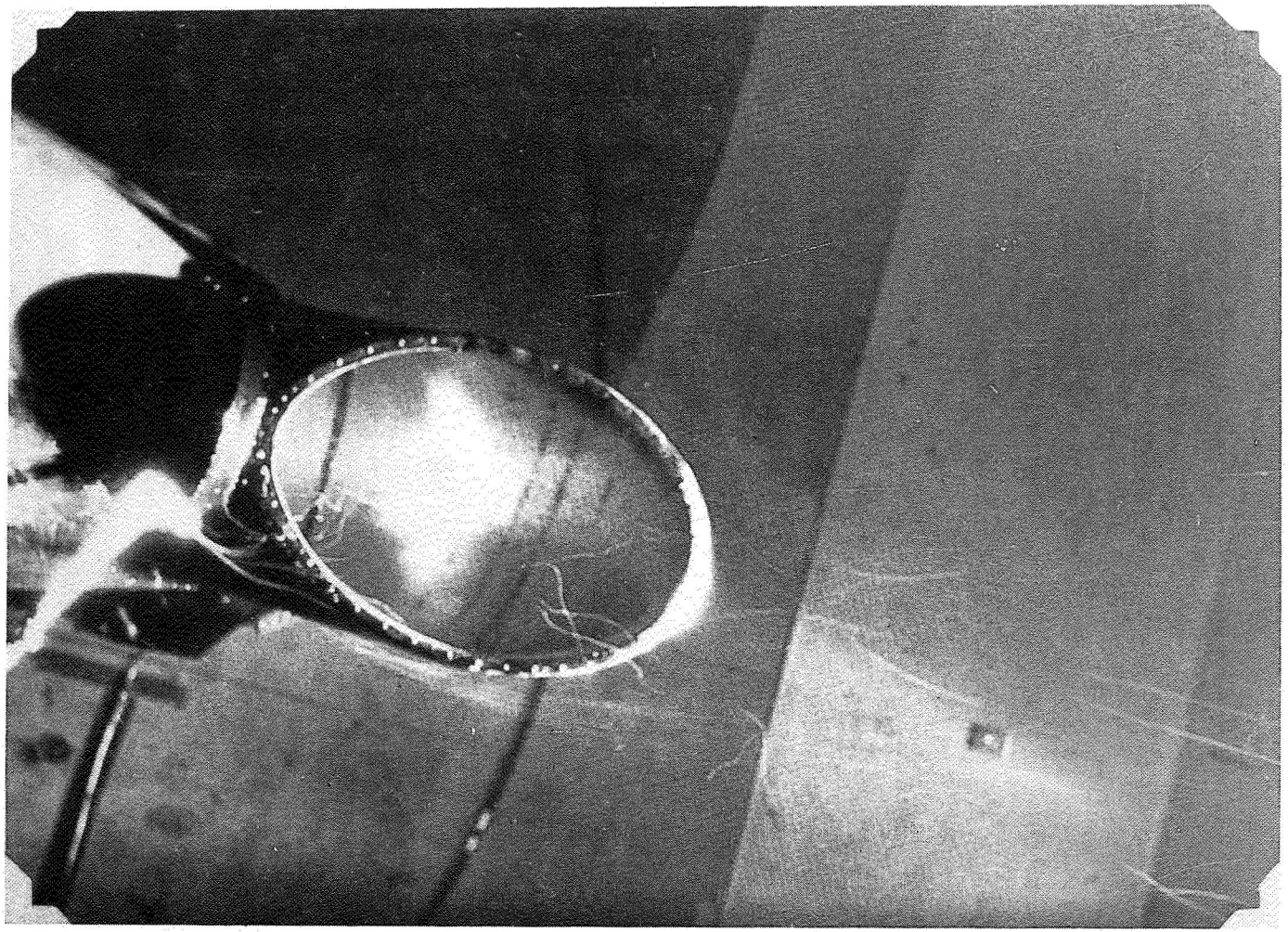

L-74-1187

(b) Top view.

Figure 11.- Concluded.

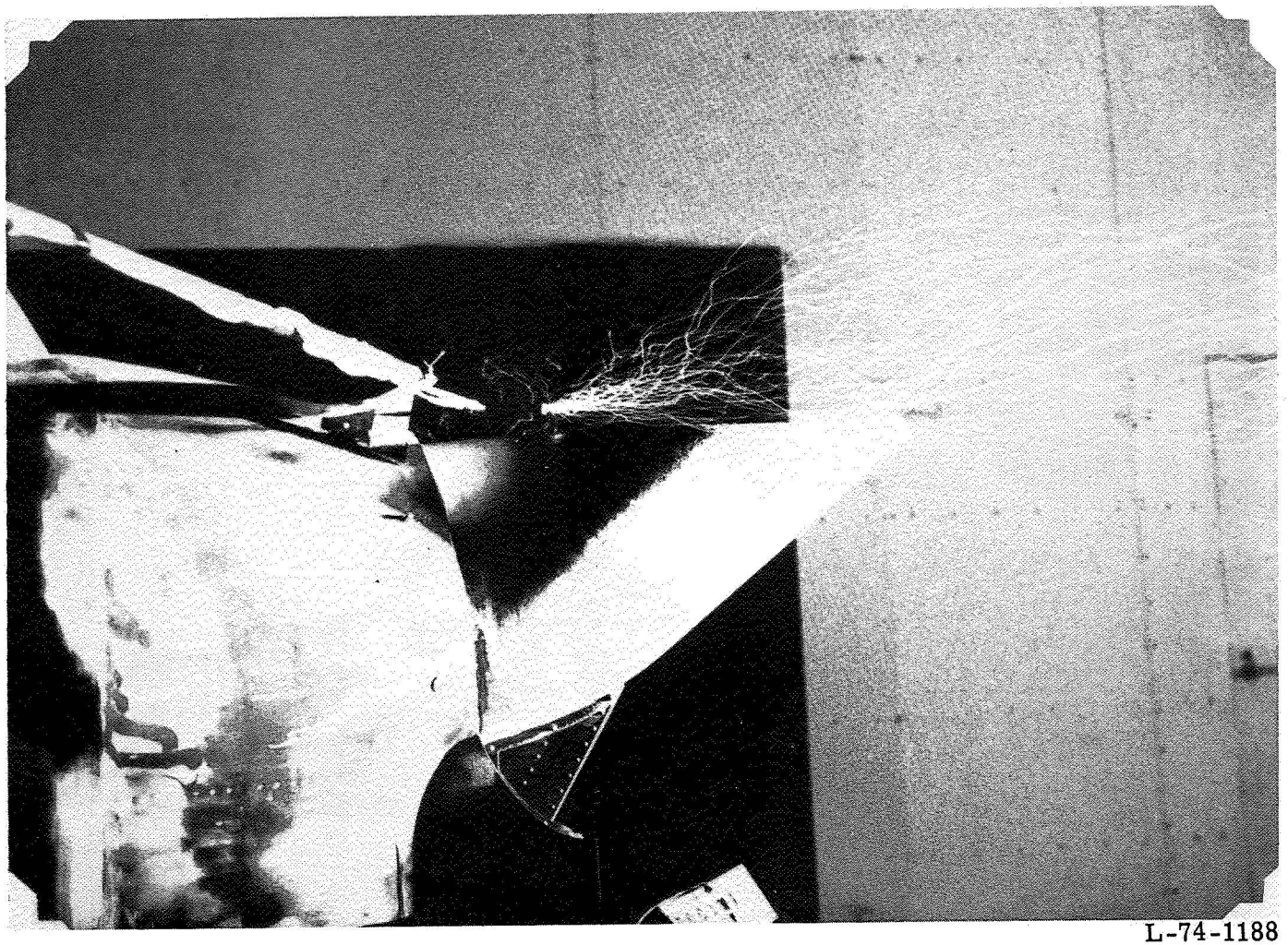

(a) $V_{eff} = 0.7$.

Figure 12.- Effects of flow deflector 1 and swirler on exhaust flow.

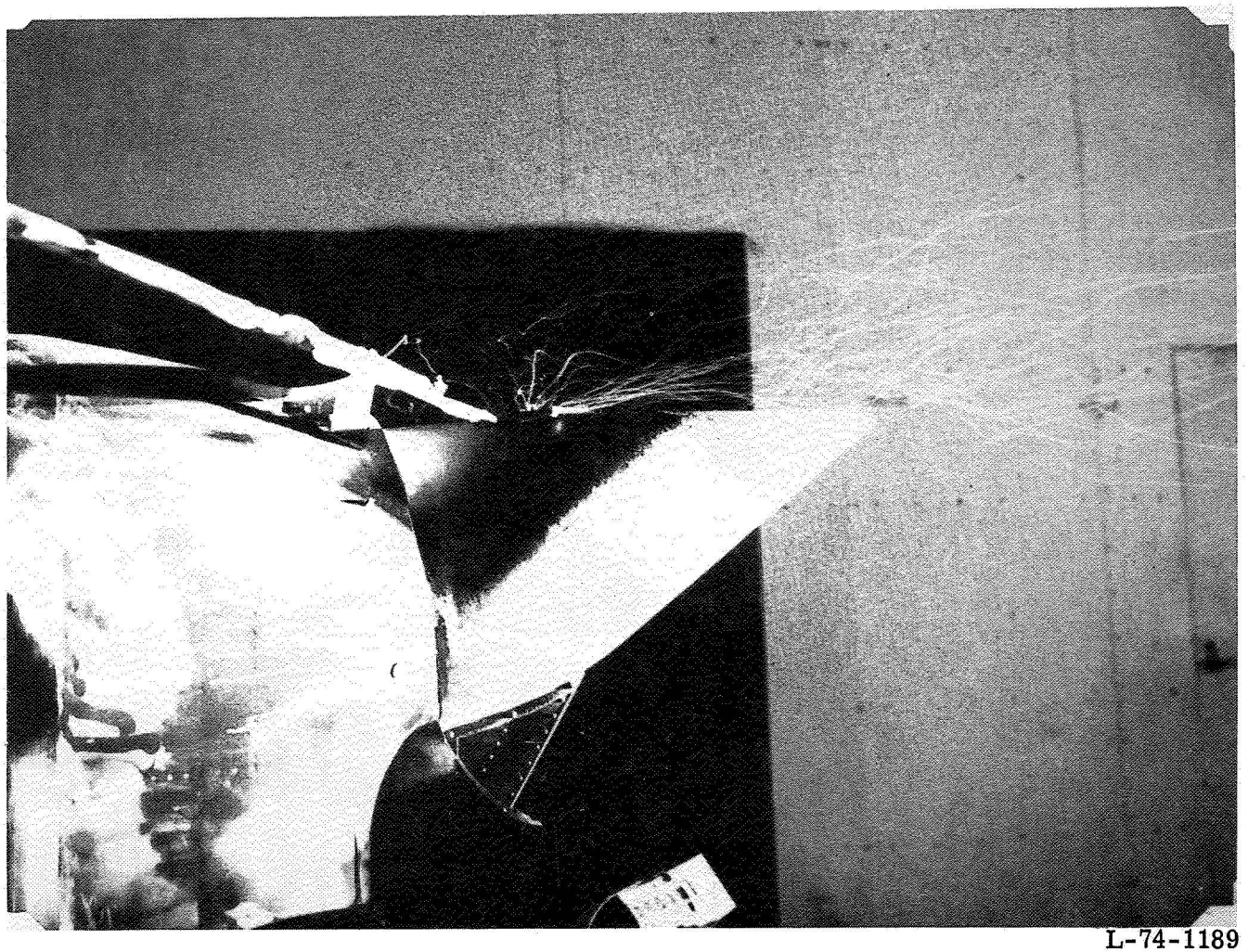

L-74-1189

(b) $V_{eff} = 1.0$.

Figure 12.- Concluded.

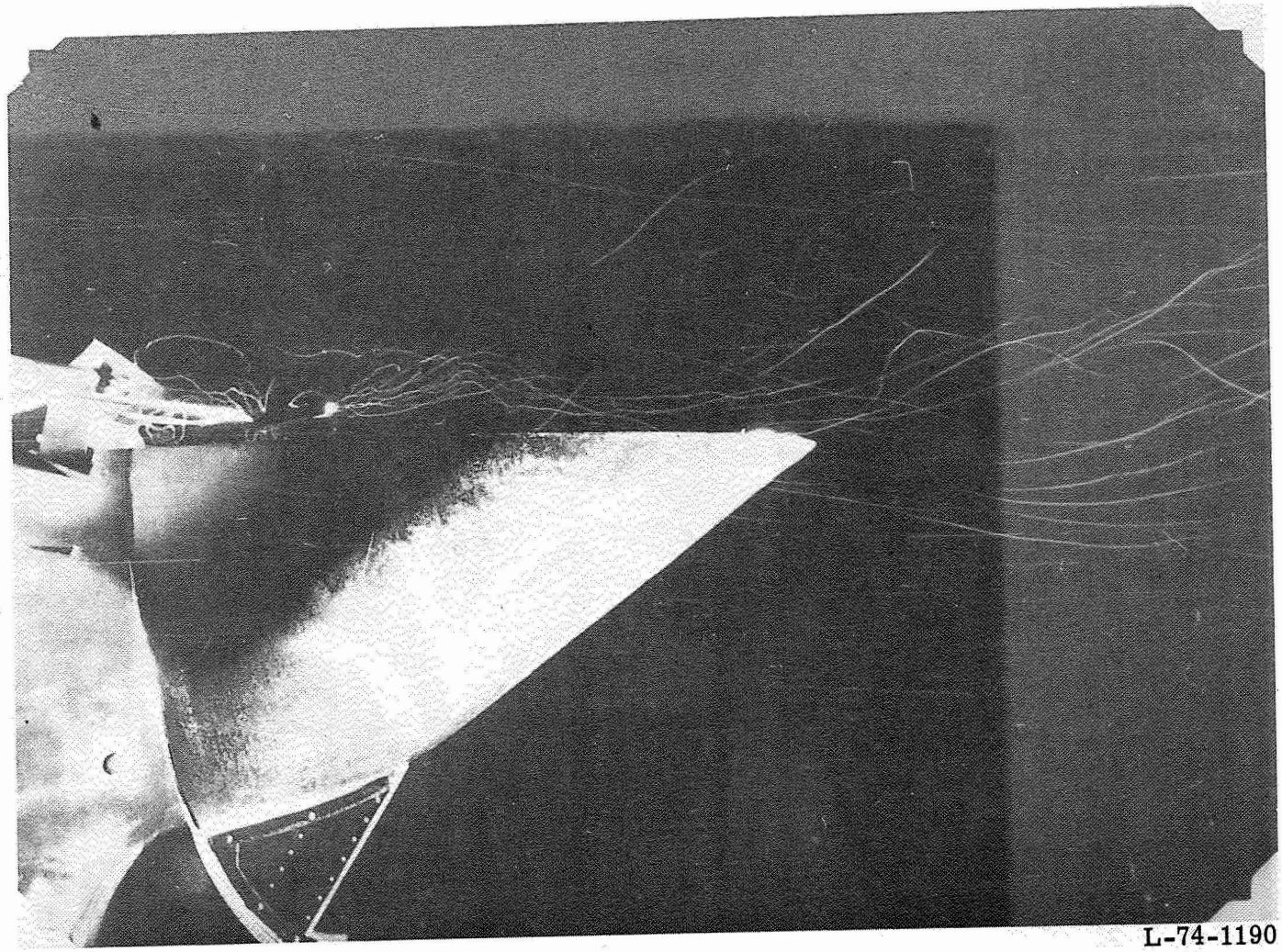

(a) Side view.

Figure 13.- Side and top views, photographed simultaneously, of effects of flow deflector 1 and swirler on exhaust flow at $V_{eff} = 0.7$.

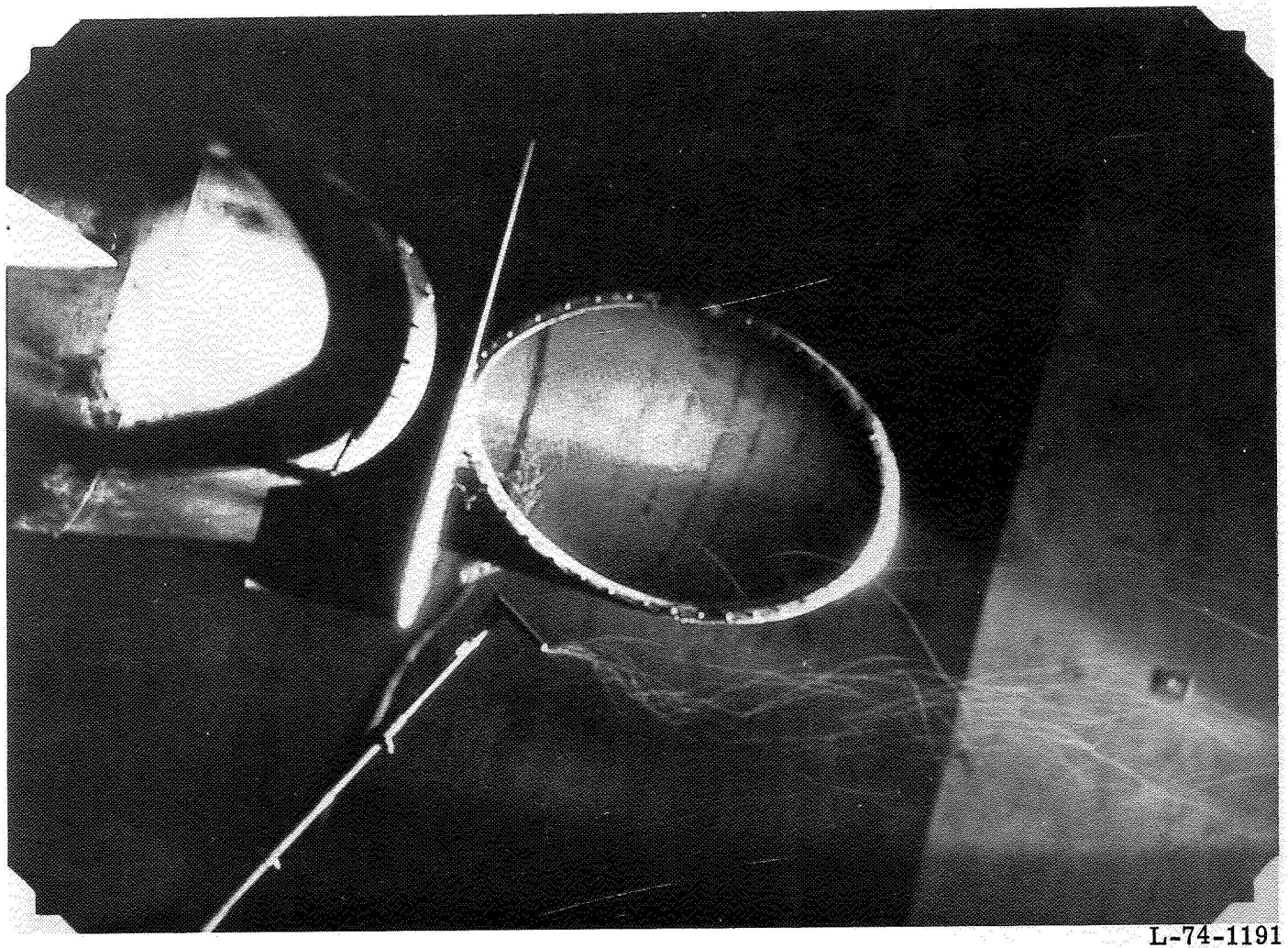

(b) Top view.

Figure 13.- Concluded.

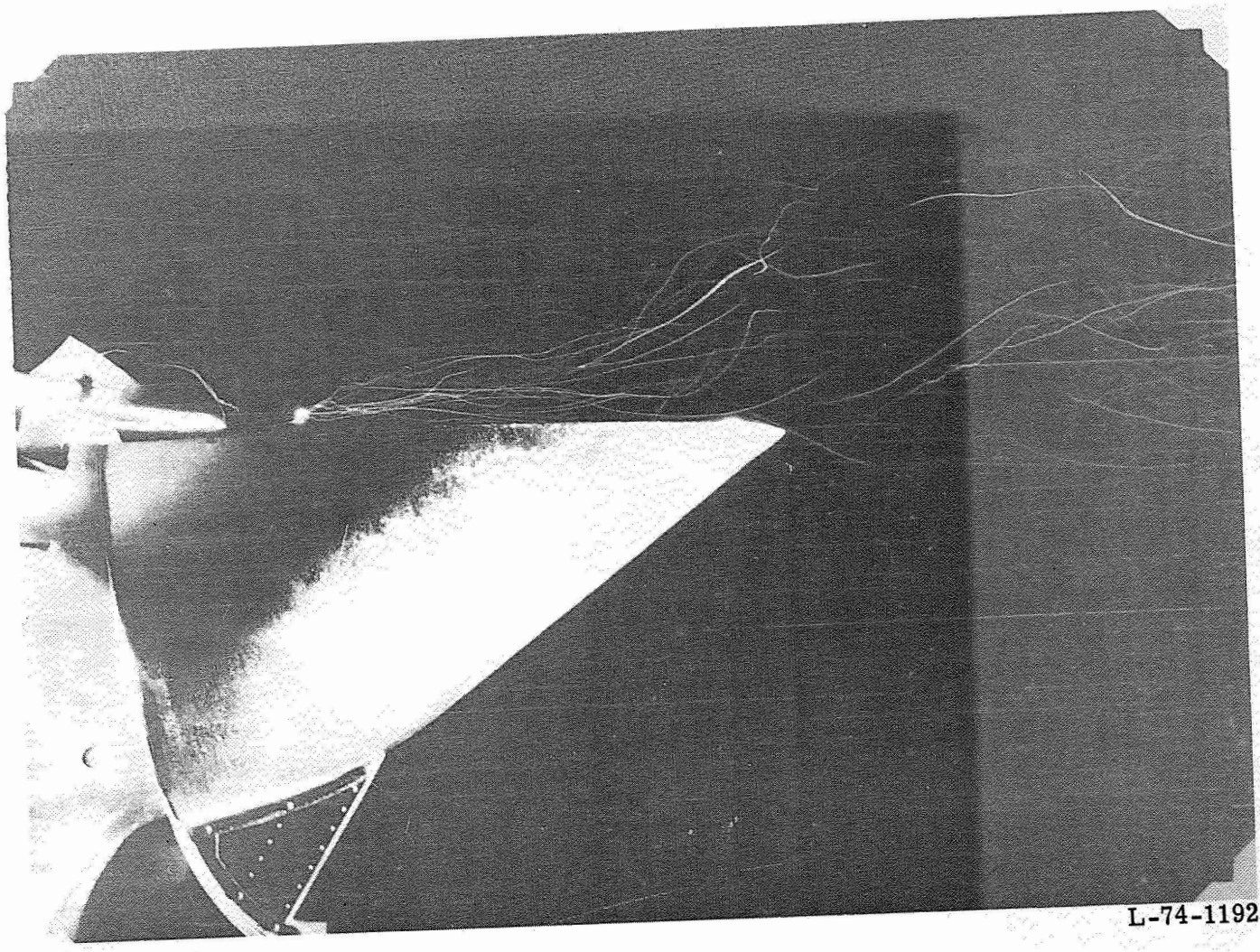

(a) Side view.

Figure 14.- Side and top views, photographed simultaneously, of effects of flow deflector 1 and swirler on exhaust flow at $V_{eff} = 0.8$.

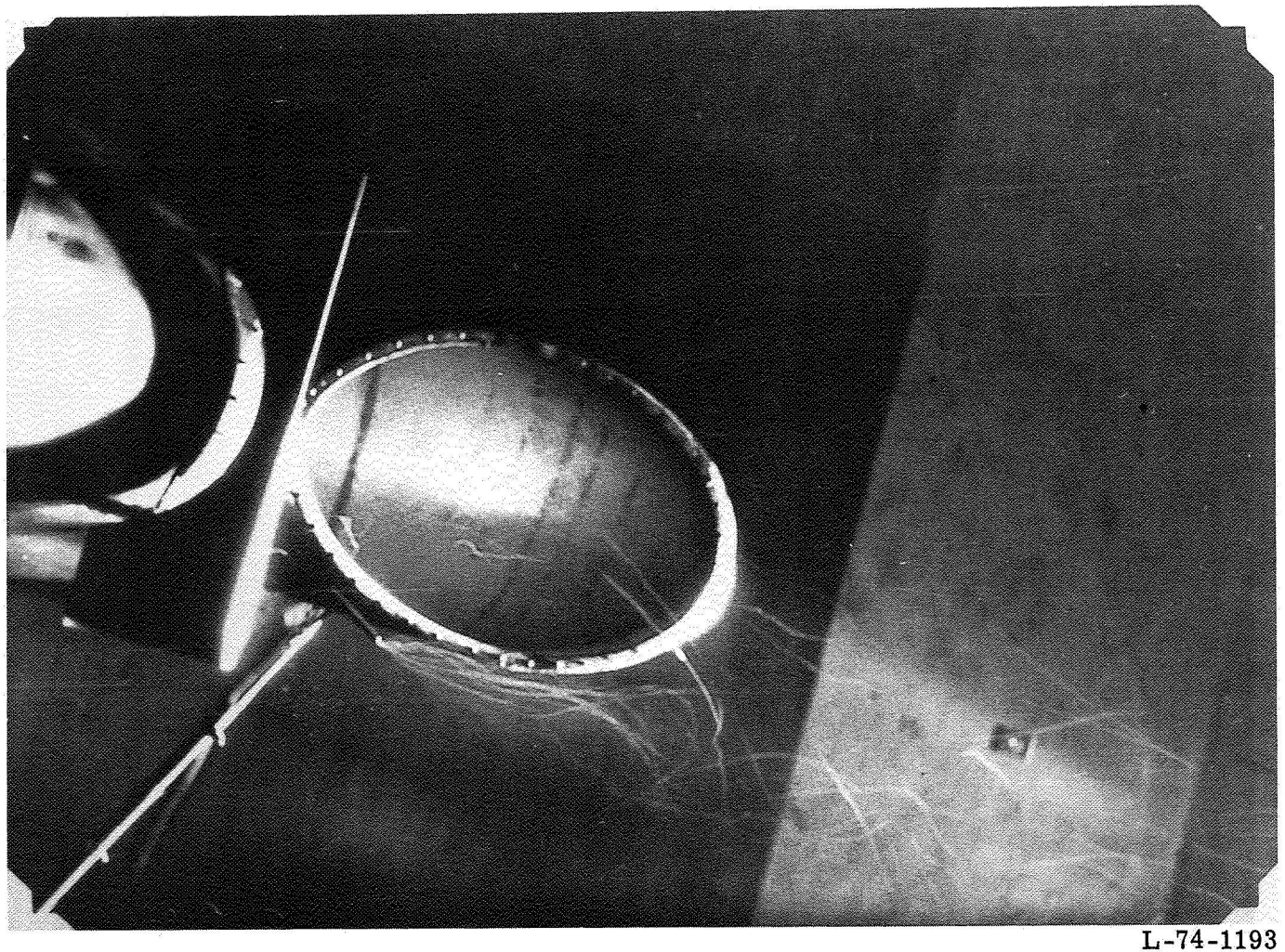

L-74-1193

(b) Top view.

Figure 14.- Concluded.

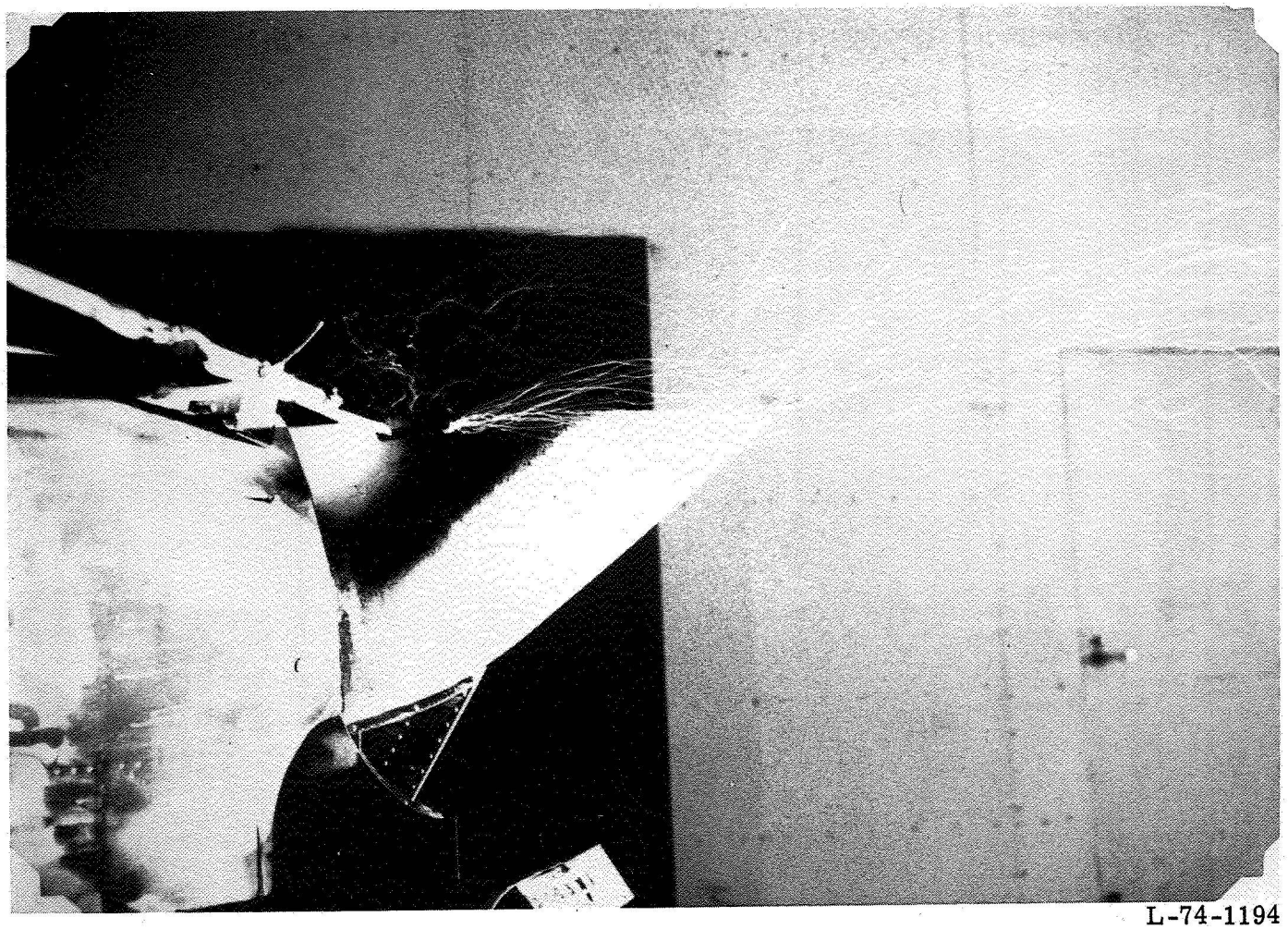

L-74-1194

Figure 15.- Effects of flow deflector 2 and swirler on exhaust flow at $V_{eff} = 0.7$.

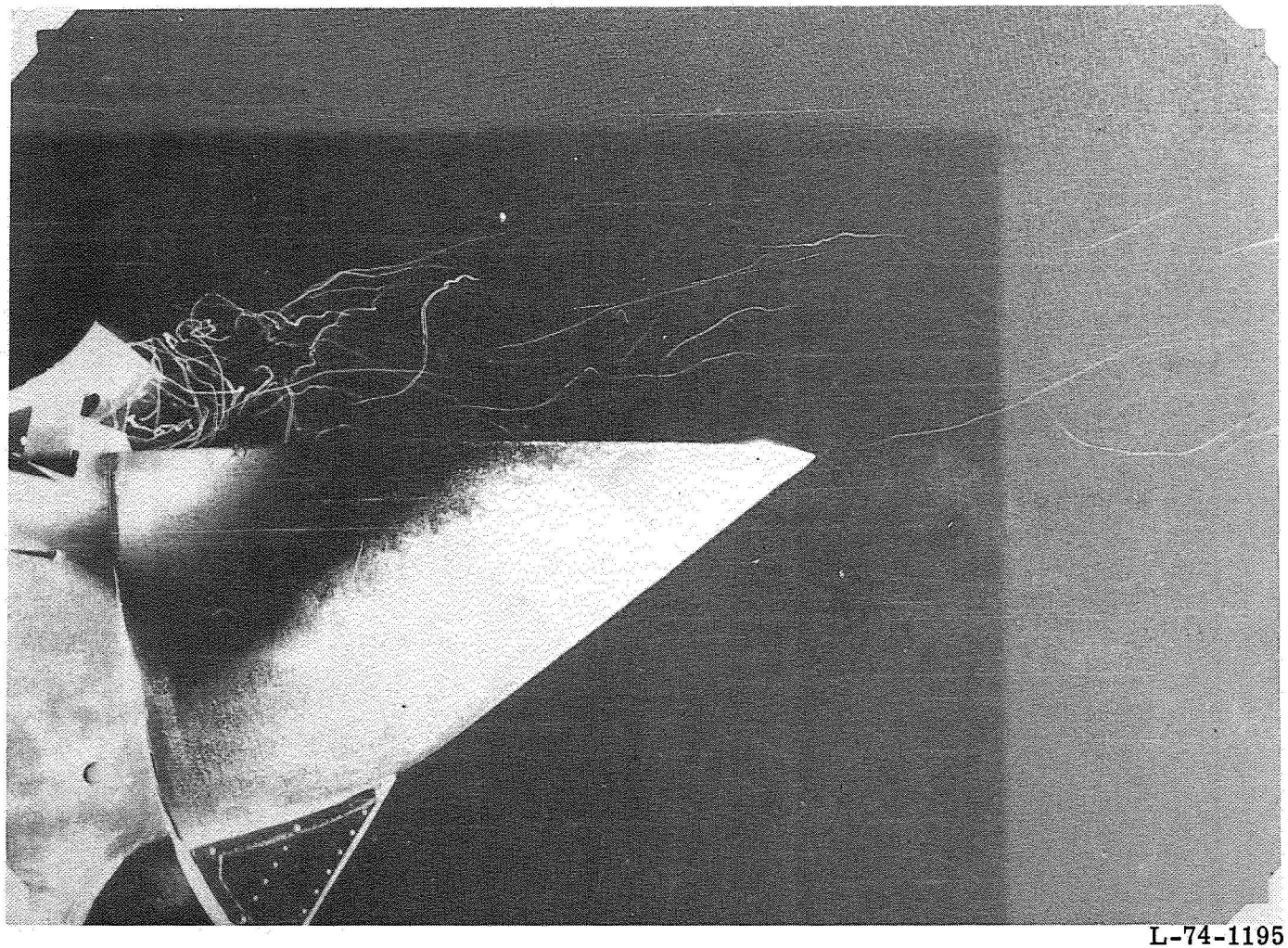

L-74-1195

(a) Side view.

Figure 16.- Side and top views, photographed simultaneously, of effects of flow deflector 2 and flow swirler on exhaust flow at $V_{eff} = 0.7$.

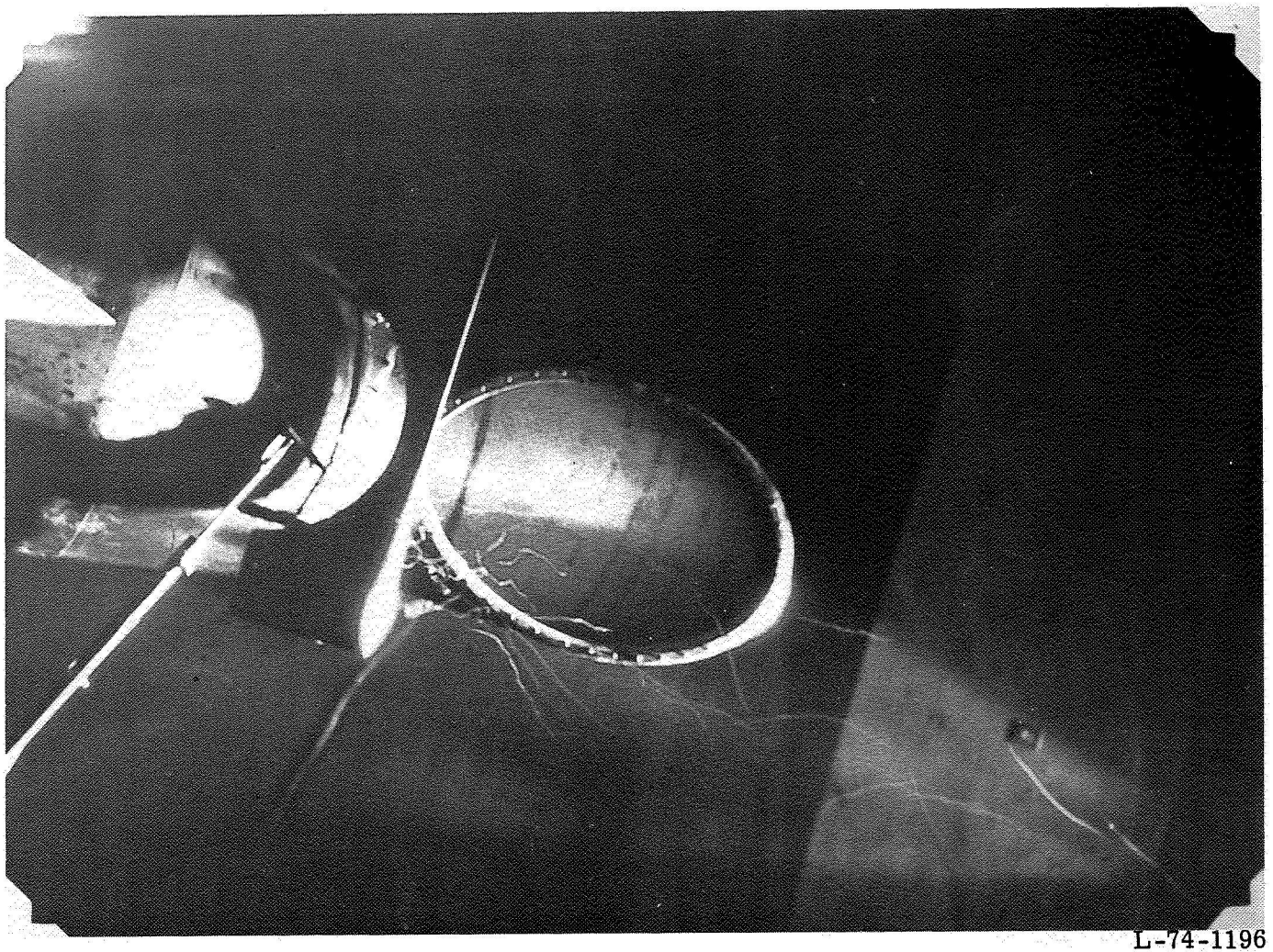

(b) Top view.

Figure 16.- Concluded.

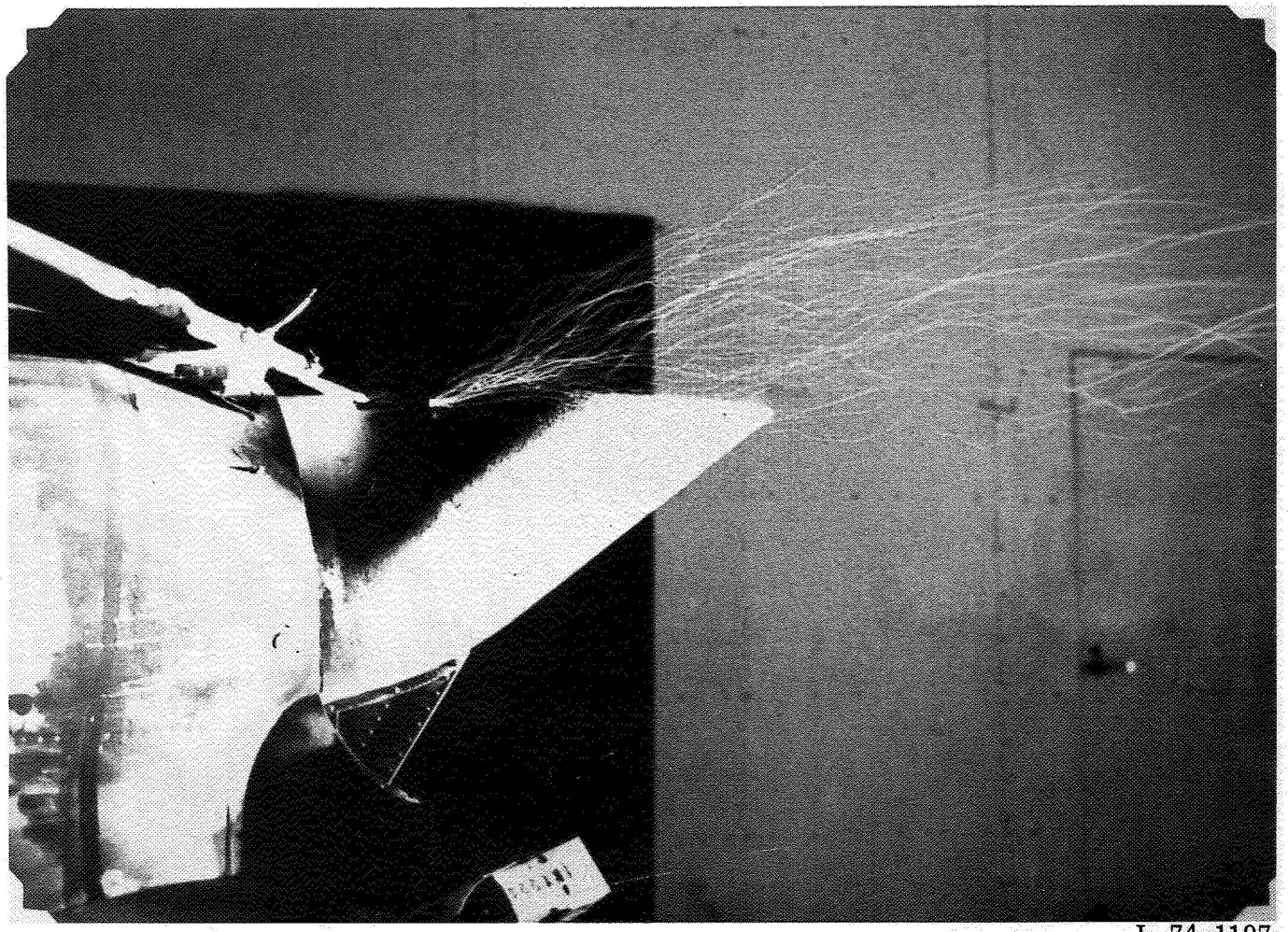

L-74-1197

(a) $\alpha = 0^{o}$.

Figure 17.- Effects of angle of attack and flow deflector 2 on exhaust flow at $V_{eff} = 0.7$.

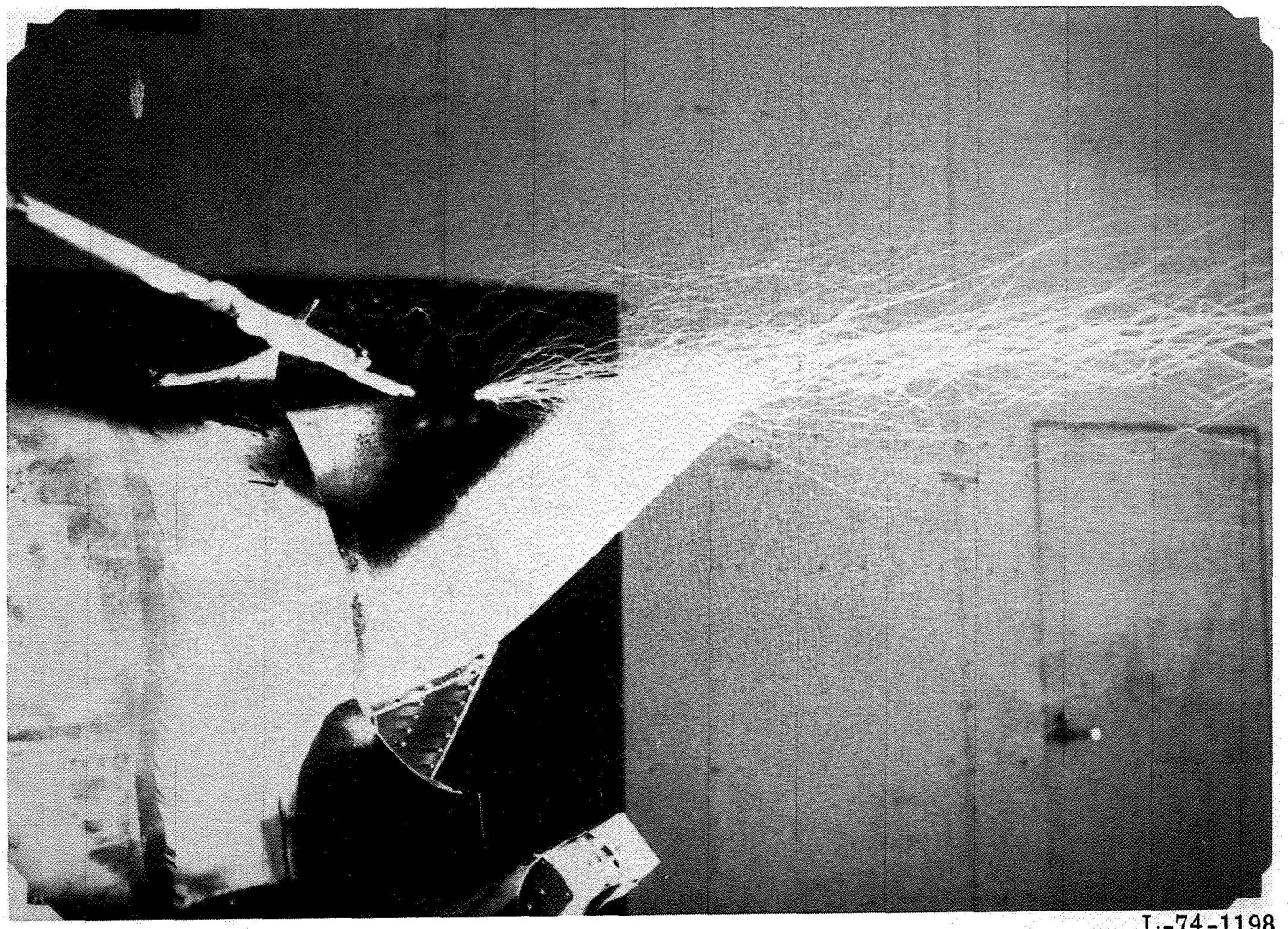

L-74-1198

(b) $\alpha = -5^{o}$.

Figure 17.- Continued.

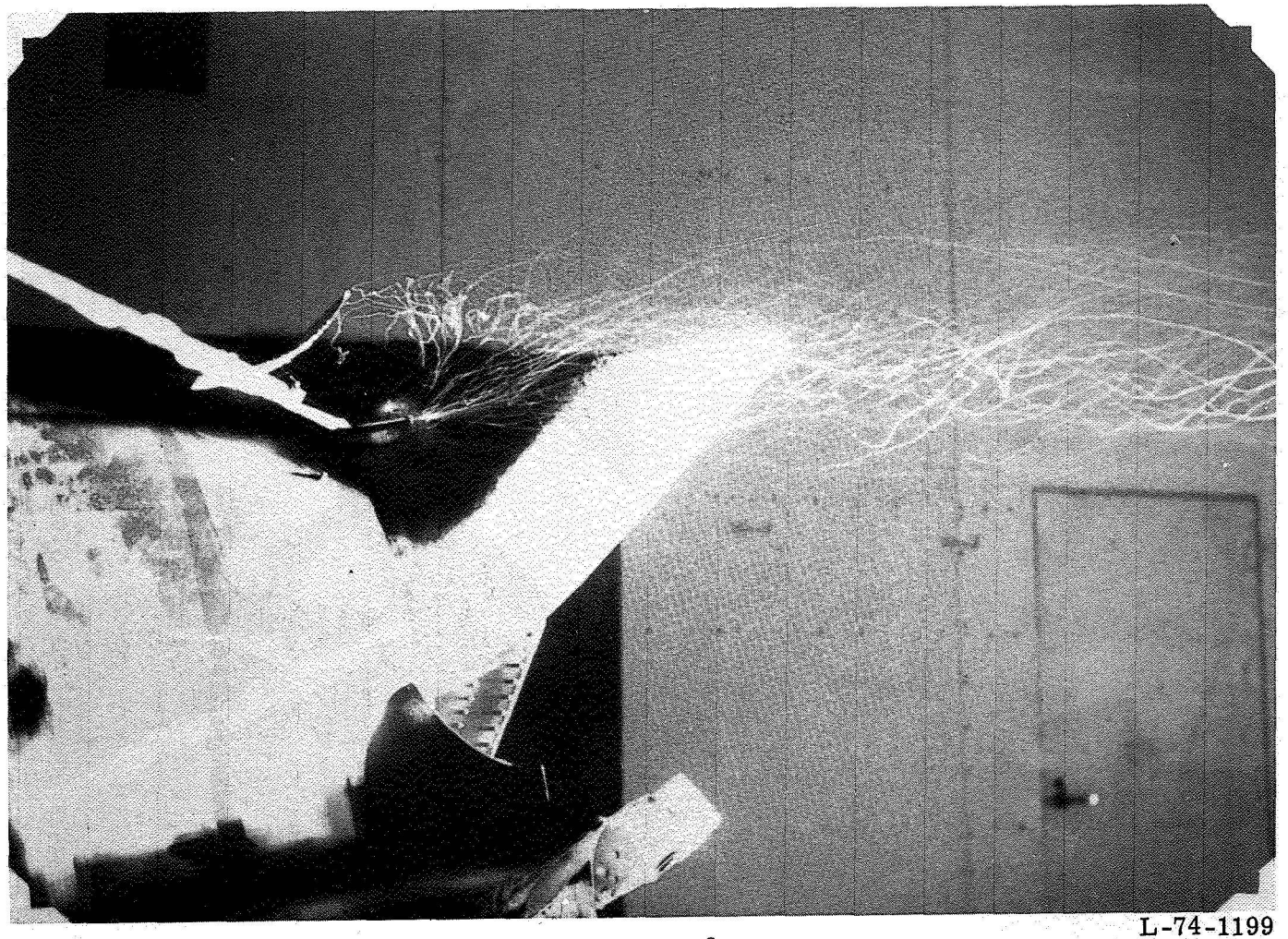

L-74-1199

(c) $\alpha = -10^{o}$.

Figure 17.- Concluded.

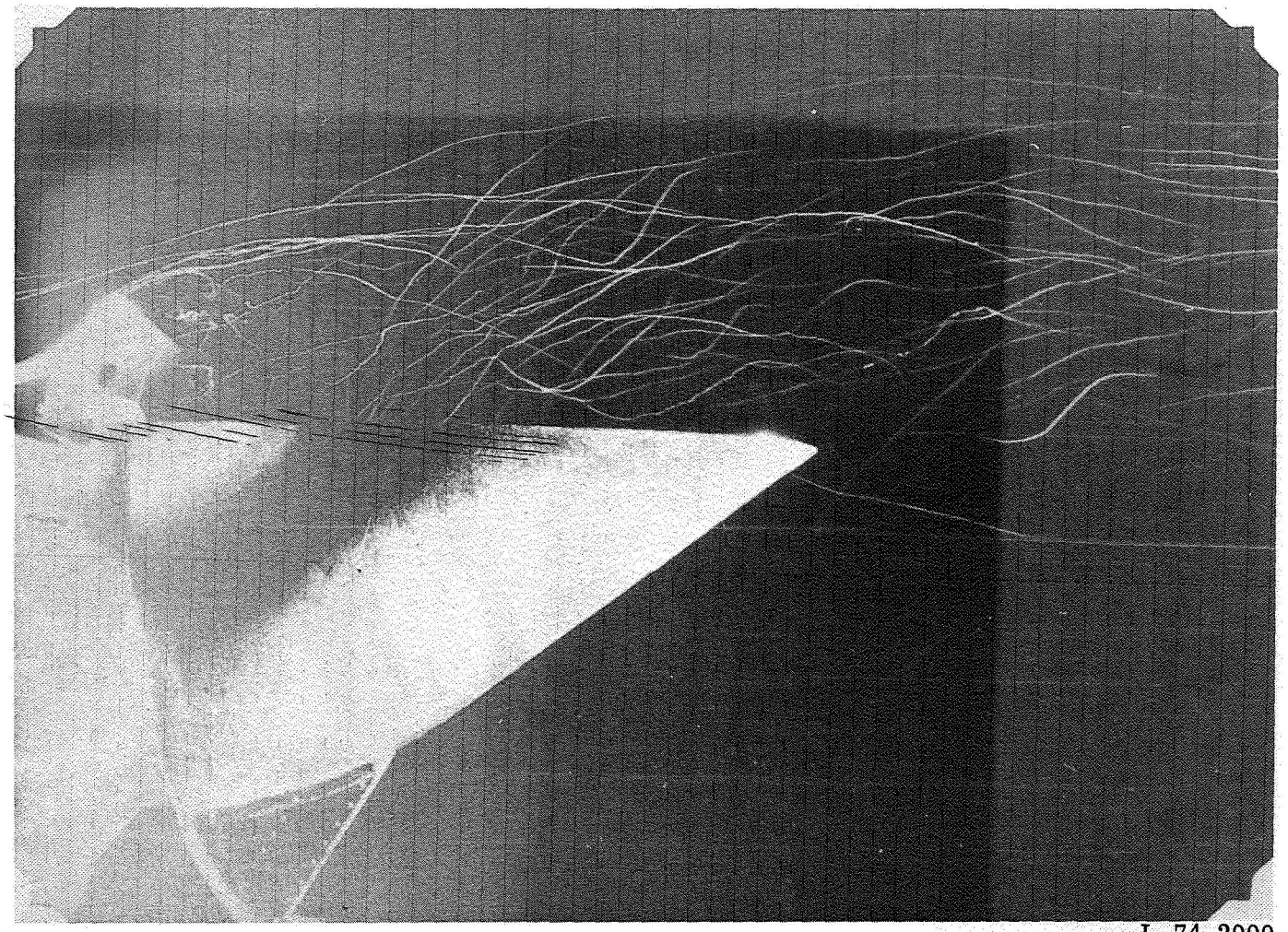

(a) Side view.

Figure 18.- Side and top views, photographed simultaneously, of effect of flow deflector 2 on exhaust flow at $\alpha = 0^{o}$. $V_{eff} = 0.7$.

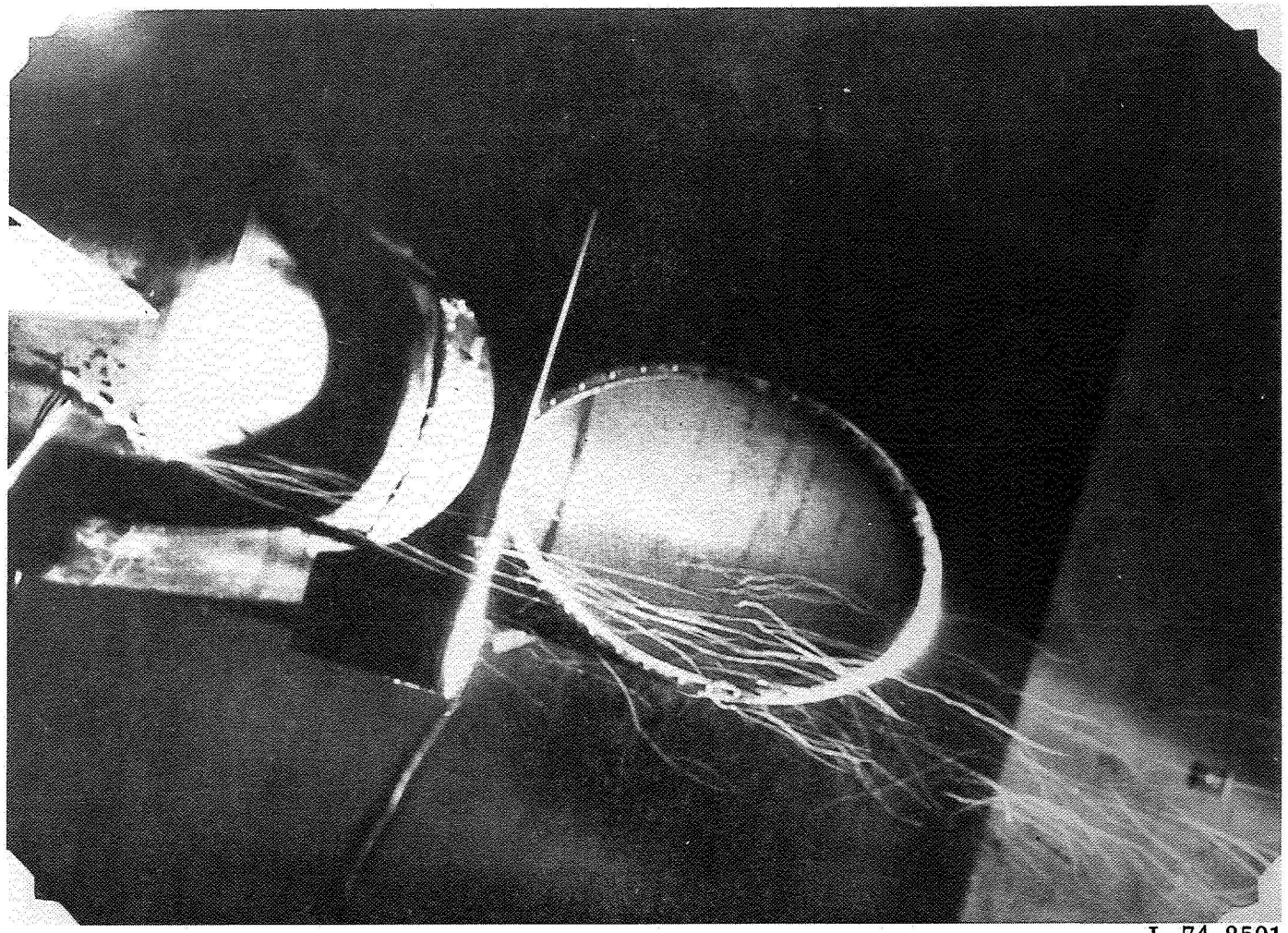

L-74-8501

(b) Top view.

Figure 18.- Concluded.

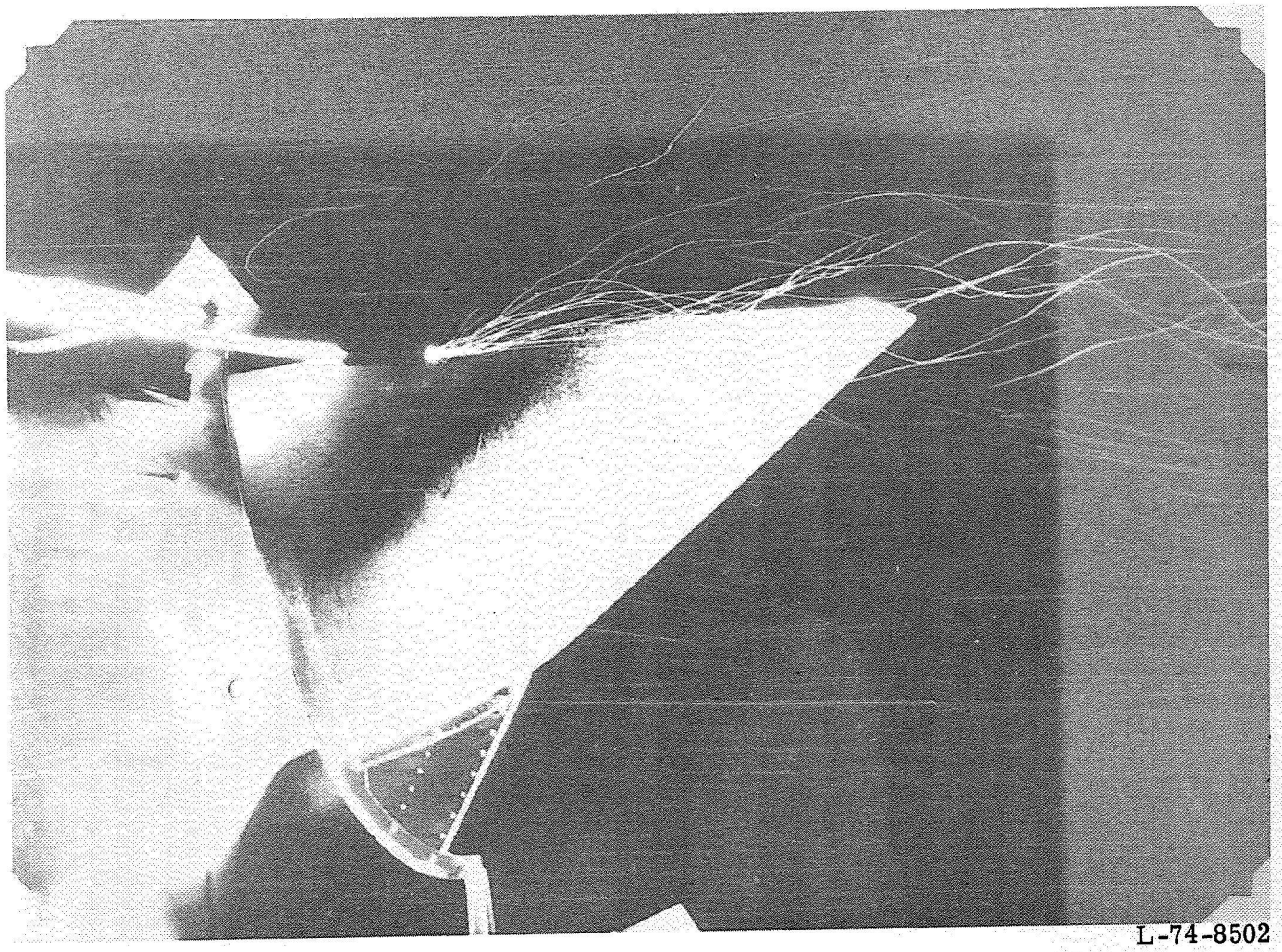

(a) Side view.

Figure 19.- Side and top views, photographed simultaneously, of effect of flow deflector 2 on exhaust flow at $\alpha = -5^{o}$. $V_{eff} = 0.7$.

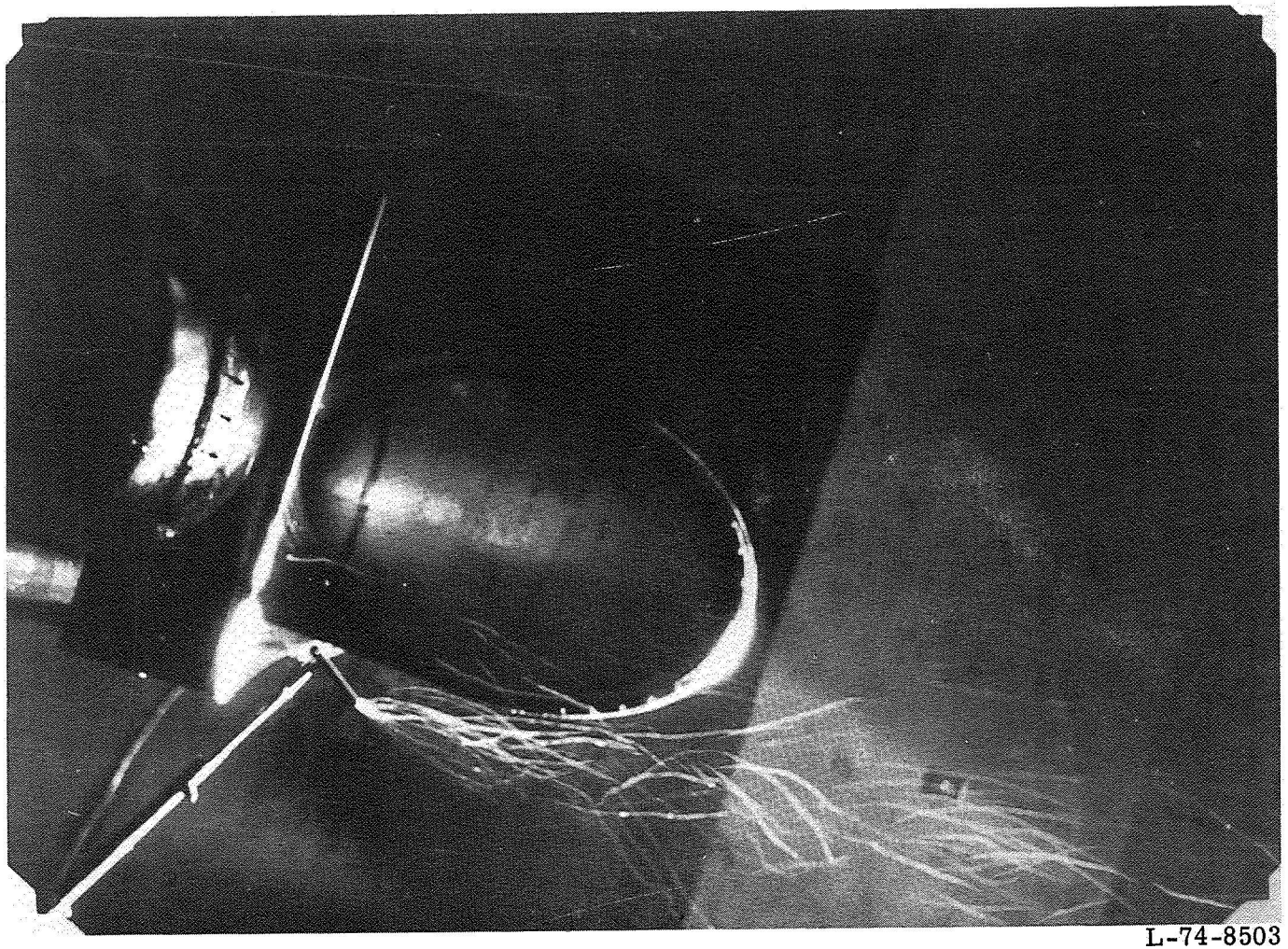

L-74-8503

(b) Top view.

Figure 19.- Concluded.

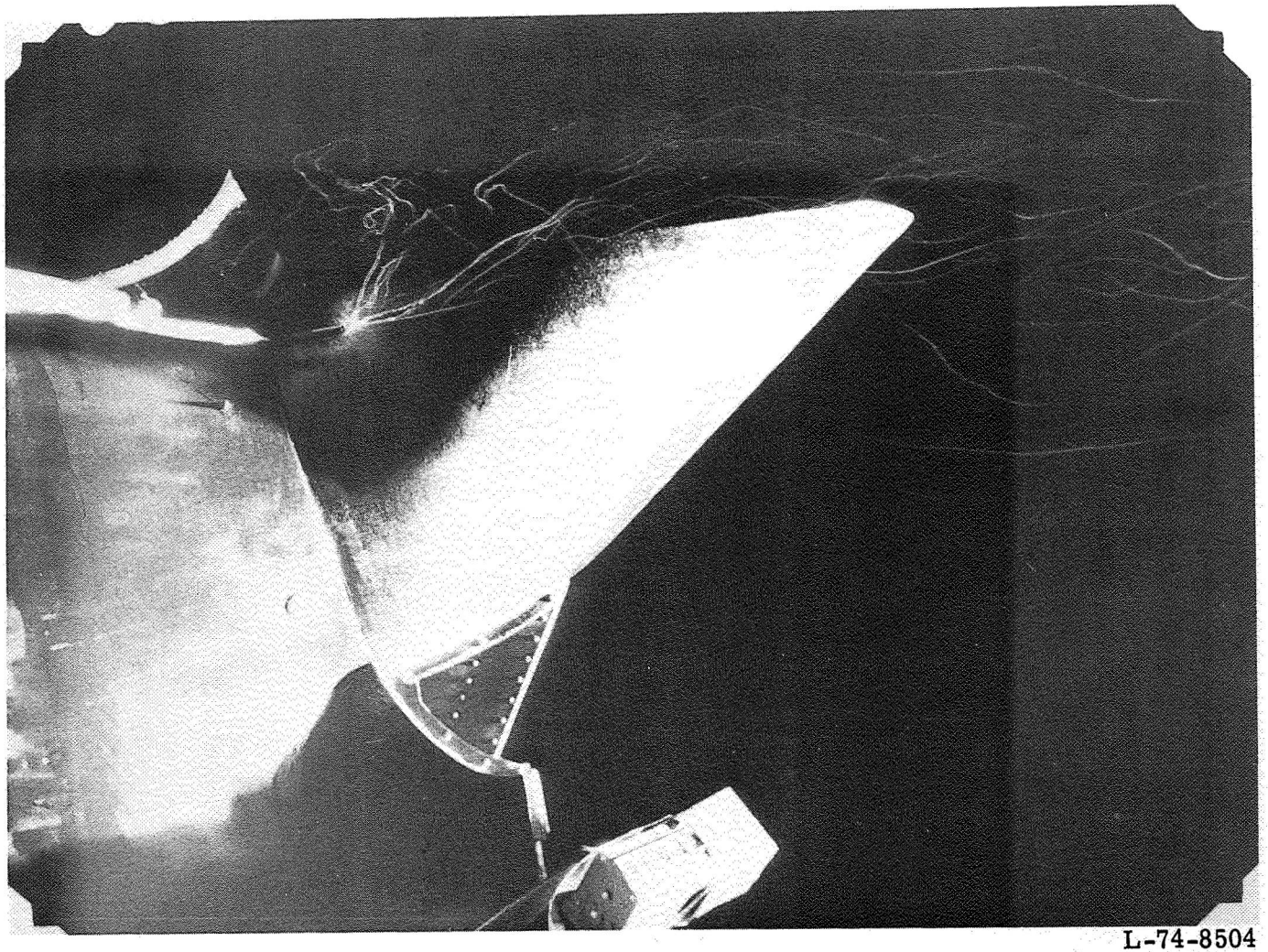

(a) Side view.

Figure 20.- Side and top views, photographed simultaneously, of effect of flow deflector 2 on exhaust flow at $\alpha = -10^{\circ}$. $V_{eff} = 0.7$.

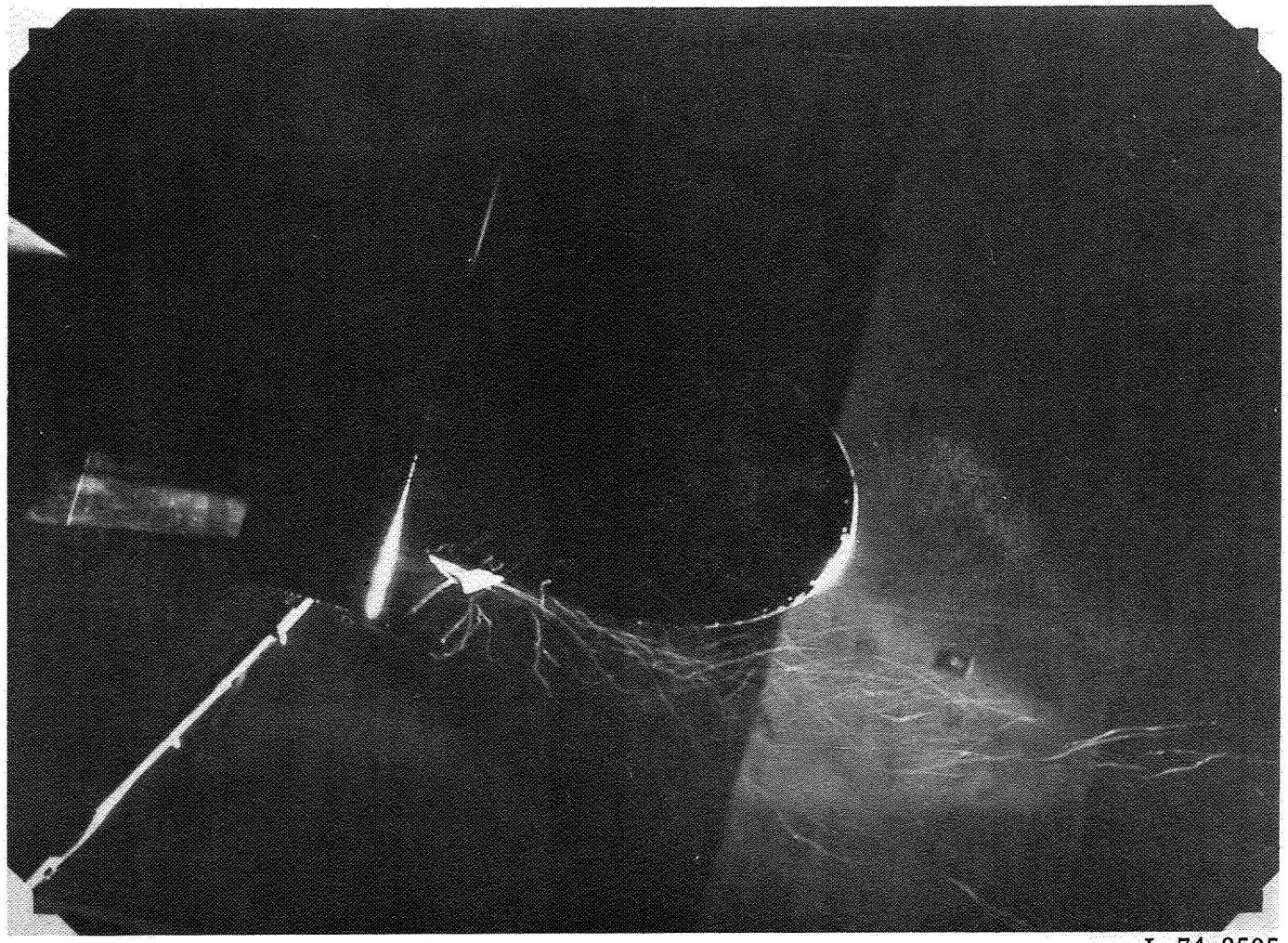

L-74-8505

(b) Top view.

Figure 20.- Concluded.

(a) $V_{eff} = 0.6$.

Figure 21.- Effects of effective velocity ratio and flow deflector 2 on exhaust flow.

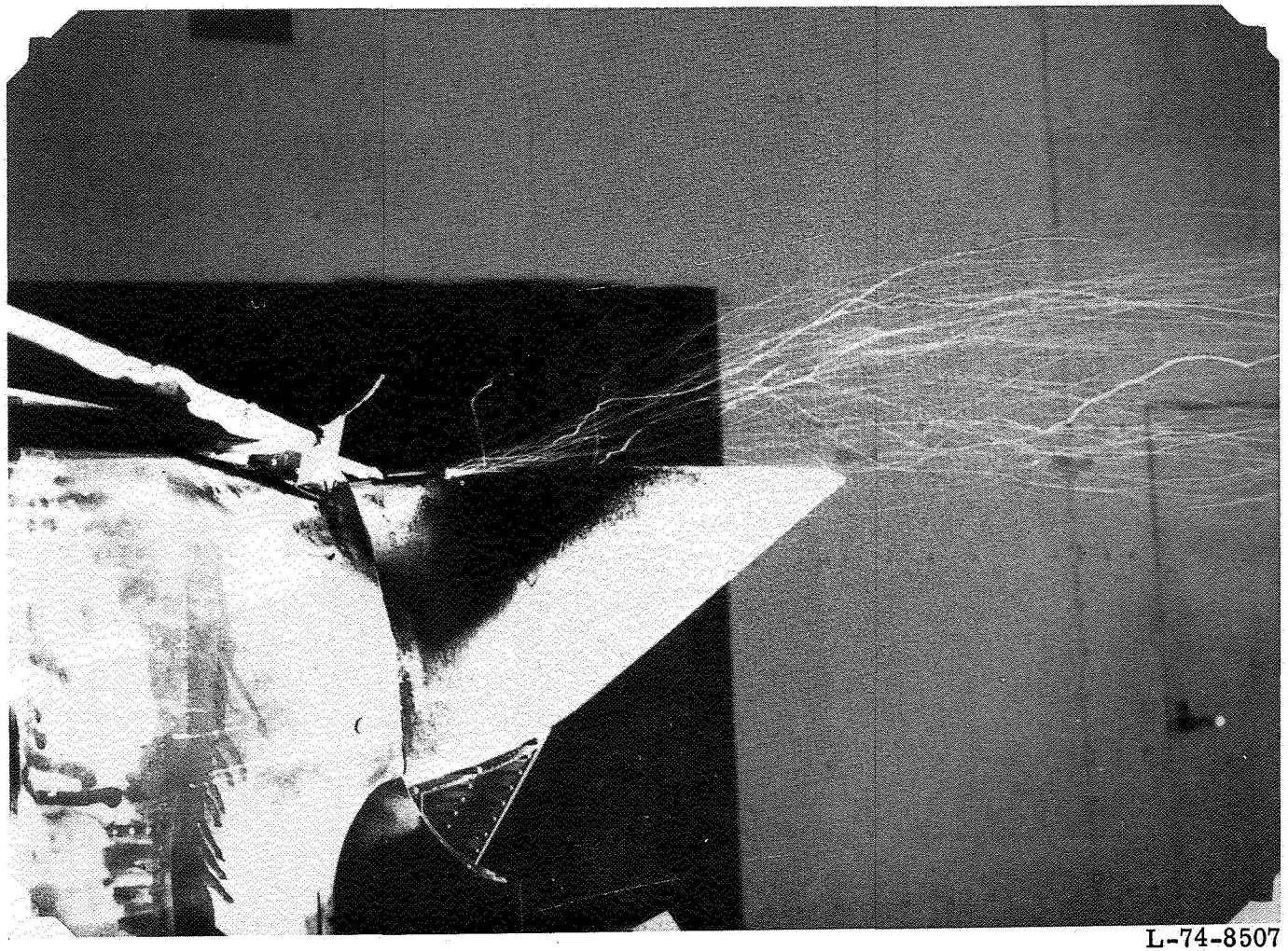

L-74-8507

(b) $V_{eff} = 1.0$.

Figure 21.- Concluded.

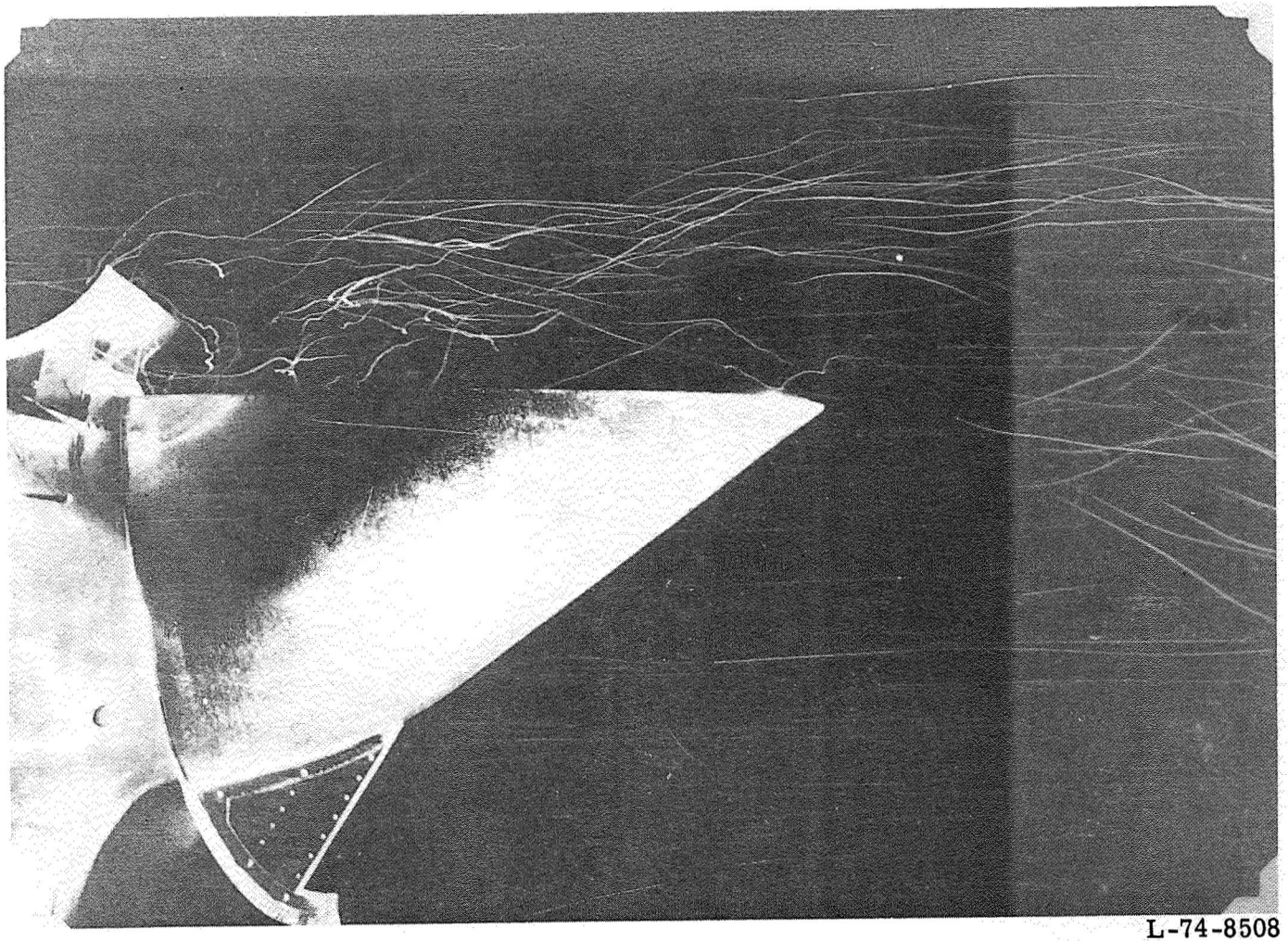

(a) Side view.

Figure 22.- Side and top views, photographed simultaneously, of effect of flow deflector 2 on exhaust flow at $V_{eff} = 0.9$.

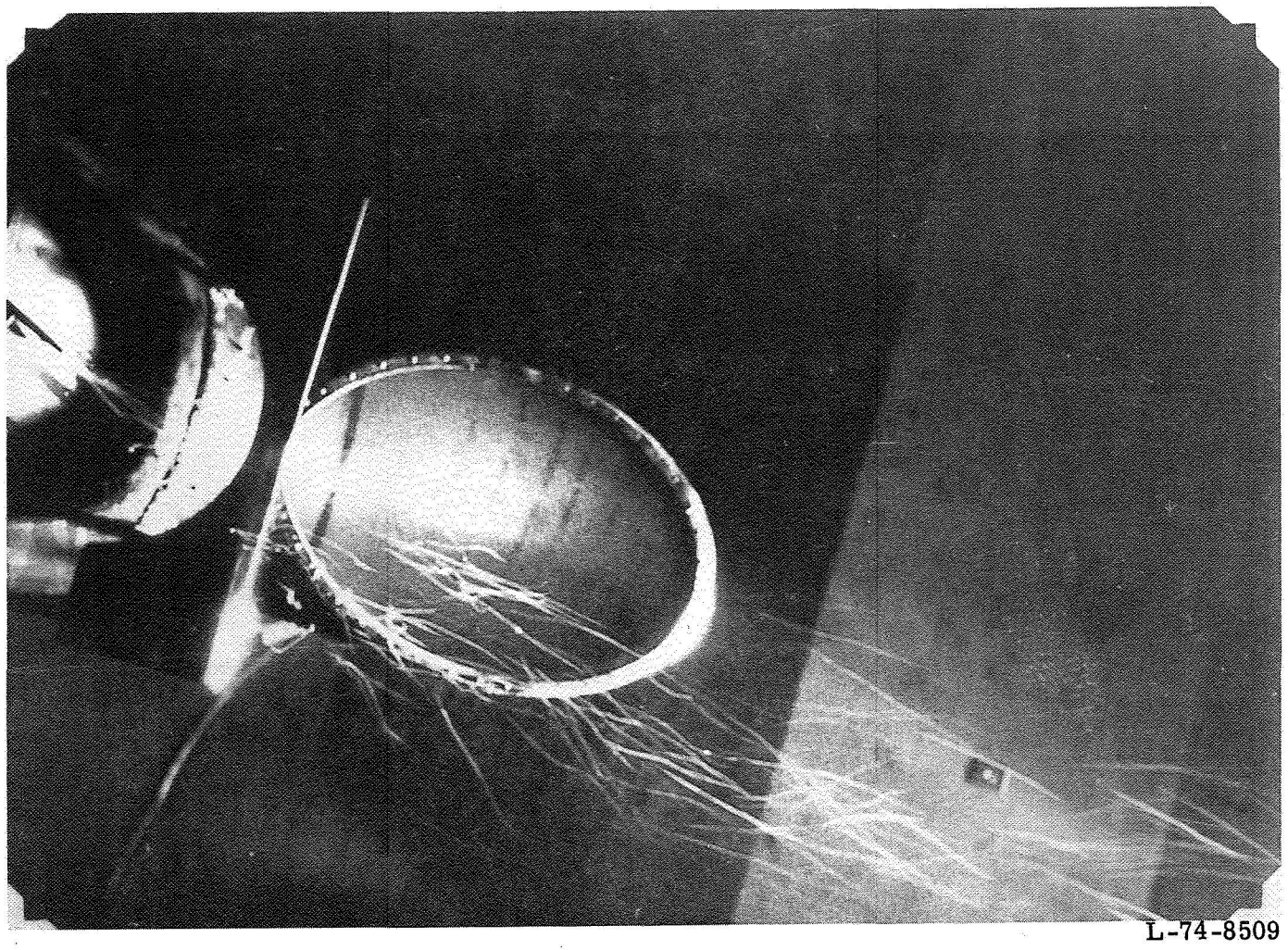

(b) Top view.

Figure 22.- Concluded.

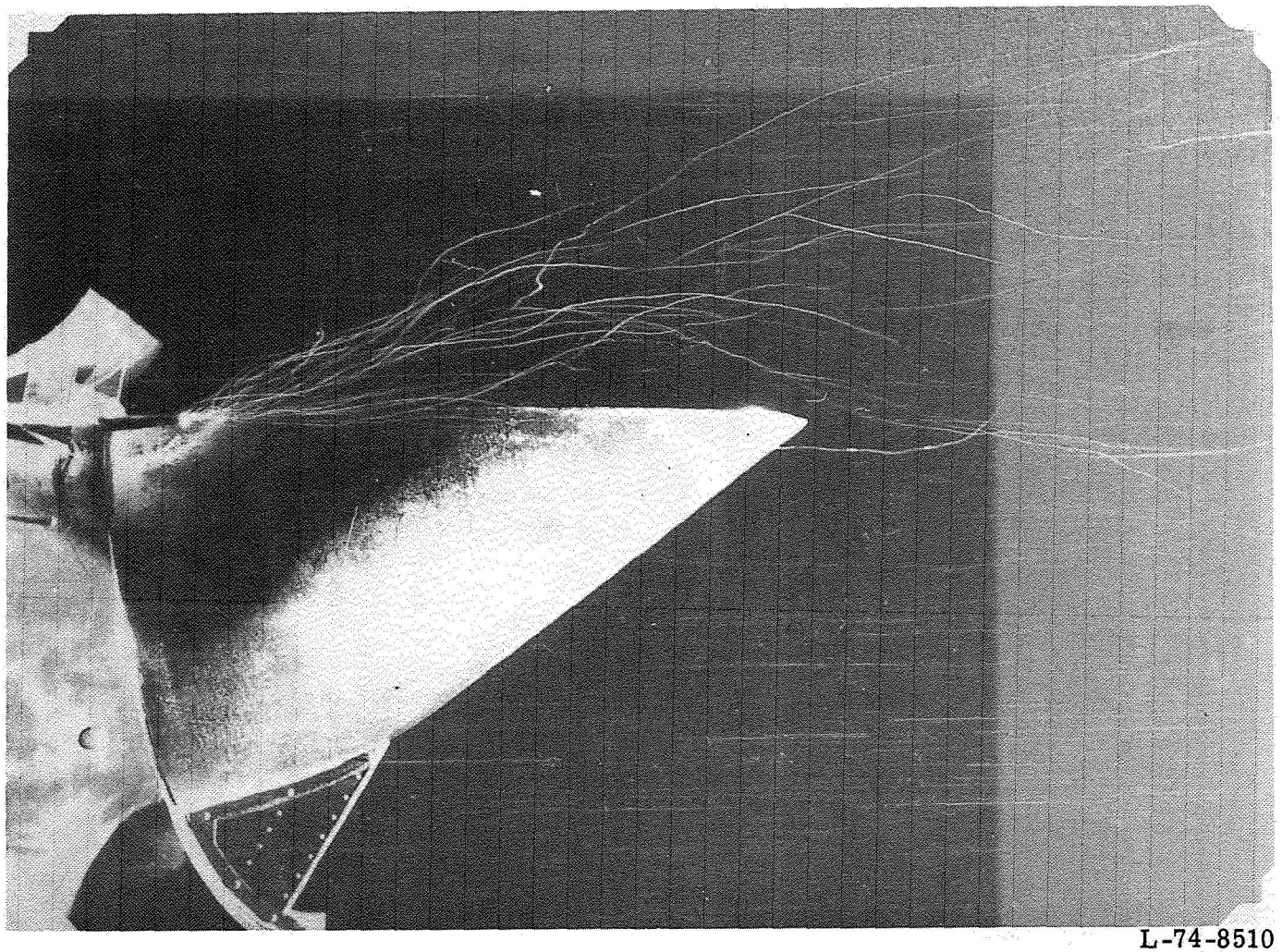

(a) Side view.

Figure 23.- Side and top views, photographed simultaneously, of effect of flow deflector 2 on exhaust flow at $V_{eff} = 1.0$.

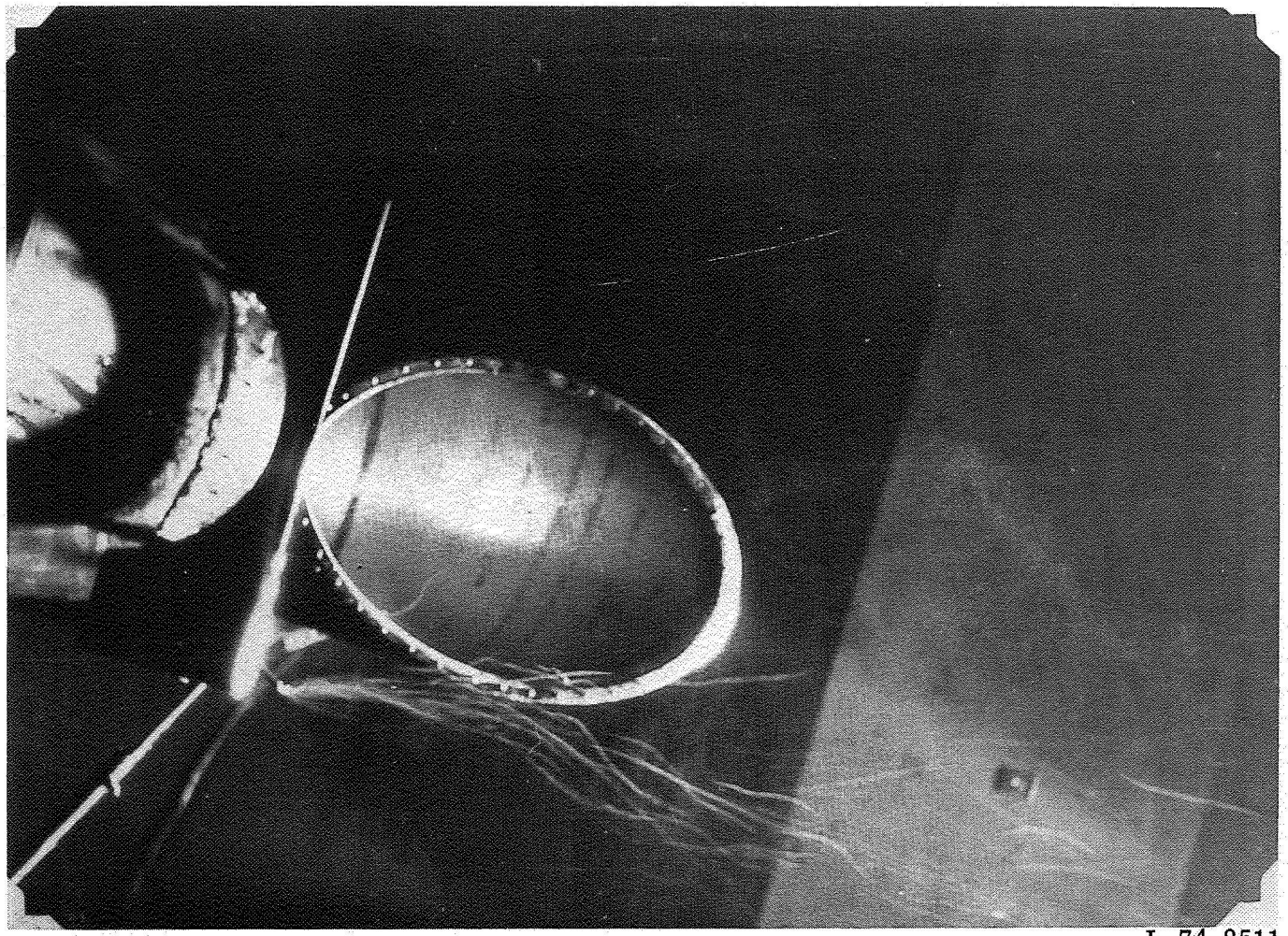

L-74-8511

(b) Top view.

Figure 23.- Concluded.

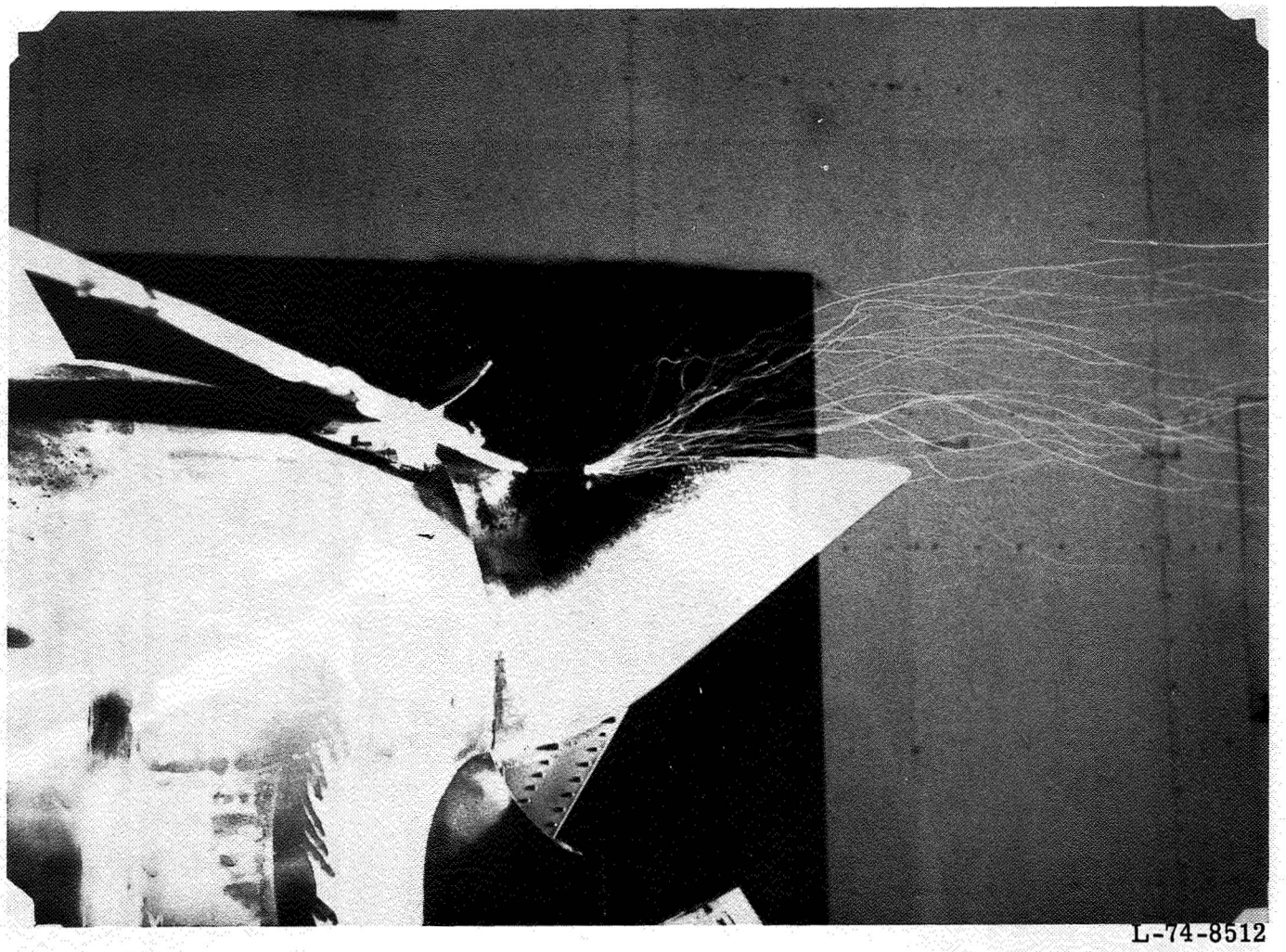

(a) $\beta = 5^{o}$.

Figure 24.- Effects of sideslip and flow deflector 2 on exhaust flow at $V_{eff} = 0.7$.

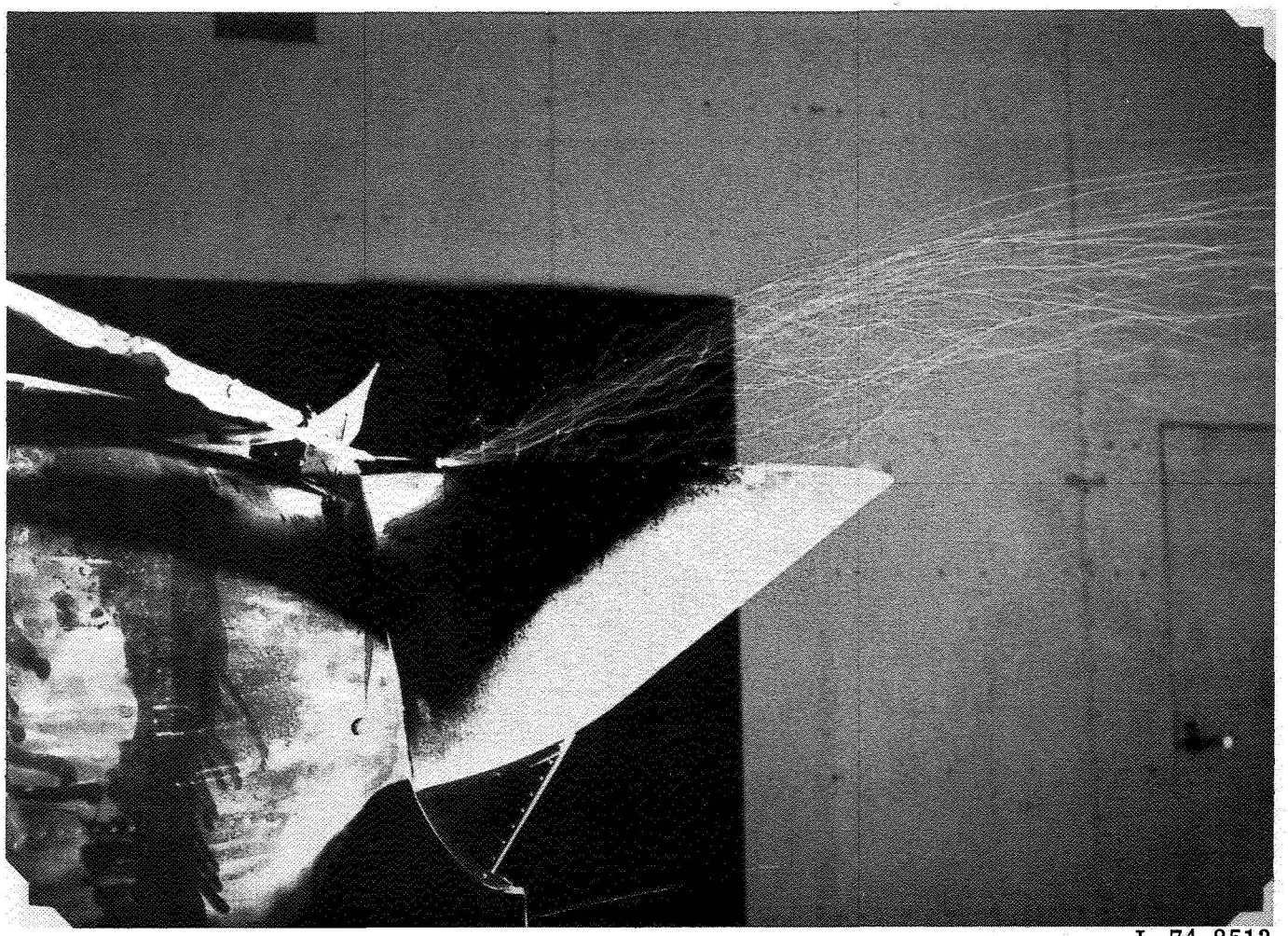

L-74-8513

(b) $\beta = -5^{o}$.

Figure 24.- Concluded.

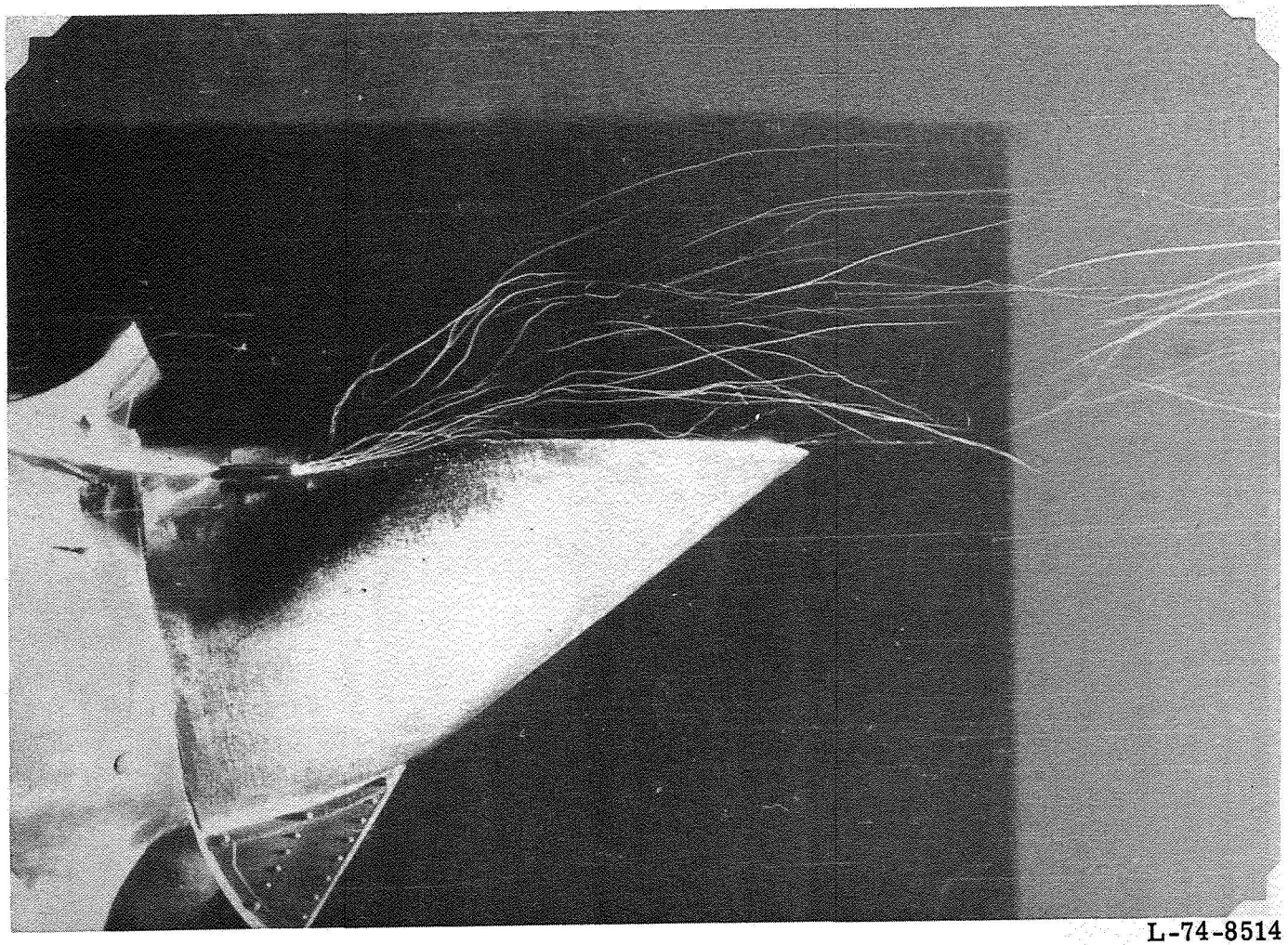

(a) Side view.

Figure 25.- Side and top views, photographed simultaneously, of effects of sideslip ($\beta = 5^{o}$) and flow deflector 2 on exhaust flow at $V_{eff} = 0.7$.

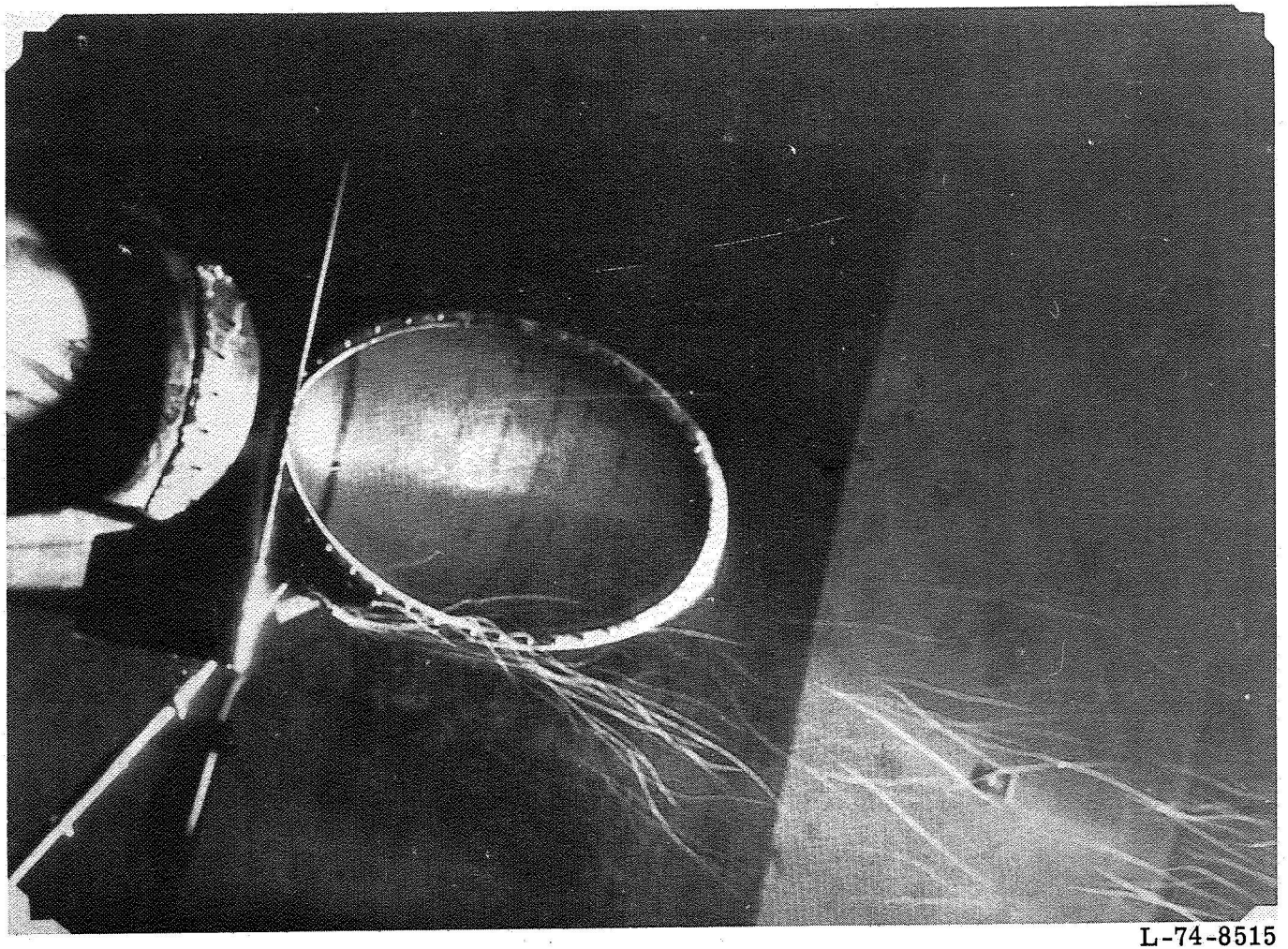

L-74-8515

(b) Top view.

Figure 25.- Concluded.

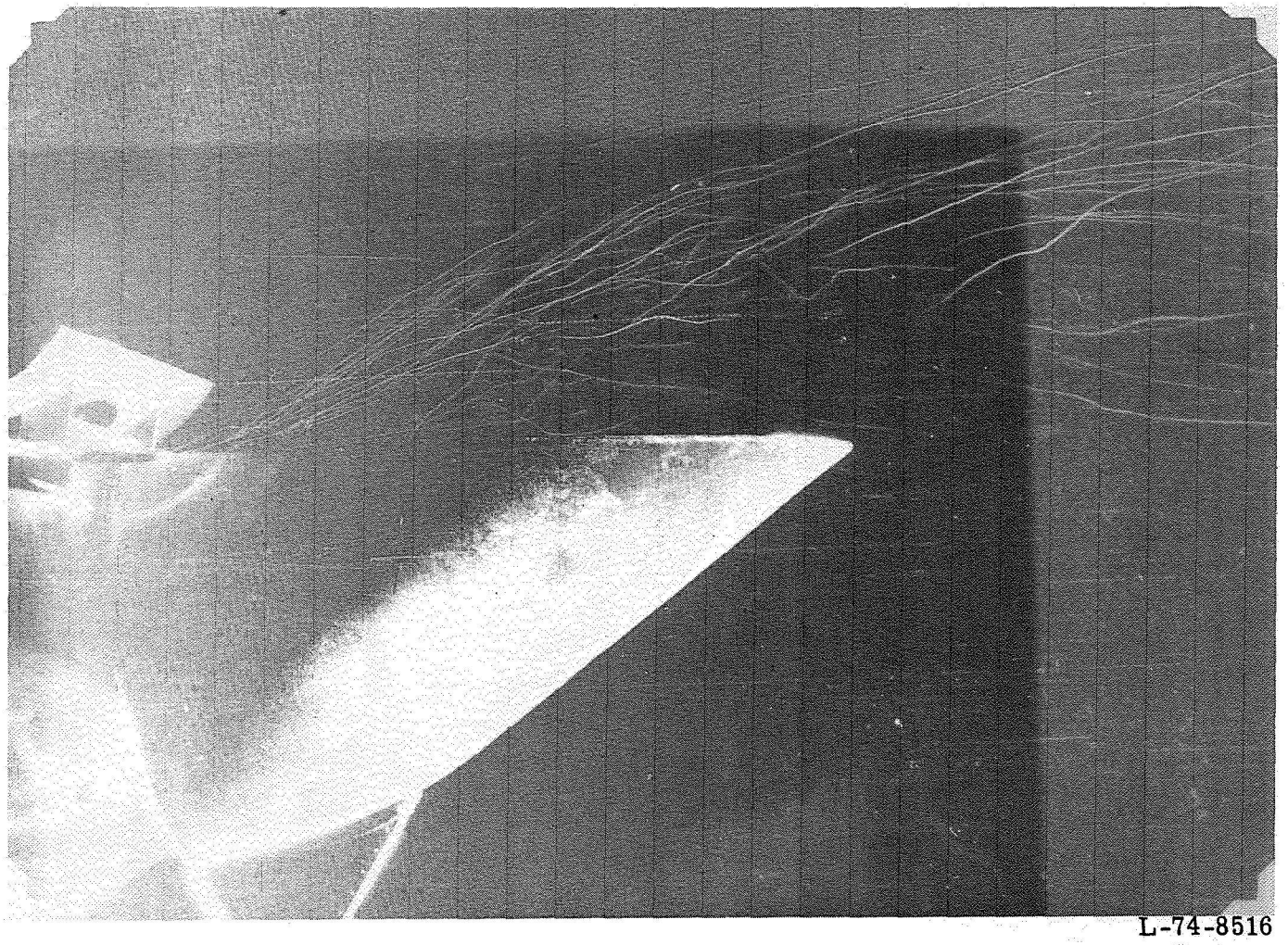

(a) Side view.

Figure 26.- Side and top views, photographed simultaneously, of effects of sideslip ($\beta = -5^{o}$) and flow deflector 2 on exhaust flow at $V_{eff} = 0.7$.

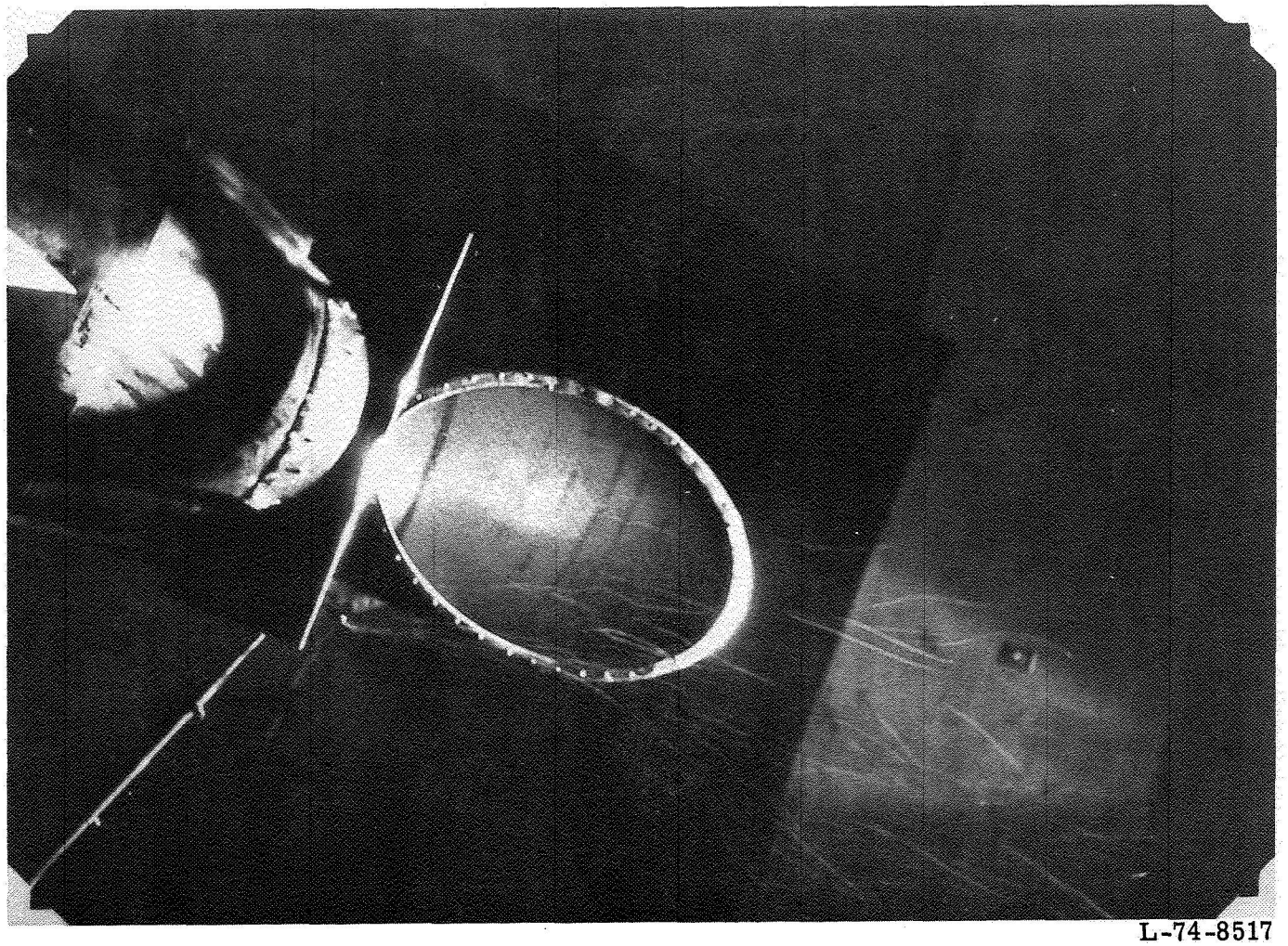

L-74-8517

(b) Top view.

Figure 26.- Concluded.

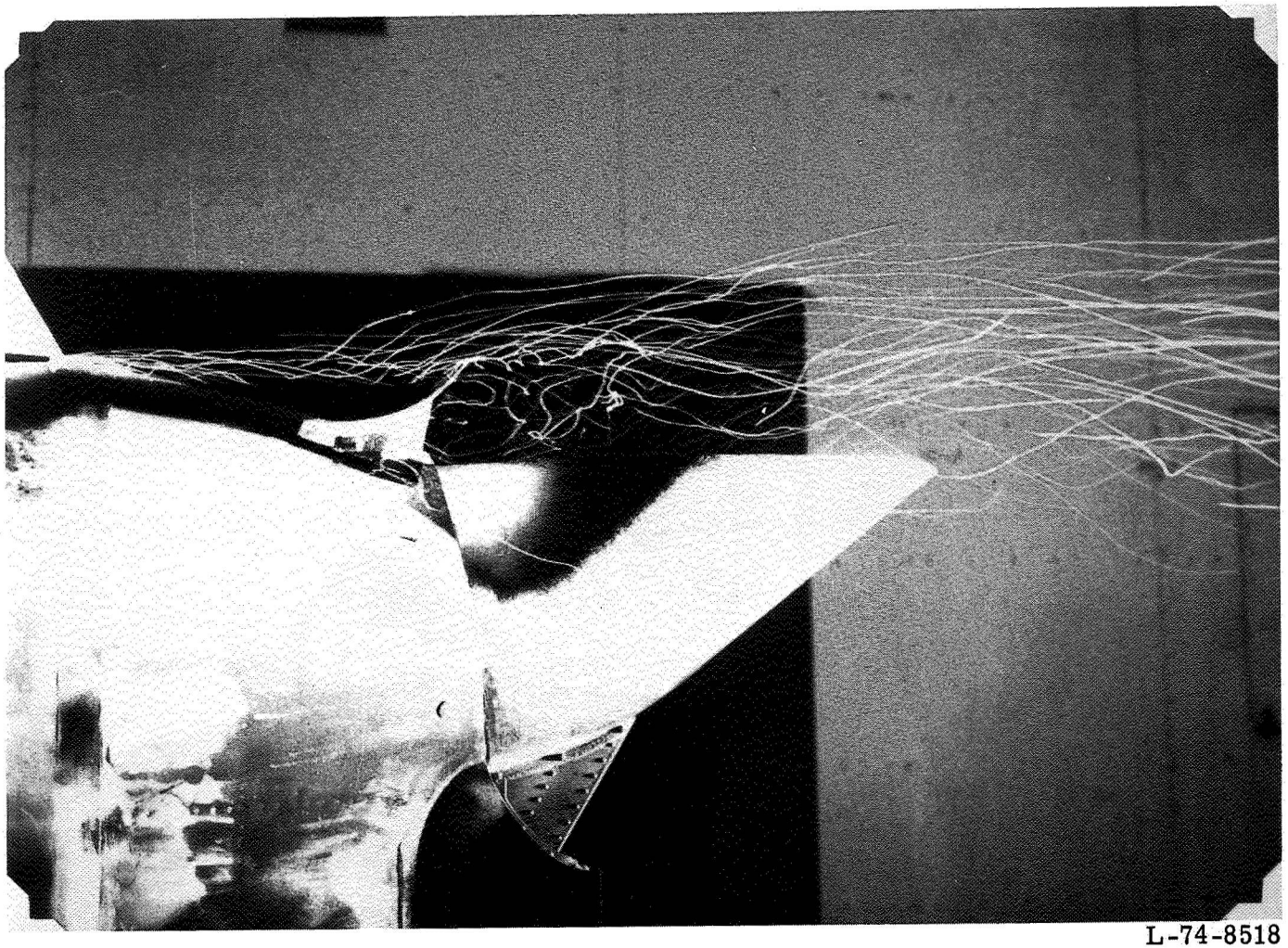

L-74-8518

(a) View 1.

Figure 27.- Views of effect of flow deflector 3 on exhaust flow at $V_{eff} = 0.7$.

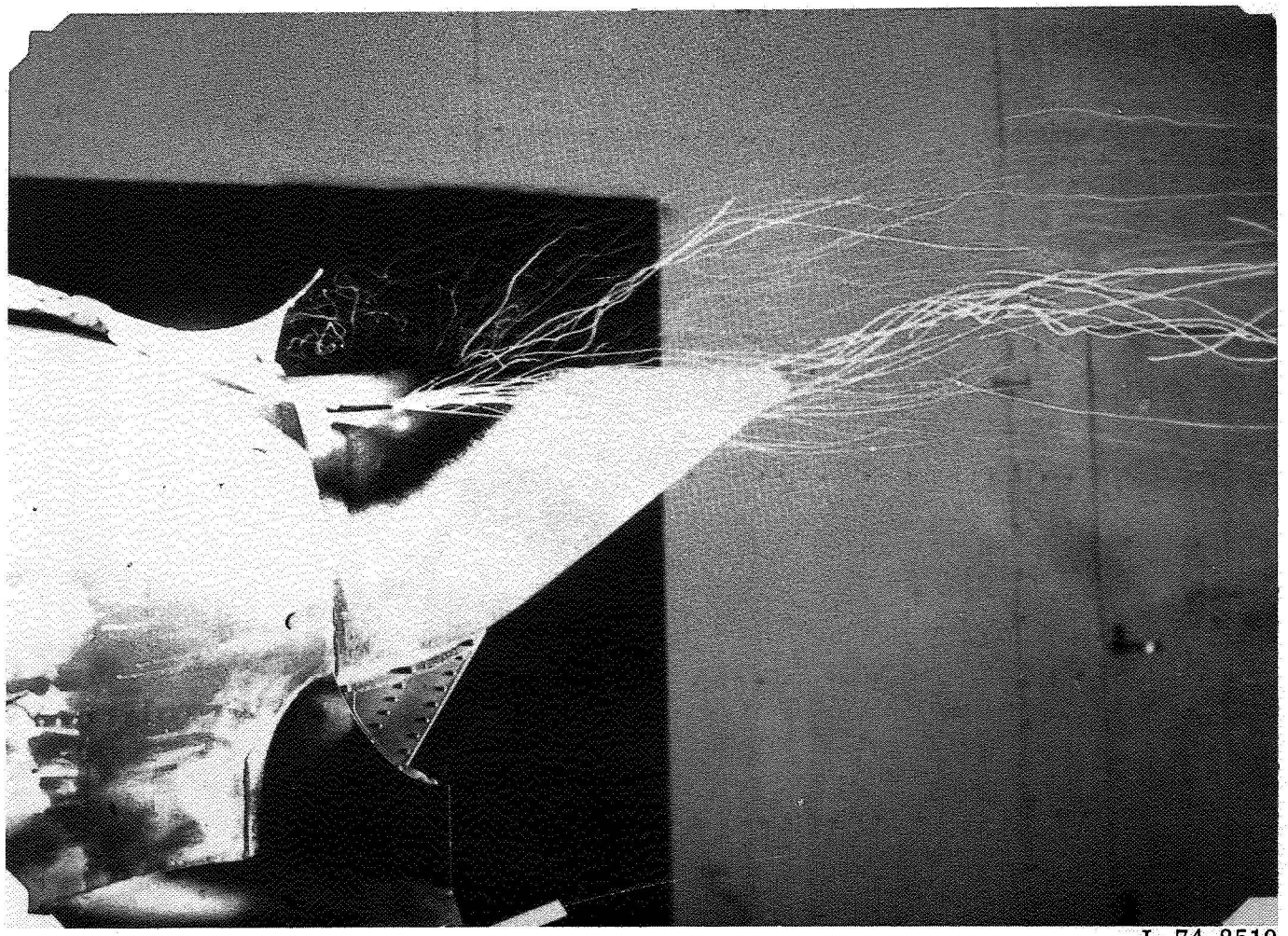

L-74-8519

(b) View 2.

Figure 27.- Continued.

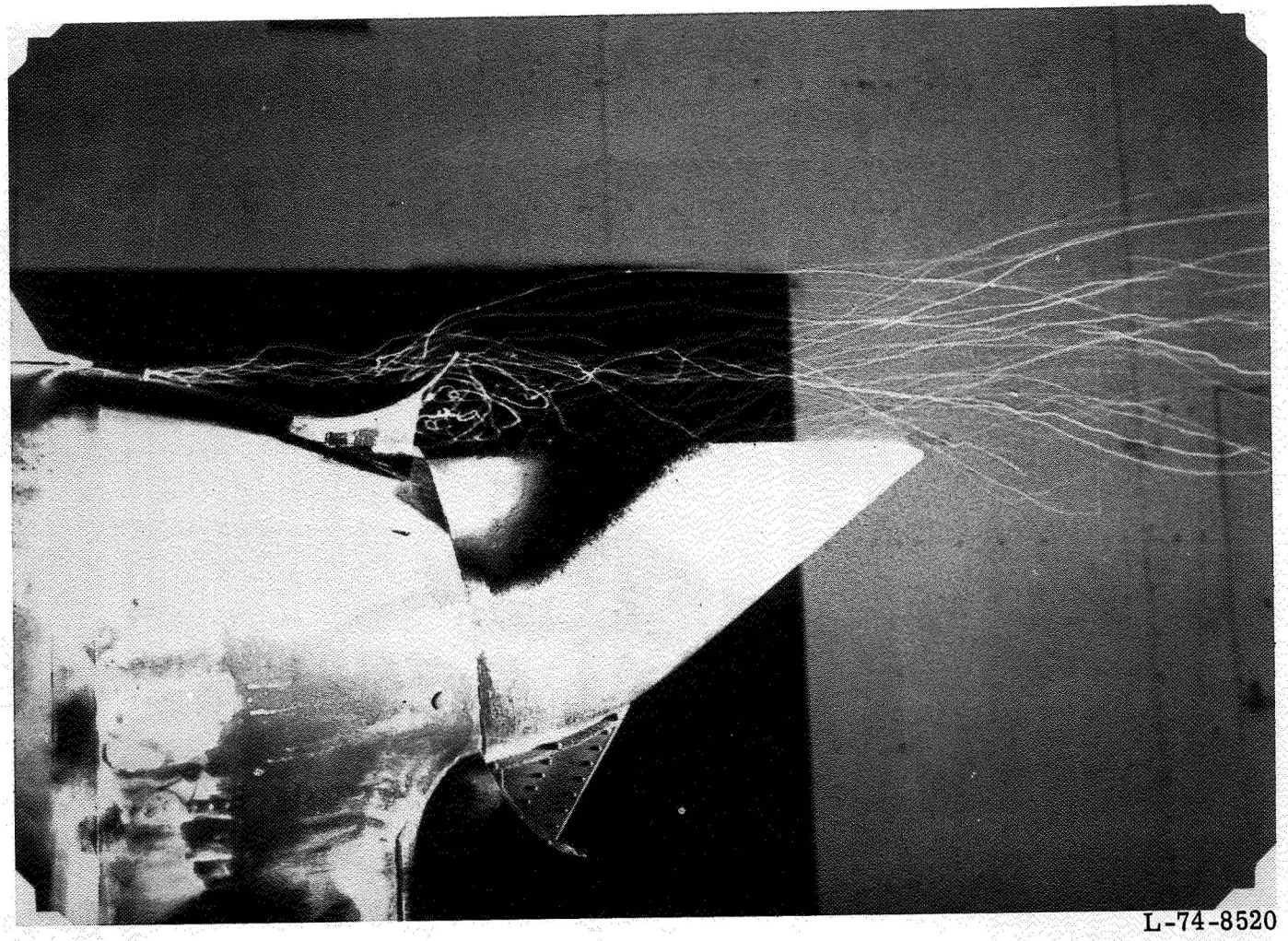

(c) View 3.

Figure 27.- Continued.

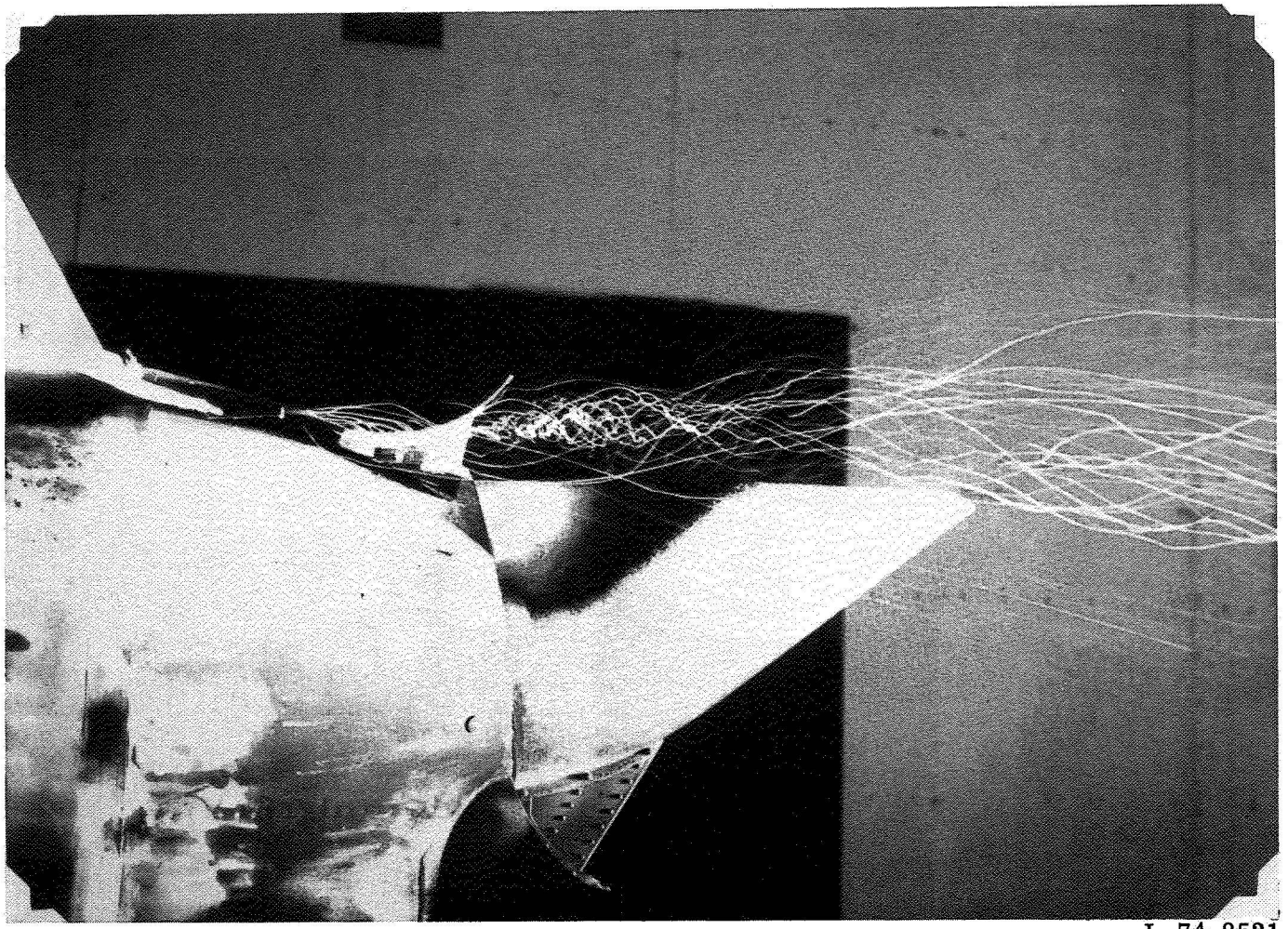

L-74-8521

(d) View 4.

Figure 27.- Concluded.

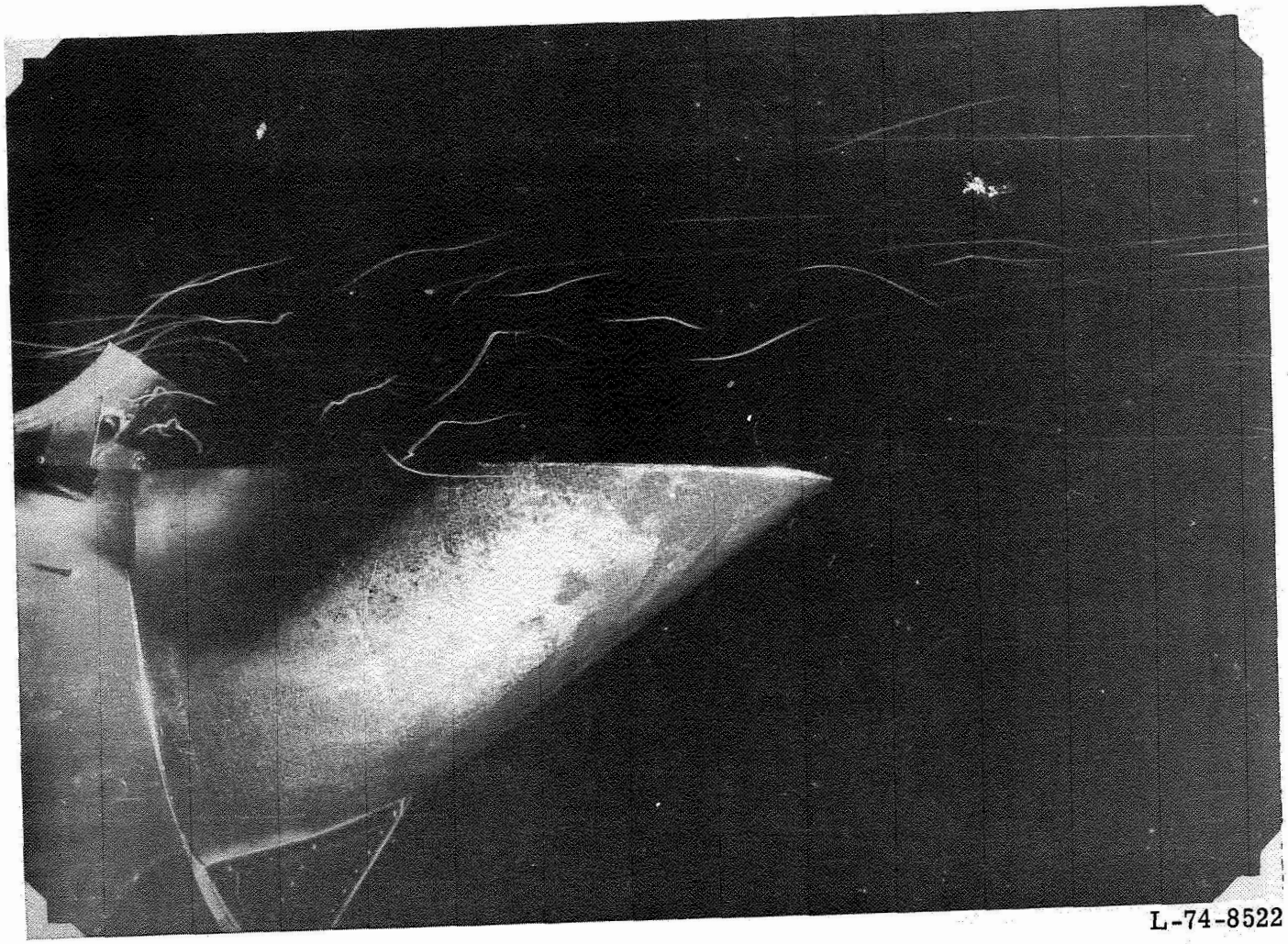

(a) Side view.

Figure 28.- Side and top views, photographed simultaneously, of effect of flow deflector 3 on exhaust flow at $V_{eff} = 0.7$.

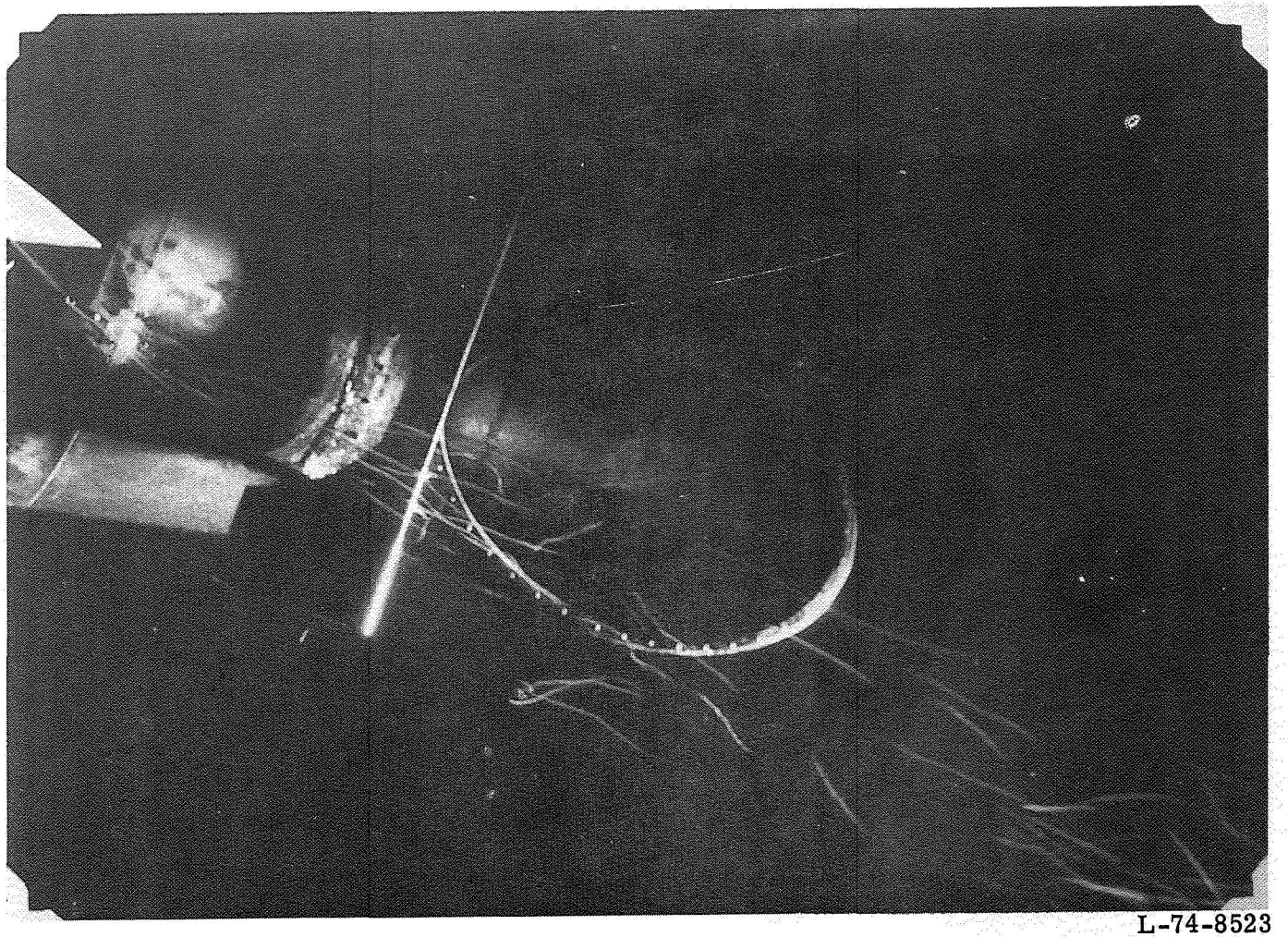

L-74-8523

(b) Top view.

Figure 28.- Concluded.

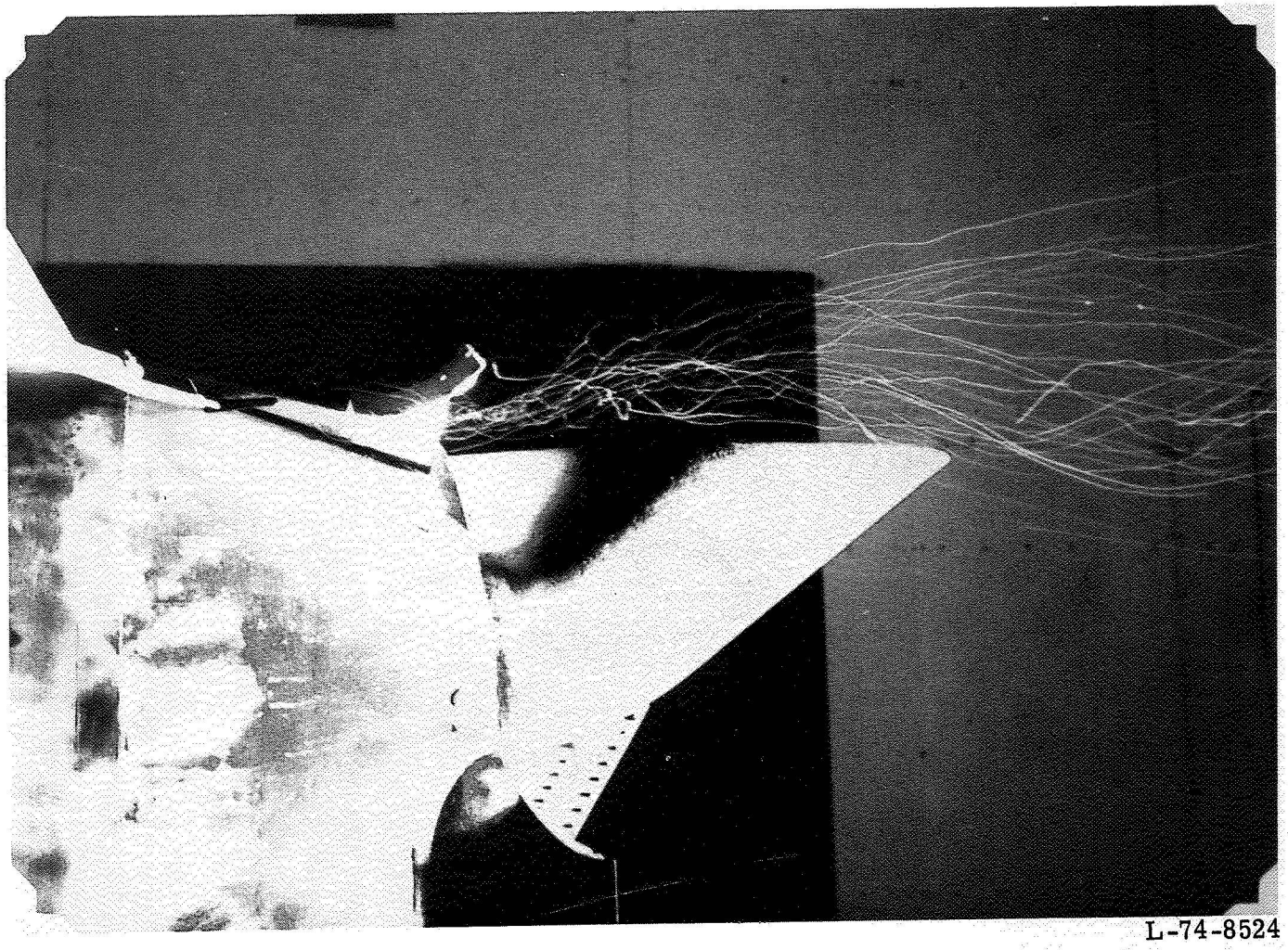

(a) View 1.

Figure 29.- Views of effect of flow deflector 4 on exhaust flow at $V_{eff} = 0.7$.

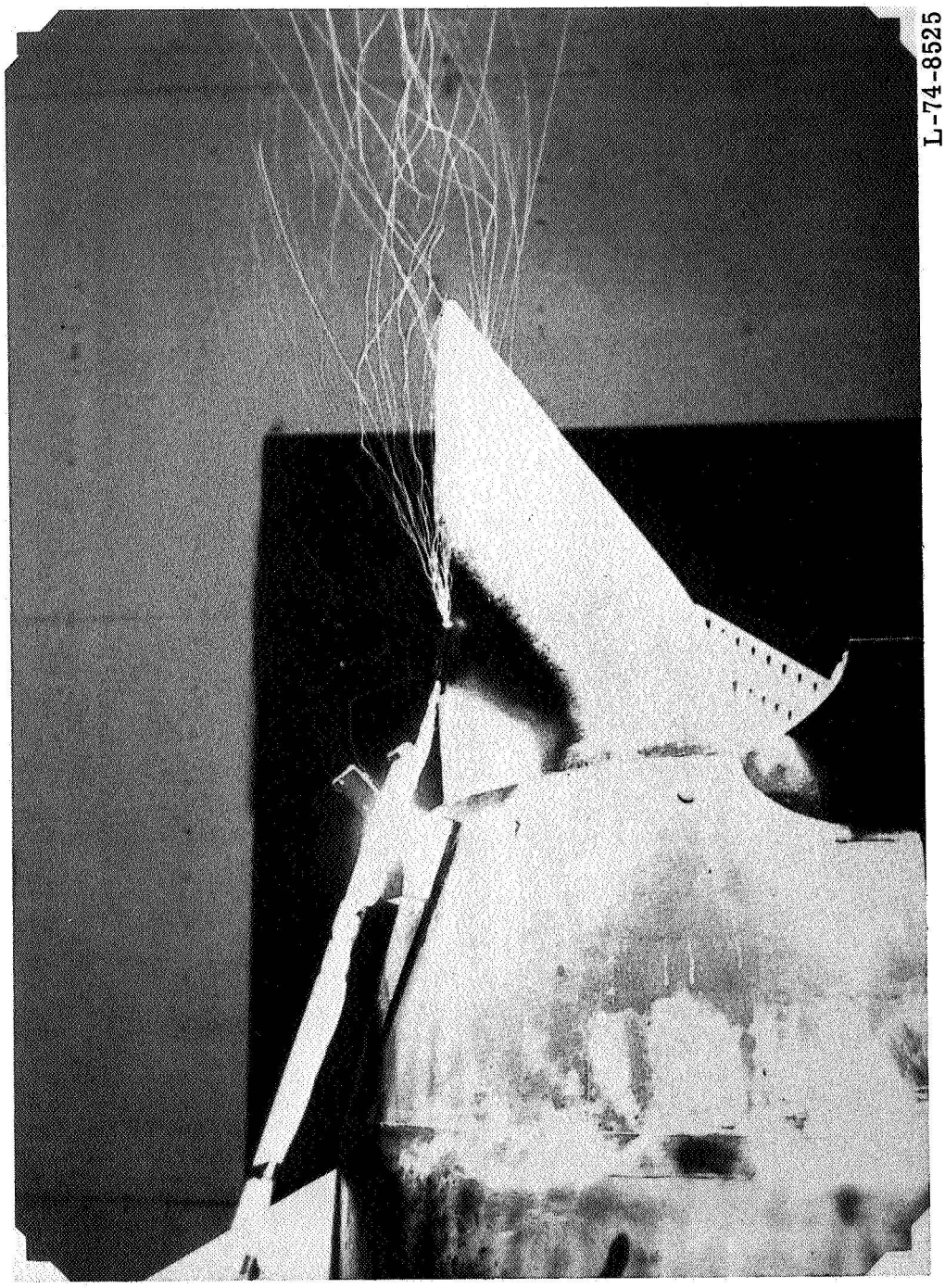

L-74-8525

(b) View 2.

Figure 29.- Continued.

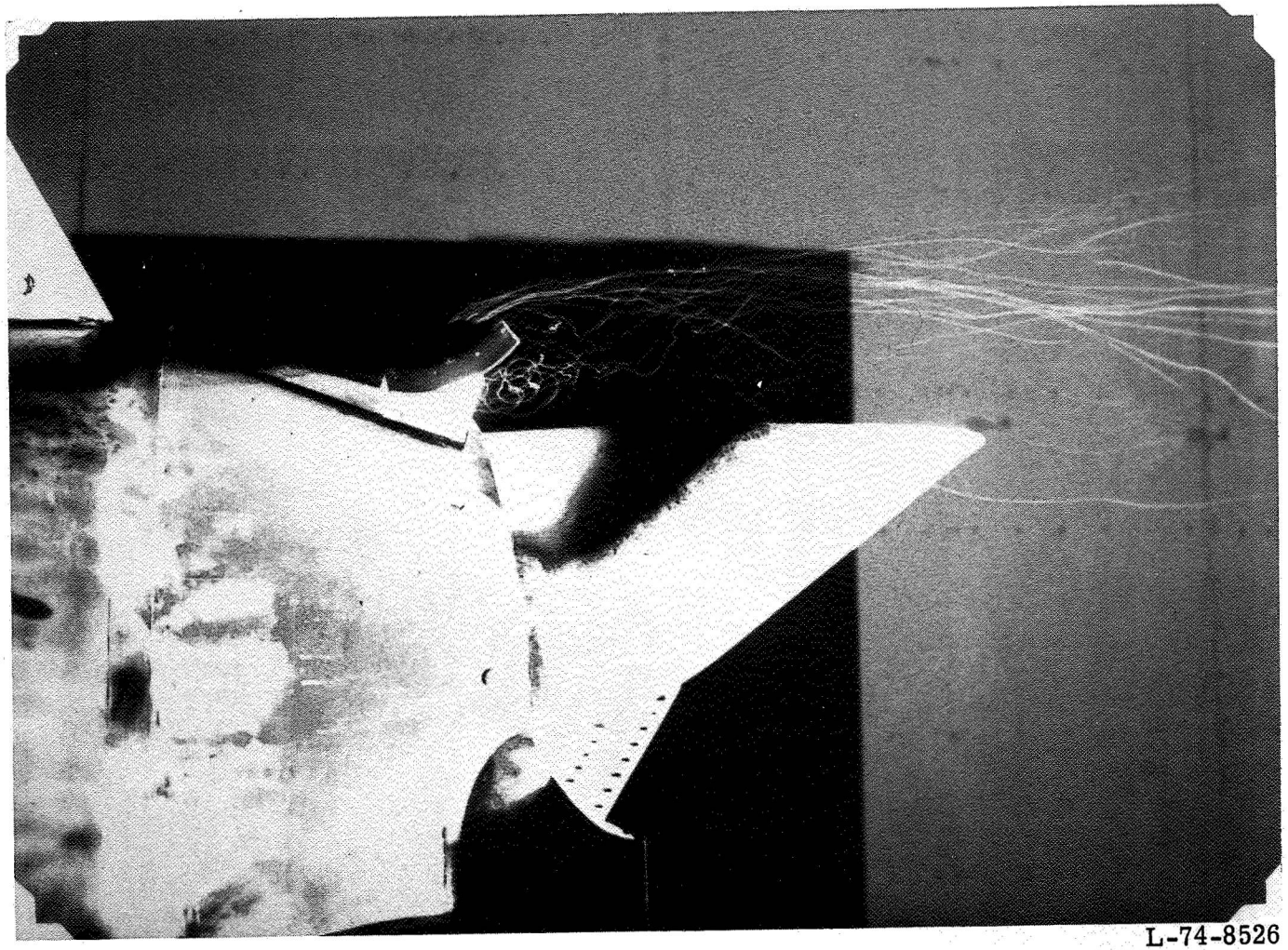

(c) View 3.

Figure 29.- Concluded.

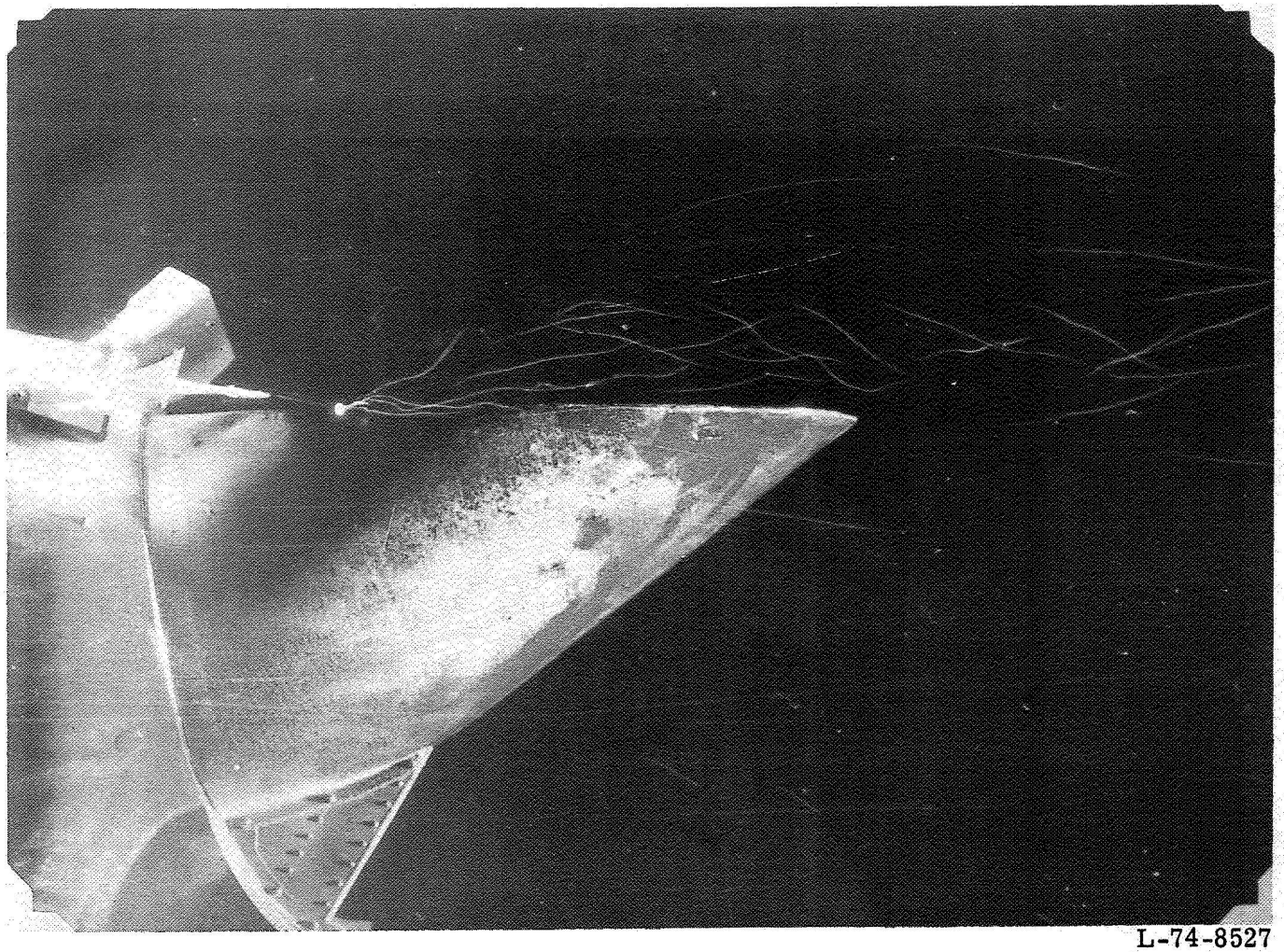

(a) Side view.

Figure 30.- Side and top views, photographed simultaneously, of effect of flow deflector 4 on exhaust flow at $V_{eff} = 0.7$.

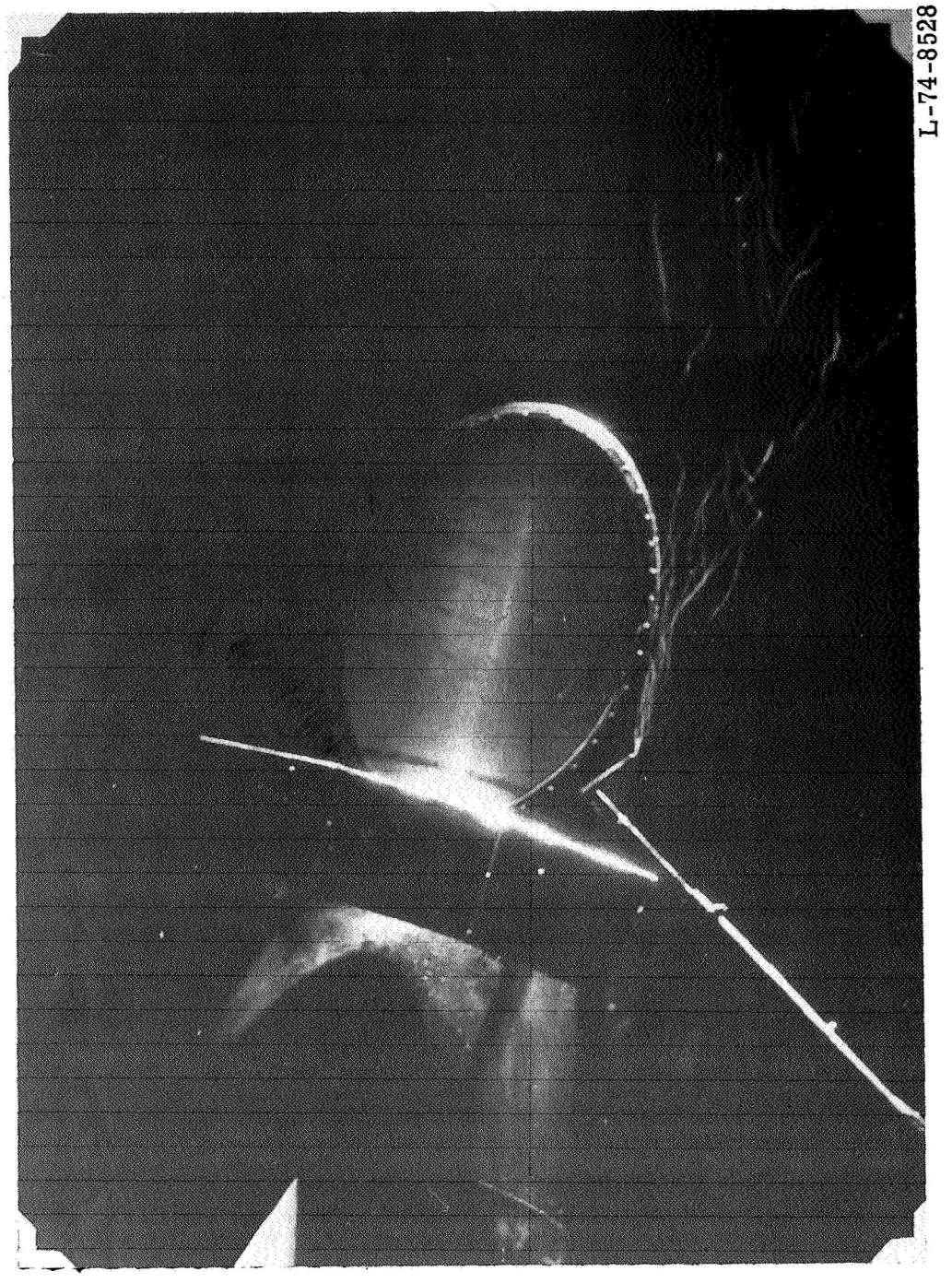

(b) Top view.

Figure 30.- Concluded.

NATIONAL AERONAUTICS AND SPACE ADMINISTRATION
WASHINGTON, D.C. 20546

OFFICIAL BUSINESS
PENALTY FOR PRIVATE USE $300

SPECIAL FOURTH-CLASS RATE BOOK

POSTAGE AND FEES PAID
NATIONAL AERONAUTICS AND SPACE ADMINISTRATION
451

U.S.MAIL

POSTMASTER: If Undeliverable (Section 158 Postal Manual) Do Not Return

"The aeronautical and space activities of the United States shall be conducted so as to contribute . . . to the expansion of human knowledge of phenomena in the atmosphere and space. The Administration shall provide for the widest practicable and appropriate dissemination of information concerning its activities and the results thereof."

—NATIONAL AERONAUTICS AND SPACE ACT OF 1958

NASA SCIENTIFIC AND TECHNICAL PUBLICATIONS

TECHNICAL REPORTS: Scientific and technical information considered important, complete, and a lasting contribution to existing knowledge.

TECHNICAL NOTES: Information less broad in scope but nevertheless of importance as a contribution to existing knowledge.

TECHNICAL MEMORANDUMS: Information receiving limited distribution because of preliminary data, security classification, or other reasons. Also includes conference proceedings with either limited or unlimited distribution.

CONTRACTOR REPORTS: Scientific and technical information generated under a NASA contract or grant and considered an important contribution to existing knowledge.

TECHNICAL TRANSLATIONS: Information published in a foreign language considered to merit NASA distribution in English.

SPECIAL PUBLICATIONS: Information derived from or of value to NASA activities. Publications include final reports of major projects, monographs, data compilations, handbooks, sourcebooks, and special bibliographies.

TECHNOLOGY UTILIZATION PUBLICATIONS: Information on technology used by NASA that may be of particular interest in commercial and other non-aerospace applications. Publications include Tech Briefs, Technology Utilization Reports and Technology Surveys.

Details on the availability of these publications may be obtained from:

SCIENTIFIC AND TECHNICAL INFORMATION OFFICE

NATIONAL AERONAUTICS AND SPACE ADMINISTRATION

Washington, D.C. 20546